

**INTEGRATED GEOPHYSICAL ANALYSIS FOR THE  
UNCONVENTIONAL POTENTIAL OF THE SEMBAR FORMATION,  
BADIN AREA, LOWER INDUS BASIN, PAKISTAN.**



**By**

**MUHAMMAD AFTAB SHABIR**

**M.Phil Geophysics**

**(2021 - 2023)**

**Department of Earth Sciences**

**Quaid-i-Azam University Islamabad, Pakistan**

بِسْمِ اللَّهِ الرَّحْمَنِ الرَّحِيمِ

*“In The Name of **ALLAH**, the Most Merciful & Mighty”*

“PAY THANKS TO ALLAH EVERY MOMENT AND GO TO EXPLORE THE HIDDEN  
TREASURES, ITS ALL FOR YOUR BENEFIT” (AL-QURAN).

DRSIM

# CERTIFICATE

It is certified that **Muhammad Aftab Shabir s/o Muhammad Shabir Khan** carried out the work contained in this dissertation under my supervision and accepted in its present form by Department of Earth Sciences, Quaid-i-Azam University Islamabad, Pakistan as satisfying the requirements for **M.Phil** degree in **Geophysics**.

## RECOMMENDED BY:

**Dr. Aamir Ali** \_\_\_\_\_

Supervisor and Chairman

Department of Earth Sciences

QAU, Islamabad.

**External Examiner** \_\_\_\_\_

DRSML QAU

## **DEDICATION**

*To my family, who has always been my source of inspiration and unwavering support throughout this journey. Your constant encouragement, love, and belief in me have been my guiding light. This thesis is dedicated to you, as a token of my gratitude for everything you have done for me. Your sacrifices and patience have made this accomplishment possible, and I hope to make you proud with my work.*

DRSML QAU

## ACKNOWLEDGEMENT

*In the name of Allah, the most merciful and most beneficent. All praises to Him who is Almighty, The One, The Everlasting, who begets none, is begotten, by no one, and there is none His equal. Alhamdulillah. I bear witness that Holy Prophet Muhammad (PBUH) is the last messenger, whose life is perfect model for the whole mankind till the Day of Judgment. I am thankful to Allah for the strengths and His blessing in completing this thesis.*

*I am nothing without your help. Please keep me always in prostration before you and let me not leave before anyone except you.*

*Foremost, I would like to express my sincere gratitude to my supervisor Dr. Aamir Ali for the continuous support of my M.Phil. study and research, for his patience, motivation, enthusiasm, and immense knowledge. His guidance helped me in all the time of research and writing of this thesis. I could not have imagined having a better advisor and mentor for my study.*

*I am extremely thankful to all of my teachers for their endless love, prayers and encouragement and my special appreciation to Yawar Amin, Ahmed Rafeh Gondal, Farman Ullah Khan Khattak and Chaudhary Umer Ghaffar who helped me in my work.*

MUHAMMAD AFTAB SHABIR  
(2021-2023)

## ABSTRACT

An ever-increasing energy demand and a huge load over natural reserves has led to a deficiency in the amount of oil and gas resources available across the globe. The compensation for such demands can only be achieved using alternative routes. Unconventional shale gas reserves therefore play a pivotal role in shaping the economic future of any country. Pakistan being an industrially burgeoning country is no different in that perspective. With that in mind, studying shale gas reserves within the basins of Pakistan is crucial for a geophysicist.

A study shows that approximately 51 TCF of shale gas reserves in Pakistan are recoverable. Major source rocks in context of unconventional resource potential in Pakistan include Sembar, Talhar, Ranikot, and Patala shales. This study focuses on demarcation and integrated characterization of Sembar formation using Tarai Deep – 02 well located in Tarai area in Central Indus Basin, Pakistan. Horizon demarcation, structural interpretation, Total Organic Content (TOC) estimation using multiple techniques, petrophysical and petroelastic properties evaluation, and TOC seismic section generation were used as the main tools for characterization of the formation.

Sembar formation was marked using seismic to well tie. Presence of normal faults pertaining to the extensional forces led to creation of extensional regime within the vicinity. Petrophysical analysis of the wells showed high shale volume (VSH) values and low effective porosity. TOC curves generated Passey's  $\Delta\text{LogR}$ , Schmoker's approach, and Schwarzkopf formulation gave reasonable TOC results for the Sembar formation, averaging 3-4%.

Rock physics modelling is done on well Tarai Deep – 02 and calculating the elastic properties of the subsurface. These elastic properties calculated now has the information of subsurface rock properties and is more accurate picture describer of the subsurface. Monte Carlo simulation is used to construct uncertainty models for shale probability in the Sembar formation of Tarai deep-02. These elastic properties are then used for stochastic inversion. Calculated TOC's are spatially distributed by the inverted volume and TOC is distributed all along the seismic

## Table of Contents

CHAPTER 1 .....	1
INTRODUCTION .....	1
CHAPTER 2 .....	6
GEOLOGY TECTONICS AND STRATIGRAPHY OF THE AREA .....	6
2.1 Tectonic Setting .....	6
2.2 Stratigraphy of the area.....	9
2.2.1 Sembar formation as a source rock.....	11
3.1 Interpretation.....	13
3.1.1 Structural Analysis.....	14
3.1.2 Stratigraphic Interpretation .....	14
3.2 Seismic Interpretation Workflow.....	14
3.3 Base Map .....	15
Construction of Synthetic Seismogram .....	16
3.5 Time Contour Maps .....	18
3.5.1 Time and Depth Contour Maps of Sembar Formation .....	18
3.5. Contour Maps of Chiltan Formation.....	20
CHAPTER 4.....	23
4.1 SOURCE ROCK CHARACTERIZATION .....	23
4.2 Methodology .....	23
4.3 Total Organic Carbon (TOC).....	24
4.4 Kerogen Type.....	25
4.5 Vitrinite Reflectance .....	26
4.6 Level of Maturity (LOM): .....	27
4.7 Well Log Response in Tarai Deep-02.....	29

4.7.1 Gamma Ray Log .....	29
4.7.2 Sonic Log: .....	30
4.7.3 Neutron Log .....	30
4.7.4 Density Log.....	31
4.7.5 Resistivity Log.....	31
4.8 TOC calculation from wireline logging.....	32
4.8.1 Passey's Log R Method .....	33
4.8.2 Sonic and Resistivity overlay.....	33
4.8.3 Schmoker's Method: .....	37
4.8.4 Schwarzkopf's Method .....	40
CHAPTER 05 .....	44
Shear Velocity Estimation and Rock Physics Modelling for Shales .....	44
5.1 Introduction:.....	44
5.2 Multilinear regression: .....	45
5.3 The development of the Shale RPM: .....	47
5.4 Voigt-Reuss-Hill (VRH) average: .....	48
5.5 SCA model:.....	48
5.6 Kuster-Toksöz (K-T) model: .....	48
5.7 Gassmann's equation: .....	49
5.8 Backus averaging method:.....	50
5.9 The shale properties analysis and rock physics model process .....	50
5.10 Rock Physics Modelling for Sembar formation: .....	52
5.11 Uncertainty Analysis using Monte Carlo Simulation: .....	57
5.12 Uncertainty Analysis of Sembar shales: .....	58
6.1 Seismic to well tie and Wavelet Extraction .....	65



6.2 Low Frequency Model.....	67
6.3 Prior Model (SI Model) .....	67
6.4 Variograms.....	68
6.4.1 Vertical and horizontal variograms.....	69
6.5 Facies Classification .....	69
6.6 Probability Density Functions (PDF's) .....	69
6.7 Inverted impedance section.....	69
6.8 Spatial Distribution of TOC.....	70
6.9 Seismic Passey TOC sections from impedance model:.....	71
6.10 Seismic Schmoker TOC sections from impedance model:.....	72
6.11 Seismic Schwarzkopf TOC sections from impedance model:.....	74
DISCUSSION AND CONCLUSIONS .....	77
REFERENCES .....	79

## CHAPTER 1

### INTRODUCTION

Global economic development is mostly based on energy resources, which necessitates a complete grasp of all available options to fulfil industrial and home energy needs. Conventional hydrocarbon resources contribute significantly to the global energy mix (Bocora, 2012; Zou et al., 2016). However, the pace of depletion of all these conventional resources has dramatically grown during the last 50 years (Miller & Sorrell, 2014). Exploration of unconventional gas has increased in recent years in order to fulfil global energy urge. Shale gas is the most important of these resources, encompassing more than half of all unconventional reserves. In recent times, shale gas resources have emerged as potential sources of energy. Shales with significant organic content, thermal maturity, and brittleness may function as commercial hydrocarbon producers. Pakistan's shale gas reserves have been predicted by the EIA to be 586 TCF, with 100-105 TCF feasible (EIA, 2013).

Unconventional reservoirs have surged in oil and gas production all over the world, with shale gas being mined in places like North America. To increase productivity on a regular basis, commercialized production requires substantial hydraulic fracturing and the use of horizontal wells (Glorioso et al., 2012). The extraction of hydrocarbons from Mississippian Barnett shale utilizing hydraulic fracturing and horizontal drilling has sparked interest in shale resource classification (Sharma and Chopra, 2013).

Because of the appropriate quantity of organic matter inherent in it, shale is regarded a possible source rock in both conventional and unconventional reservoirs (Passey et al., 1990). According to data, shale gas accounts for more than 70percent of Pakistan's basin (Hasany & Saleem, 2012). Lower Goru, Ranikot, Sembar, and Patala Formation shales are the chief possible source rocks in Pakistan's basin. Based on its depositional context, shale may exhibit severe textural and compositional differences. Such intricacy needs the development of unique but dependable approaches for shale rock classification that take into account the geology of the region of concern (SDPI, 2014).

Several methods for assessing the age and kind of source rock using well log data have been established during the recent years (Meyer et al., 1984). The total organic content (TOC) and organic maturity of the putative source rock are used to define it (LOM). Vitrinite reflectance (Re)

and the evolutionary state of kerogen (Welte & Tissot, 1984; Peters & Cassa, 1994). TOC has a considerable impact on shale gas resource potential. Because of the presence of organic materials, source rock has a short transit time, high resistivity, and low density. Several ways of estimating TOC have been developed by various researchers. Geophysical well-log data may be used to determine shale potential. Wireline log analysis makes identifying shale plays simple (Swanson, 1960; Passey et al., 1990). Myers and Jenkyns (1992) devised a density log-based approach for estimating TOC. Passey (1990) suggested AlogR, a method for identifying shale play that takes the resistivity (LLD) log and either the density (DT), neutron porosity (NPHI), or sonic (DT) logs into consideration. Despite the fact that the processes are often effective, they are limited by the need for calibration through the analysis of core samples collected from certain source rocks (Myers & Jenkyns, 1992).

Shales often have relatively complex mineralogy, which influences their brittleness. As a result, reliable lithology and mineralogy predictions are required. For this goal, many laboratory measurement analyses are employed. Elemental log analysis is one such technique that uses well log data to quantitatively evaluate the formation based on mineral composition. However, it requires a greater level of interpretative attention and aptitude (Vishal et al., 2022).

Because of their diverse composition, TOC, thermal maturity, and depositional conditions, organic shales have a significant degree of anisotropy (Liu et al., 2012). Because their minerals line easily, shale rocks may be modelled as VII media (Chesnokov et al., 2009; Wenk et al., 2007). Furthermore, traditional rock physics models overestimate anisotropy in shale gas deposits. As a result, identifying reservoir dynamic characteristics and, as a result, estimating gas reserves is challenging. To model biological shales, the anisotropy in the shale matrix caused by variations in clay minerals and pores must be taken into account. Carcione (2000), Dewhurst et al. (2011), Slätt & Abousleiman (2011), and Wenk et al. (2007). By adding organic shale features into a rock physics model, many ideas have been established. (Carcione et al., 2011; Khalid et al., 2019) created a RPM for organic shale that takes into account kerogen as a load-bearing matrix in addition to minerals and pores. Zhu et al., (2012) proposed a more accurate shale gas RPM. Bandyopadhyay et al. (2012) investigated the variance associated with organic shale rock characteristics using Zhu's model. Zhang et al. (2017) developed a model by considering anisotropic formation, pore size, and shale mineral distribution. The rock physics framework given

here for various shale rock compositions takes matrix, kerogen, fluids, pores, and so on into consideration.

Because shale has poor permeability, hydraulic fracturing is necessary to recover hydrocarbons from shale gas. The Petro-clastic properties of the rock may be used to discover shale oil/gas drilling zones. Based on the created Rock physics model, Petro-elastic properties are analyzed to find probable drilling sites. The organic content of the source rock could also have an effect on the Petro clastic characteristics. For efficient hydraulic fracturing in shale gas drilling zones, low permeability (K), high brittleness index (B), and moderate Young's modulus (E) are desired.

Uncertainty analysis is a technique for ensuring the variability of log data predicted using rock physics templates. Deterministic correlations between input components and output variables such as  $V_p$ ,  $V_s$ , and so on are provided by rock physics models. Monte Carlo simulation attempts to measure the uncertainties associated with every parameter and thereby anticipates the output using the probabilistic distribution function (PDF). The shale distribution is represented by probabilistic models, which may also be utilized to estimate the production impacts on elastic characteristics (Adjei et al., 2019).

The most effective method for characterizing a reservoir is to use seismic amplitude versus offset (AVO) reflection coefficient modelling. AVO analysis aids in the extraction of subsurface rock properties from surface seismic data, which is then used to determine lithology, porosity, and fluid saturation. Anisotropy in shales has a significant influence on AVO evaluation (Blangy, 1994; Mallick, 2001; Tsvankin et al., 2010). Carcione (2000) and Sayers (2013) investigated the theoretical underpinnings of RP as well as AVO behaviour in shale. Commercially, the AVO technique has shown to be a useful tool for hydrocarbon estimation.

Finally, using post-stack inversion, the implications of the derived rock physics model are extended to seismic sections. Seismic inversion gives a more detailed answer at geological boundaries, allowing variation in reservoir characteristics simpler to trace (Ali et al.2018). It may also be used to compute reservoir characteristics including porosity, Hydrocarbon, permeability, and water saturation (Gavotti et al., 2014).

Table 1.1 Detail of Sembar formation is discussed in the table i.e. top and bottom depth of the formation, thickness and age in each well.

Well Names	Total Depth	Sembar Depth(m)	Thickness(m)	Formation age
Tarai 1	3106.75	<b>Top</b> 2355.38	658.64	Upper Cretaceous
		<b>Bottom</b> 3014.02		
Tarai deep-02	3143.43	<b>Top</b> 2252.362	690.643	Upper Cretaceous
		<b>Bottom</b> 2943.005		
Tarai deep-03	3289.66	<b>Top</b> 2368.18	668.39	Upper Cretaceous
		<b>Bottom</b> 3036.57		

The specific objective of this thesis is to assess the hydrocarbon potential of the Sembar Formation in Pakistan's Lower Indus Basin (LIB) Badin block besides modelling the TOC and Petro-elastic characteristics using seismic data and conventional logs in the frame of reference of unconventional resource production. Badin, Ranikot, Talhar and Sembar shale are both source rocks in the LIB, although Sembar shale is regarded as the primary source rock because of its composition, broadly distributed dispersion, huge thickness, and depth in comparison to the other shale formations (Ahmad et al., 2011; Abbasi et al., 2014). To achieve the goals, 3D seismic and log data were used, which included 3D seismic data (13 x 13 kilometres) and well log/vertical seismic profiling (VSP) data recorded in Tarai-01, Tarai deep-02, and Tarai deep-03 of the Badin block of the Lower Indus Basin, Pakistan. The Sembar shale is the target formation; consequently, in Table 1.1, the depths, thicknesses, and ages of wells (A, B, and C) are columnized in relation to the Sembar Formation. This study provides and pertains to a novel workflow (Figure 1.1) for estimating TOC, one of the most important parameters for shale gas evaluation, as well as other Petro-elastic parameters such as ratio, BI, shear modulus, and E in the study area, using 3D seismic and log data in three stages.

In the first step, a synthetic seismogram is developed to link the seismic and well data. The synthetic seismogram is then overlaid on the seismic sections and horizons, and faults of the Sembar and Chiltan formations are indicated across the inline to provide time contours, depth contour lines, and isopach maps.

The second step is estimating TOC and petro-elastic parameters in wells (Tarai-01, and Tarai deep-02) using log data. Passey's AlogR, Schmoker, and Schwarzkopf's techniques are used to calculate TOC because they yield the best possible results in all wells. The assessment of these features is critical as they have a substantial influence on the recovery and expansion of unconventional assets when compared with conventional reservoirs (Mavko et al., 1998; Zhang et al., 2020).

The third step is to build a rock physics model for the well's petro-elastic parameters using the Backus average. In addition, a probability model for the Sembar formation is being developed.

The fourth step is to create an inverted seismic model for the TOC calculated from the wells and using the rock physics model velocities.

DRSML QAU

## CHAPTER 2

### GELOGY TECTONICS AND STRATIGRAPHY OF THE AREA

#### 2.1 Tectonic Setting

Geological information, such as the tectonic setting, stratigraphy, structural styles, and depositional environment of any given region, plays an extremely important part in the process of hydrocarbon exploration and production because it contributes to the selection of technique for the appraisal of particular reservoirs (whether conventional or unconventional). For the purpose of compiling geological knowledge, prior studies as well as public and unreported company reports are important (Onajite, 2013). The geological data is necessary to differentiate reservoir rocks from non-reservoir units, which is particularly important for hydrocarbon extraction. Because of this, it is vital to have a short talk on the geology of the region.

Geologically speaking, Pakistan is located on the Indian Plate, which, roughly 50 million years ago, collided with the Eurasian Plate farther to the north, giving rise to the Himalayan region as a consequence of the impact. In addition, the Tethyan and Gondwana landmasses may be distinguished as two distinct regions on the Indian Plate. The Tethyan domain extends throughout most of northern and western Pakistan, encompassing the regions of Kohistan, Ladakh, Makran, the Karakorum Ranges, Kharan, and Chagai. In contrast to the Gondwana landmass, which includes the Salt Range, the Kirther fold and thrust belt, and the On the western side of the Indus Basin are the Cholistan and Thar deserts, as well as the Sulaiman fold and thrust belt, all of which are located in eastern Baluchistan (Kazmi and Jan 1997). The Indus, Baluchistan, and Kakar Khorasan basins are the three most important basins in Pakistan. Each of these basins is further subdivided into smaller basins, as described by Kadri (1995). The sediments of the Indus Basin are the primary targets for petroleum exploration in Pakistan. These sedimentary rocks contain significant conventional and unconventional reservoirs from the Cretaceous and Eocene epochs. Energy corporations are conducting exploration in every basin because each basin has a unique mix of sources and reservoir formations. In the LIB, only a small number of Lower Goru's sand strata are considered to be conventional reservoirs, but the Sembar shale is regarded as a substantial source rock (Alam et al., 2002).

During the Cretaceous epoch, when the plate movement was as fast as around 20 to 30 centimeters per year, the Indus Basin first began to form (Farah et al., 1984; Gnos et al., 1997).

Tectonically, the Indus Basin seems to be quite active north of Pakistan (Upper Indus Basin), and it has a significant potential for tectonic events because it is located at the primary compressional boundary of the Eurasian and Indian plates. Because of this, the majority of the thrust and fold belts are exposed throughout the boundaries of the Upper Indus Basin, and these also include the Main-Mantle-Thrust, Main-Boundary Thrust, and Salt-Range-Thrust. In contrast, the northern section of the basin, which is known as the Upper Indus Basin, is significantly more active than the southern part of the basin, which is also known as the Lower Indus Basin. Both parts of the basin are referred to as the Indus Basin. The Lower Indus Basin is often characterized by an extensional regime, with major normal faults and a few minor reverse faults indicating an extensional regime (Farah et al., 1984, Kadri, 1995). During the Cretaceous period, tectonic instability in the Indus Basin led to the formation of an extensional regime, which marked the start of the development of the Lower Indus Basin (Farah et al., 1984). In the neighbourhood of the Thar platform, the rift zone may be found as the Sargodha High, which delineates the dividing line between both the UIB and the LIB (Kadri, 1995). Horst and graben formations are largely developed below the Tertiary unconformity, comprising Cretaceous and earlier strata, as a result of rifting and doming that occurred during this time period (Alam et al., 2002), as illustrated in figure 2.1.

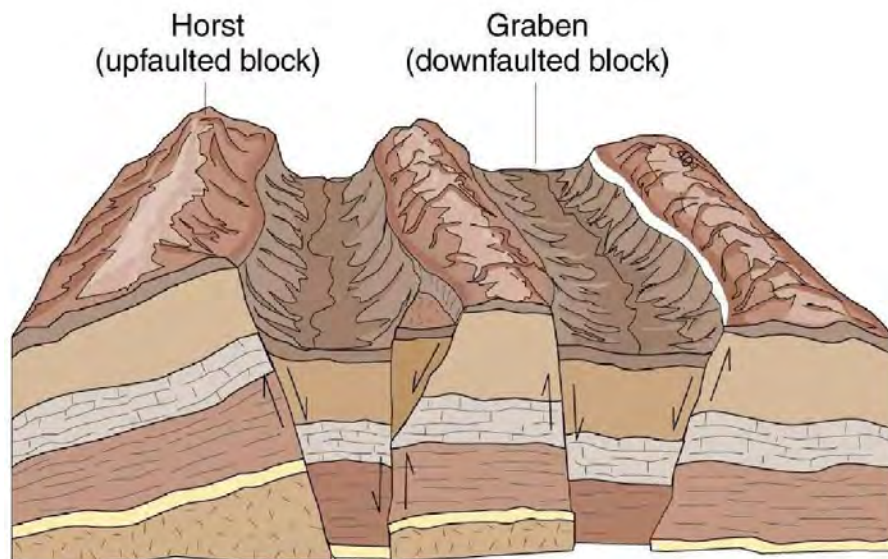


Figure 2.1 Model illustrating extensional regime.

Our research focuses on the Badin block, which is located in the LIB about 160 kilometres east of Karachi at coordinates  $24^{\circ} 5' N$  to  $25^{\circ} 25' N$  and  $68^{\circ} 21' E$  to  $69^{\circ} 20' E$  (Kadri, 1995; Alam



et al., 2002; Ahmed et al., 2013; Munir et al., 2014). As a result of its distance from the primary zone of deformation, this region (the eastern side of LIB) is experiencing a doming and rifting process at a relatively modest intensity. The rate of distortion increases as one move from east to west, and the region is characterized by inclined normal faults (Farah et al., 1984; Kadri, 1995; Alam, 2002). These faults may be observed and mapped as deforming the Cretaceous as well as earlier layers on seismic data (Kadri, 1995; Alam et al., 2002). The majority of traps in this region are of the structural kind (Kemal, 1991). The structural and tectonic framework of Pakistan is shown in Figure 2.2, along with geographical information; the study region is denoted by a red polygon on the map.

DRSML QAU

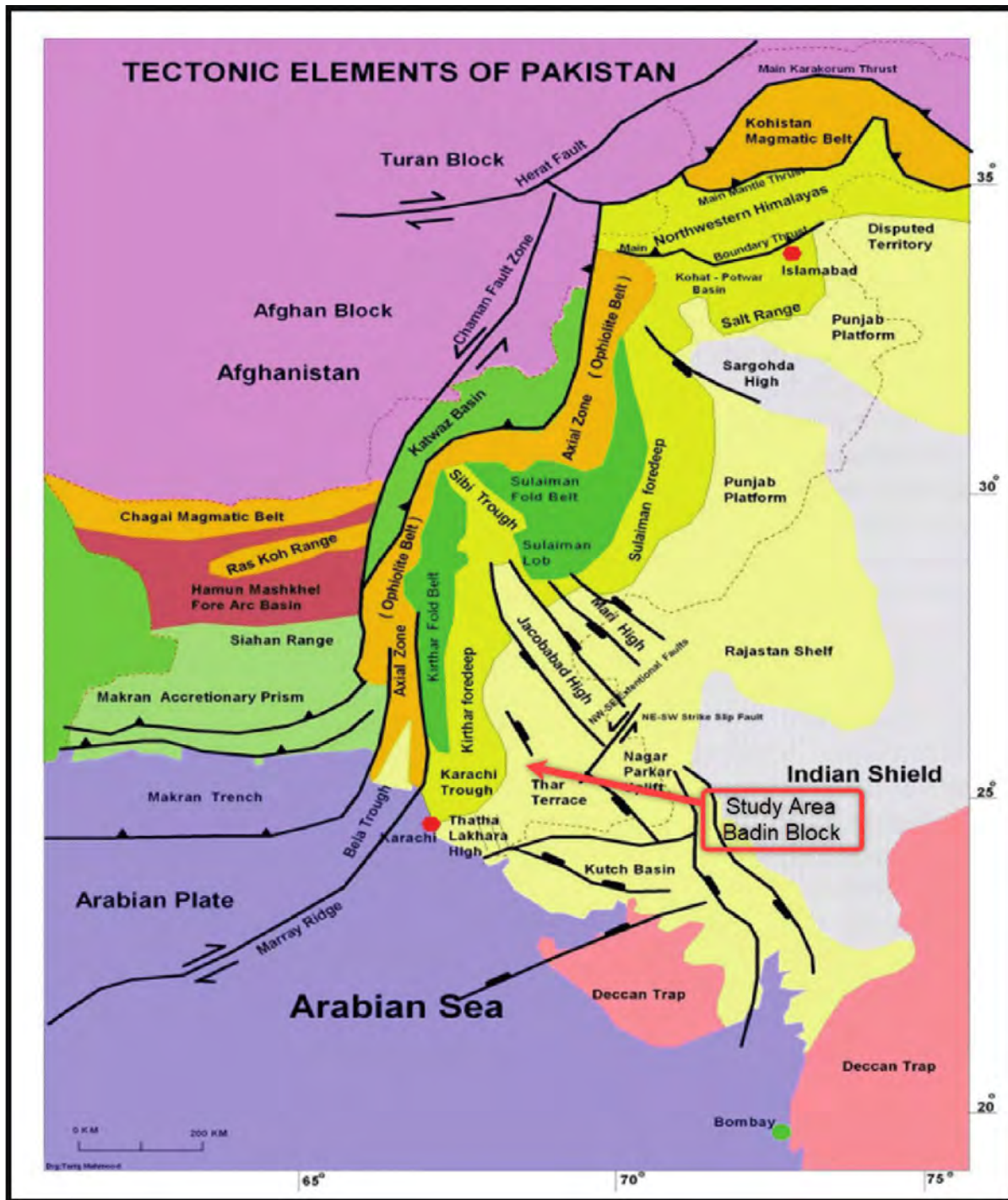


Figure 2.2 The structural and tectonic framework of the Badin area, Pakistan (Kazmi and Snee, 1989).

## 2.2 Stratigraphy of the area

In terms of stratigraphy, the age of the formations in the Indus Basin may be anywhere from the Cambrian to modern, and it includes erosional and non-depositional periods. On the other hand, the age of the formations in the study region can be anywhere from the Jurassic to the

Tertiary (Alam et al., 2002). Major prospective conventional and unconventional sources in the LIB may be found in the Sembar Formation, as well as in various shale sections of the Lower Goru and Ranikot formations (Abbasi, 2014). The Sembar shale in the north of the Kirther Range has a modest HC potential, although this potential increases as one move toward the range's south and southeast portions. The Cretaceous Sembar and Goru formations (which belong to the Cretaceous period) were deposited in a shallow marine setting during the deposition process. These formations are formed on top of Jurassic Chiltan limestone that has been eroded regionally along the passive borders of continental areas. The Sembar is a kind of sedimentary rock that is composed mostly of shale, with just trace quantities of silt and sand present. The Sembar formation is made up mostly of shales, with only trace amounts of sand and silt, while the Lower Goru formation is a combination of interbedded shale and sandstone. Deposition took place on the shelf and in shallow marine environments throughout the Late Cretaceous, which led to the formation of carbonate rocks such as those found in the Parh, Fort Munro, and Moghal Kot. Because it contains regressive sands, the Pab Formation has characteristics of a near-shore environment (Eckhoff and Alam, 1991, Porth and Raza, 1990, Ahmad et al., 2013; Wandrey et al., 2004).

AGE (Ma)	PERIOD	EPOCH	FORM	LITHOLOGY	NOMANCLATURE	HC SIGNIFICANCE			
						RES.	SOURCE	SEAL	
85          94          134          164	CRETACEOUS	UPPER	PARH		CHALAK & LIMESTONE				
			UPPER GORU			UPPER GORU			
					MARL & SHALE				
		LOWER	LOWER GORU			UPPER SAND			
						UPPER SHALE			
						MIDDLE SAND			
						LOWER SHALE			
						BASAL SAND			
		UPPER	SEMBAR			SEMBAR SHALE & SAND			
				CHILTAN		CHILTAN LIMESTONE			



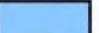



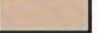
	MARL & SHALE		SHALE		SOURCE
	SANDSTONE		LIMESTONE		SEAL
					RESERVOIR

Figure 2.3 The summary of stratigraphic column of Badin area, LIB, Pakistan.

### 2.2.1 Sembar formation as a source rock

The Sembar, together with the shale layers of the Lower Goru and Ranikot formations, are regarded as confirmed source rocks in the Lower Indus basin. But the Sembar formation that may be found in the research region is the primary source rock (Ahmad et al., 2011; Abbasi et al., 2014), Based on the classification systems used by oil firms, the reservoir rocks known as the Lower Goru sands may be broken down into the categories of A, B, C, D, Upper, and Basal sands. The Basal Sand is the primary objective, although the Massive Sand is also

responsible for the production of HCs in certain regions of the LIB (Kadri, 1995, Abbasi et al. 2014). According to Zaigham and Mallick's hypothesis, Chiltan limestone has the potential to become another HC-bearing rock (reservoir) in the future (2000). Rock formations such as the Sembar, Bara Lakhra, Laki, Ghazij, and Kirther in the Southern Indus Basin serve the function of seal rocks (Zaigham and Mallick, 2000). Within the LIB study region, the primary seal and cap rocks that come together to produce a full HC play are the interbedded shales of the Lower Upper Goru (Kadri, 1995).

In spite of the fact that the LIB has many strata with significant shale and clay, the Sembar formation is regarded as the principal source rock due to the chemical characteristics, width, depth, and maturity of this rock. William was the very first person to adopt the word "Sembar" in 1959. He called it after the type of location of "Sembar Pass" which is located in the Mari highlands. The thickness of the formation varies in various parts of the landscape, with an overall average of around 300 meters. Iqbal and Shah's study from 1980, Raza et al., study.'s from 1990, Wandrey's study from 2004 and Ahmad et al., study.'s from 2013 are all cited in this article.

The Sembar Formation is made up of dark grey shales but also includes lenses of sand and silt (Raza et al., 1990). Its characteristics vary throughout the basin, with minor quantities of argillaceous limestone and glauconite (Eckhoff and Alam, 1991; Shah, 2009), whereas phosphate and pyrite are formed in the lower part of the formation. Average mineral compositions (in percentage) for clay, quartz, calcite, and pyrite, respectively, are 47, 42, 10, and 1. Gas contents of CO<sub>2</sub> range from 1 to > 70; N ranges from (Shah, 2009).

Previous research has indicated that the Sembar Shale is a prospective source rock in the Lower and Middle Indus basins because it contains type-II and -III kerogen (EIA/ARI, 2013); TOC 1 and 29.48 wt.%, which indicates that it is immature to mature source rock. The total organic carbon content ranges from around 0.5 to 3.5 wt.% in the region under investigation, whereas the formation average is 1.4 wt.%. Another sign that the shale has reached its mature state is when the vitrinite reflectance (Ro) is between 0.6 and 1.3%. To the west, where it was buried for a long time, the thermal maturity level is quite high; to the east, where the depth is not as great, the maturity level is lower. The geothermal gradient is lower than 20 to 45 degrees Celsius every kilometer, and the depth spans from 1 to 3 kilometers (OGDCL, 1988; Ahmad et al., 2013).

# CHAPTER 03

## SEISMIC INTERPRETATION

### 3.1 Interpretation

Interpretation is a process that may be used to convert all of the seismic data into a model of the subsurface that is either structural or stratigraphical in nature. Interpretation is used to try to locate the real anomalous zone because the seismic section is a description of the geological stratum model of the earth. Real geology is rarely known in a satisfactory way; therefore, it is unusual for the accuracy or incorrectness of an interpretation to be determined. The criteria for excellent interpretation are consistency instead of accuracy. To accurately interpret seismic data, it is necessary to have a comprehensive understanding that encompasses not only seismic information, but also gravitational and magnetic data, well parameters, surface geology, and various geological and physical principles. (Telford et al, 1999) Conventional seismic interpretation entails picking and tracking seismic reflectors that are laterally consistent in order to map geologic formations, stratigraphy, and reservoir geometry. Identifying hydrocarbon accumulations, determining their extent, and estimating their amounts are the objectives. The conventional method of interpreting seismic data is an art that requires a high level of skill and extensive practical experience in geology and geophysics. In the last three decades, there's enormous breakthroughs in data equipment, and seismic processing procedures in order to meet the need of investigating ever more complicated targets. Due to this development, seismic analysis is now a highly computational science. The fact that computer-based processing (processing and interpretation) is much more accurate, precise, efficient, and satisfying frees up more time for further data analysis. The whole of this task is accomplished by the use of many pieces of software, one of which is referred to as the Kingdom 2021. Our main goal is to render the reflection as transparent as possible so that we can simulate the underlying structure and stratigraphy. When the acoustic impedance changes, the reflection indicates the boundaries to a geologist. We connect the well characteristics to the seismic data in order to discern between both horizons using the seismic data. Data has been analysed using well-log data has been used to connect the seismic data. The best possible seismic data is used to determine the structure and estimate of sedimentary layers, acoustic velocity, seismic succession, and rock properties (Dobrin & Savit, 1988). There are several ways for interpretation:

1. Structural Examination
2. Identification of mechanical features
3. Stratigraphic investigation
4. Identification of stratigraphic boundaries

### **3.1.1 Structural Analysis**

In the instance of Pakistan, where the vast majority of the hydrocarbons are already being extracted from structural traps, this kind of study is very well-suited. The analysis of reflector geometry using reflection times as the primary data source. The search for mechanical traps that may hold hydrocarbons is the primary application of structural interpretation of seismic sections. The primary application of analysis of structures is as described above. Instead of structural maps, that are designed to portray the geometry of multiple selected reflections, the vast bulk of structural interpretations rely on two-way reflection durations. This is because these maps are easier to calculate. There are certain seismic portions that include pictures that can be deciphered with a minimum of effort, and in other cases with no effort at all. Faults may be easily identified by discontinuous reflections, and folded beds can be uncovered by undulating reflections (Sheriff, 1990).

### **3.1.2 Stratigraphic Interpretation**

Because genetically linked sedimentary sequences frequently comprise of plus standard strata that illustrate discordance with sequences both above and below them, seismic stratigraphy is used to determine both the depositional processes and the environmental conditions that existed at the time of deposition. Formations, stratigraphic traps, and unconformities may all be determined with its assistance, which is another advantage. Using this methodology makes it easier to identify the key pro-gradational sedimentary sequences that have the most potential for hydrocarbon production and accumulation. These sedimentary sequences provide the biggest potential for hydrocarbon generation and accumulation. The use of stratigraphic analysis thus significantly improves one's chances of effectively identifying hydrocarbon traps in an environment consisting of sedimentary basins.

## **3.2 Seismic Interpretation Workflow**

Figure 3.1 demonstrates the procedure used for seismic data interpretation. The base map is created by importing SEG-Y into the Kingdom software. Horizons of concern are marked

manually as well as automatically when the tracking mode is set to auto. Initially, horizons are identified using a synthetic seismogram created from well data. During this step, faults are spotted and then marked for further investigation. In order to determine the structural highs and lows, fault polygons and horizon contours are created. Following this step, time and depth contours are produced. Utilizing the well point velocity allows for the generation of depth contours.

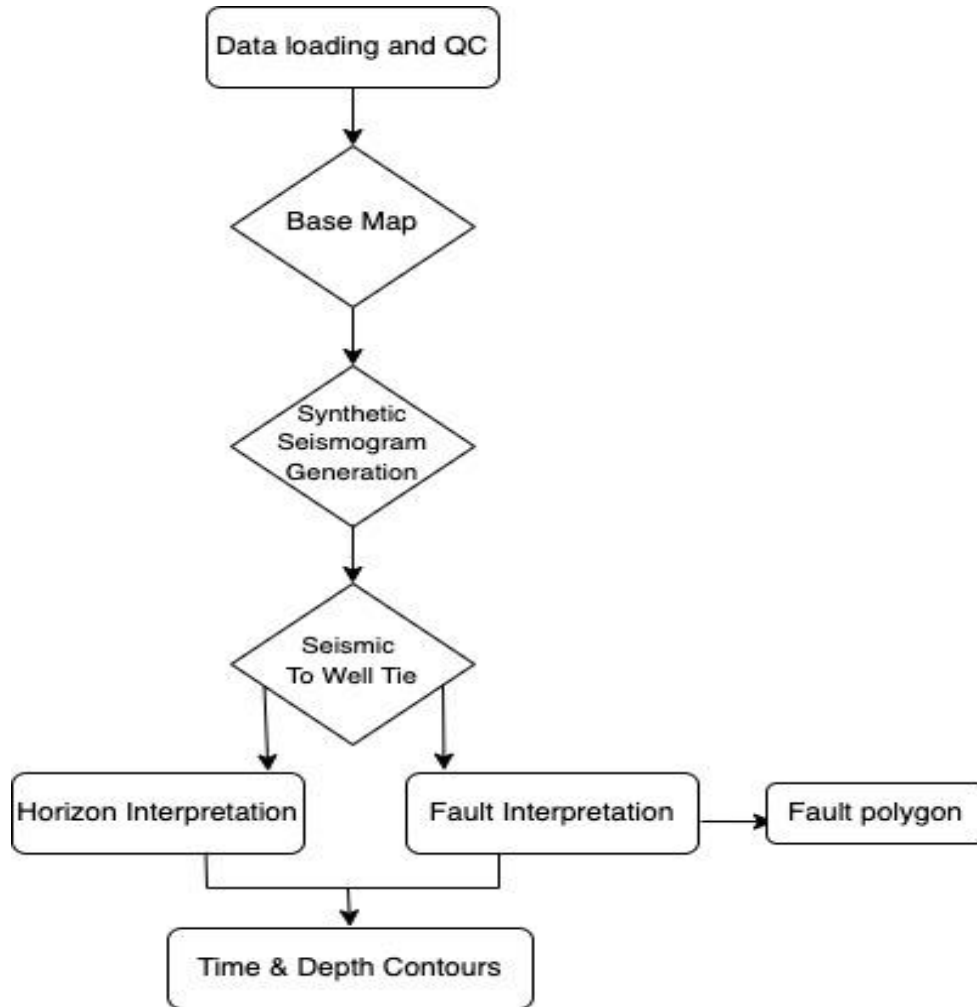


Figure 3.1 Workflow for seismic data interpretation

### 3.3 Base Map

Due to the fact that it displays the geographical location of each panel of the seismic section, the base map is an essential component of the interpretation process. For a geophysicist, a base map is a map that either comprises a number of Inlines and Xlines on which a geophysical survey is being conducted out or one that depicts the orientations of seismic lines and identifies sites at which seismic data were gathered. The locations of lease and concession borders, wells, seismic survey sites, and other cultural data like as buildings and roads, together with geographic



coordinates such as latitude and longitude, are often included on a base map. It is a map that shows the normal locations of wells and seismic survey stations, as illustrated in Figure 3.2.

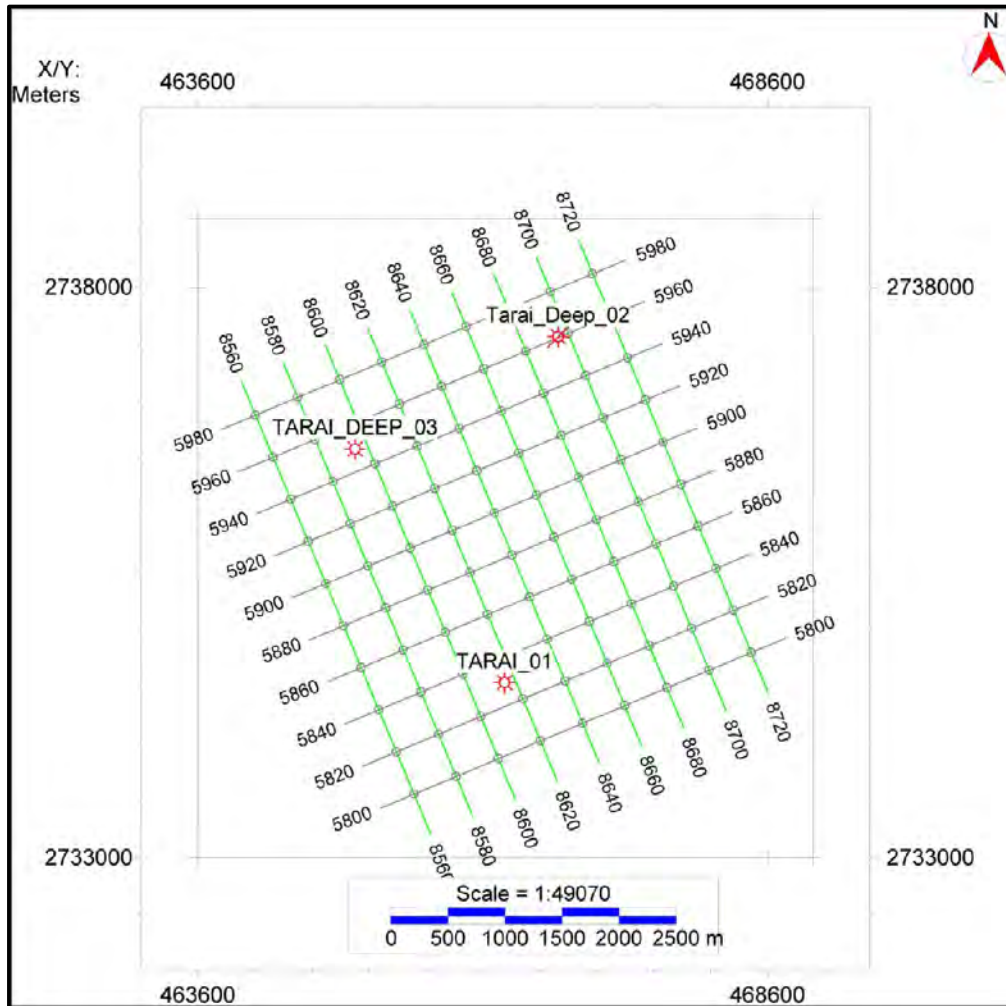


Figure 3.2 Demonstrate the base map of the study are i.e. Badin Tarai.

### Construction of Synthetic Seismogram

The construction of synthetic seismograms requires two-way time for each well top. Depth, sonic log data, and area replacement velocity generate two-way time for each well top or reflector. The preparation of the time depth chart involves employing two-way time in comparison to the top depth of each well. The recovered wavelet with a frequency of 25 Hz is convolved with the well data to produce the synthetic seismogram at the end. Tie this synthetic seismogram to the Seismic data. The synthetic seismogram of Tarai Deep 2 is shown in figure 3.3 respectively.

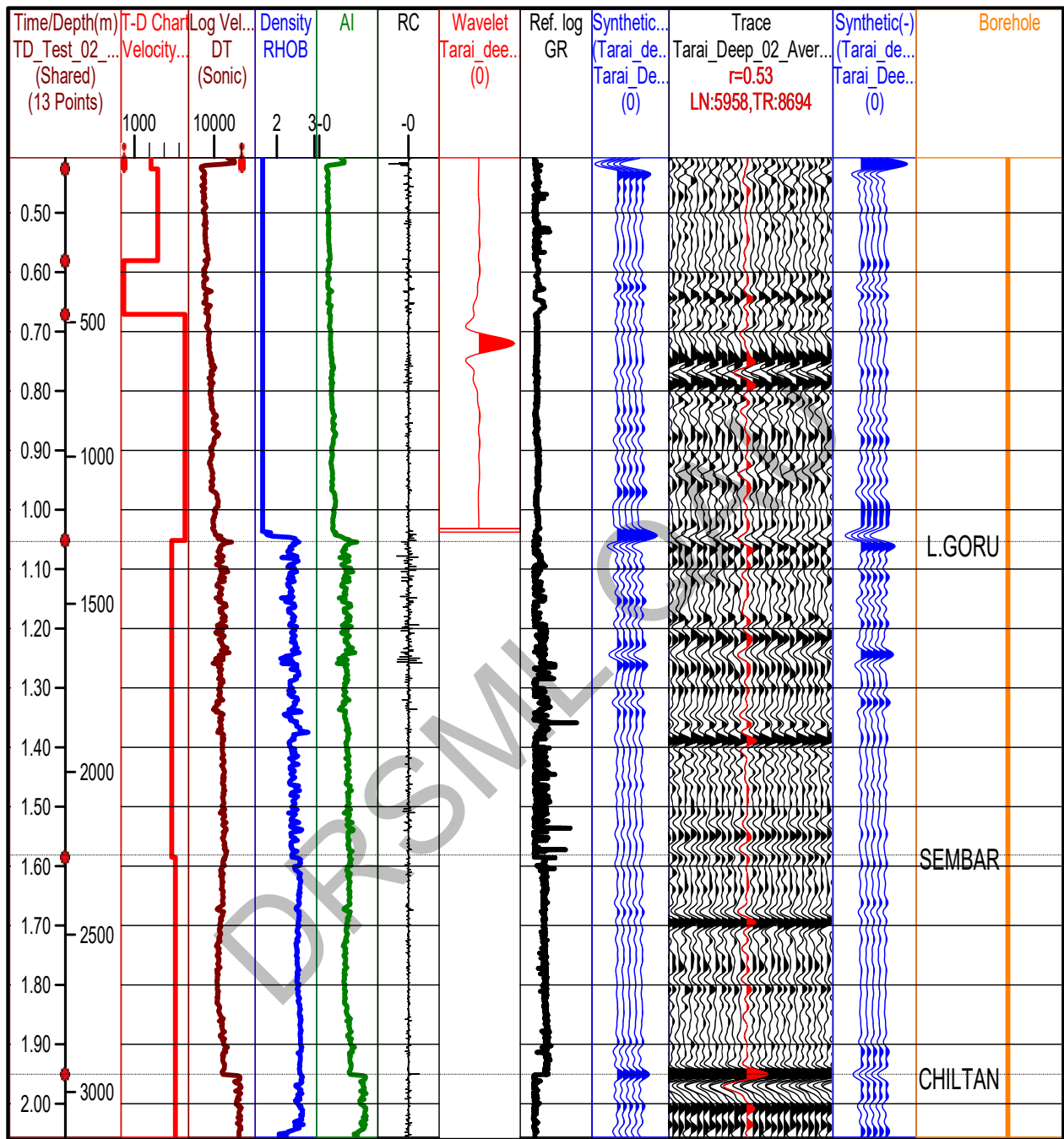


Figure 3.3 Synthetic Seismogram of Tarai Deep 2.



Sembar is the main zone of interest of the study area from the hydrocarbon exploration point of view. Time and depth contour maps of Sembar formation are used to understand the structural trap present in the reservoir.

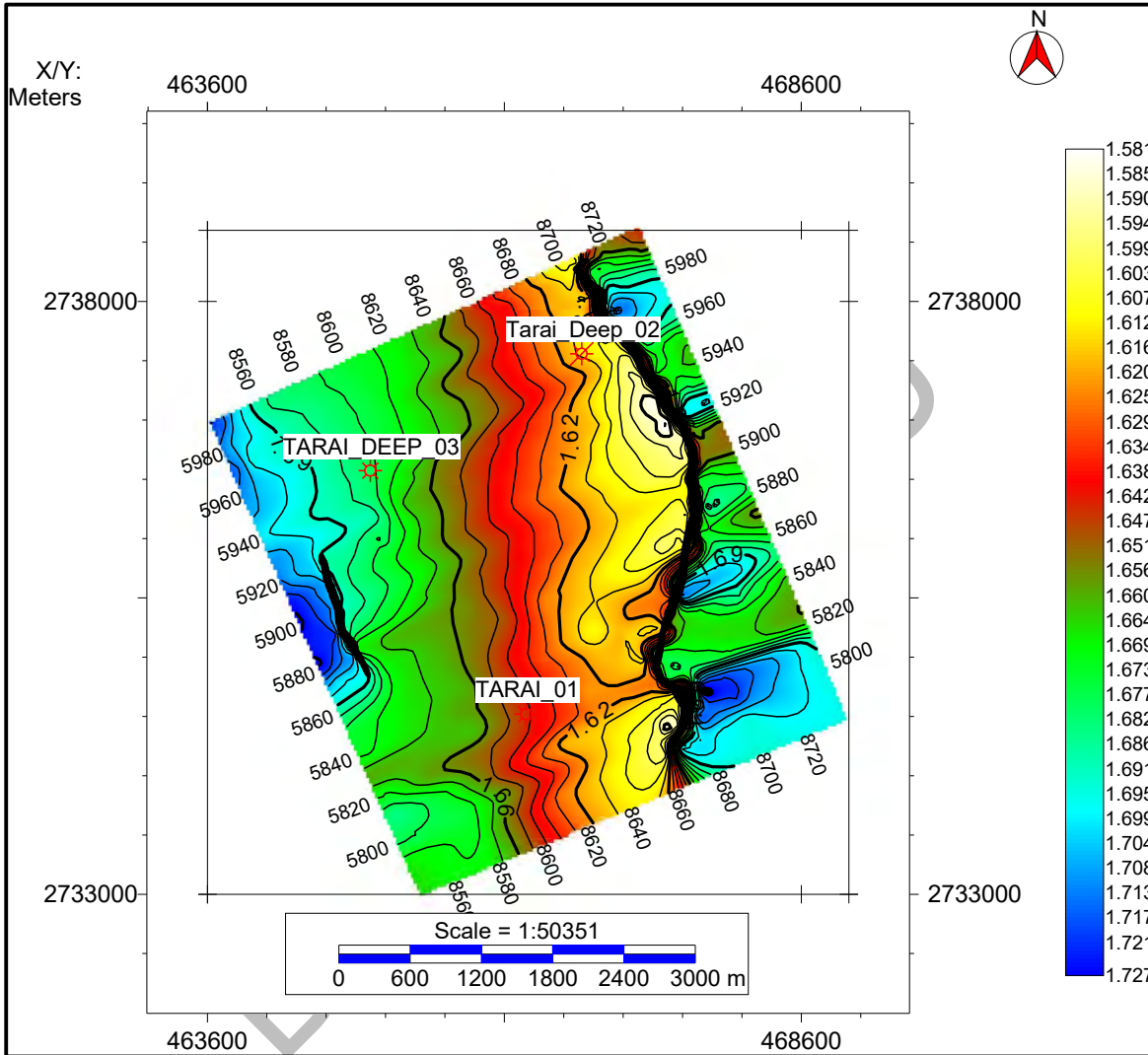


Figure 3.5 Time contour map of Sembar formation.

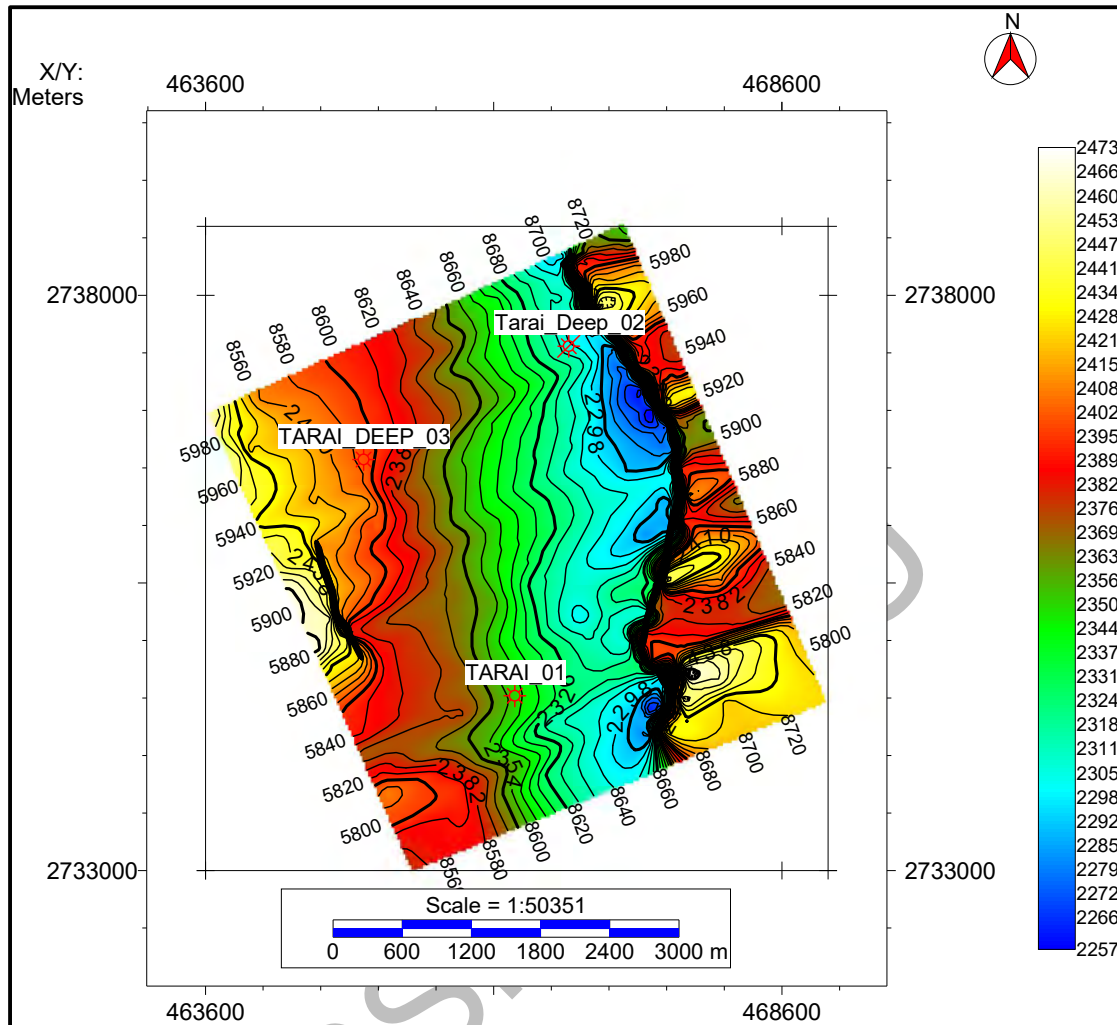


Figure 3.6 A map showing the depth contours of the Sembar geological formation.

Sembar horizon map the top of the Sembar formation, the map illustrates the pattern of the formation as shown by the Figure 3.5, and 3.6 respectively.

### 3.5. Contour Maps of Chiltan Formation

Chiltan is the main zone of interest of the study area from the hydrocarbon exploration point of view. Time and depth contour maps of the Chiltan formation are used to understand the structural trap present in the reservoir.

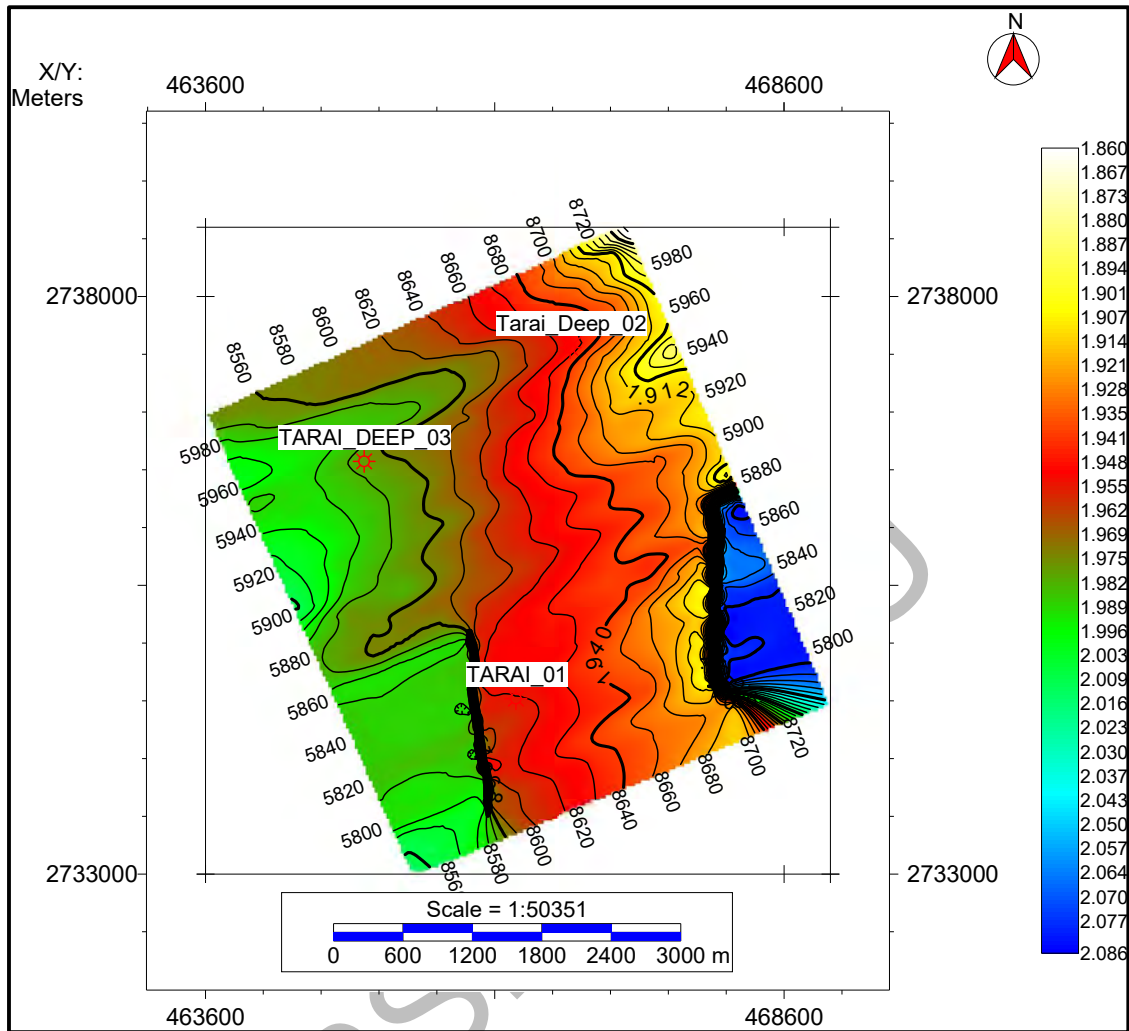


Figure 3.7 Time contour map of Chiltan formation

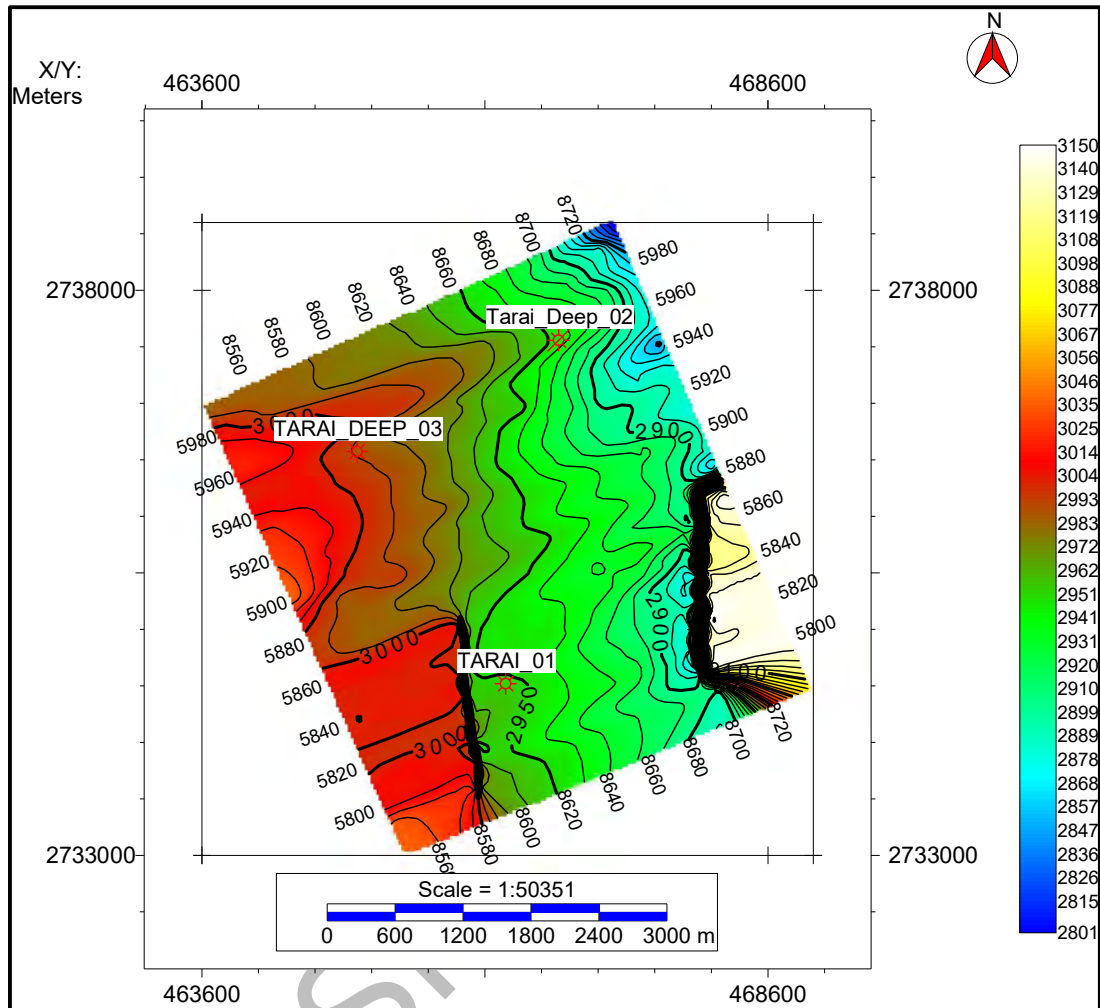


Figure 3.8 Depth contour map of Chiltan formation.

Chiltan marks the base of the Sembar formation, the map also displays areas of high and low values, which can reveal patterns of the formation. The map may show places with a high value of the Chiltan formation as illustrated in the Figure 3.7, and 3.8

## CHAPTER 4

### 4.1 SOURCE ROCK CHARACTERIZATION

When it comes to petroleum play, shale deposits and lime mudstones that contain significant quantities of organic material are regarded as source rocks. On the other hand, sandstone and carbonates are often referred to as reservoir rocks. There is also the possibility of discovering less than one percent of organic material in rocks that are not sources (Passey et al., 1990). In today's environment, one of the challenges that geophysicists are attempting to overcome is the diagnosis and quantitative evaluation of the many resources that may be available. Shales that have a significant potential for organic content are often the first focus for estimates, despite the fact that this presents a challenge because of the scarcity of economical and timely information (Bowman, 2010). Shale typically has a composition consisting of minerals such as feldspar, iron oxide, and calcite, 30% clay minerals, and a favorable proportion of quartz. Shale also contains a negligible amount of organic material (Blyth and Freitas 2017).

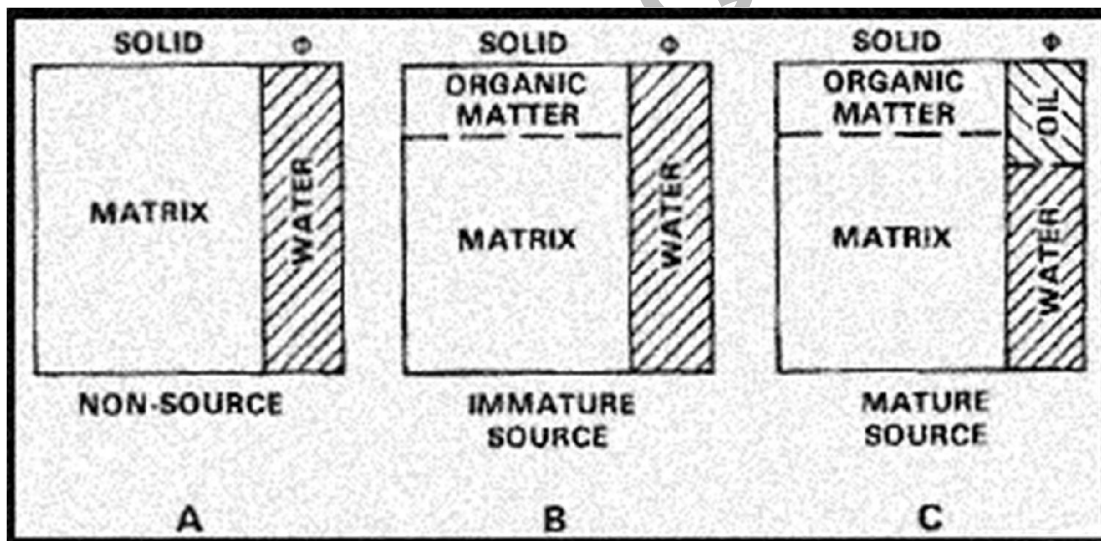


Figure 4.1 A graphical representation of the source rock and the non-source rock in its configured state (Passey et al., 1990).

### 4.2 Methodology

Shale gas is a self-developed and self-gathered deposit, in contrast to the non-source rocks, which are used as a comparison. A source rock may carry either absorbed gas or free gas, and this is determined by the quantity of TOC that is now present (Holmes et al., 2011).

The objective formation for the evaluation of organic content was the Sembar formation of the Tarai Deep 2 well. In this thesis, a number of techniques were used to conduct a study of the



hydrocarbon perspective using the wireline logs that were recorded at the well. The goal was to determine the amount of total organic carbon present. In order to generate TOC logs, the Passey LogR technique makes use of either the density log, the NPHI log, or the sonic log in conjunction with the LLD log. The approach is used by superimposing any of the three logs on top of the resistivity curve (LLD) after it has been appropriately scaled (Passey et al., 1990). Schmoker developed yet another method for locating TOC, and he did so by making use of the density log in order to locate the TOC estimations. To determine total organic carbon, Schwarzkopf arrived at an equation by first postulating a number of assumptions (Schwarzkopf, 1992).

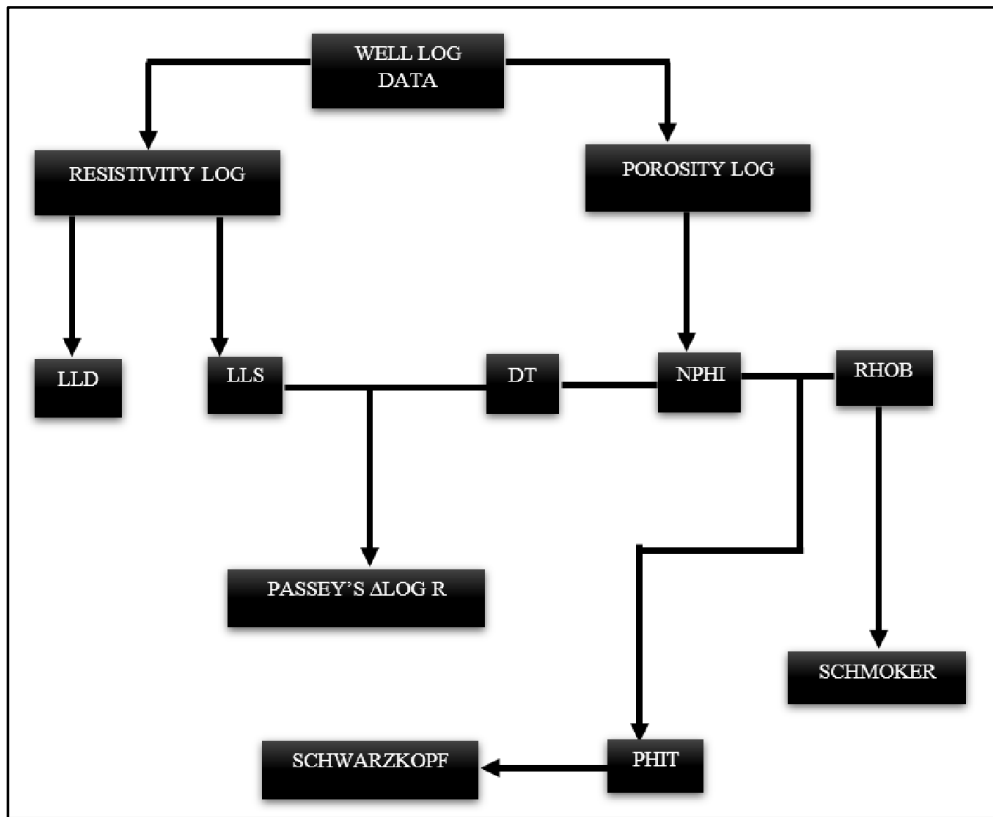


Figure 4.2 Workflow for calculating TOC logs using different techniques.

### 4.3 Total Organic Carbon (TOC)

The amount of total organic carbon is expressed as a percentage of the total weight (in wt.%). Shale gas evaluation is performed based on the total organic carbon content, which has a direct effect on the planning of hydraulic fracturing (Sondergeld et al., 2010; Passey et al., 2010). The presence of organic materials is often abundant in rocks with high TOC levels. A formation

is deemed mature when its TOC value is between 2 and 10%, and as a result, there is interest in the rock in regard to unconventional sources. When the total organic carbon values of rock are less than 2%, there is insufficient organic matter present for the formation of any potentially interesting zone. To be termed an immature rock, a rock must have TOC values that are higher than 10%. A suitable scale for determining TOC levels and potential is shown in Table 4.1. (Passey et al., 1990; Passey et al., 2010).

Table 4.1 According to Alexander et al., 2011, the following table presents a source rock's ability to contain organic matter as assessed by the total organic carbon (wt.%) values of the rock.

Total Organic Carbon (wt. %)	Resource Potential
<0.5	Very Poor
0.5-1	Poor
1-2	Fair
2-4	Good
4-10	Very Good
>10	Immature

#### 4.4 Kerogen Type

Kerogen is the name given to a certain class of chemical compounds that may be present in organic materials. When a source rock that has a sufficient amount of kerogen is subjected to the appropriate temperature and pressure, hydrocarbons are produced (Selley, 1985). The kind and amount of kerogen present in rocks are what determine their status as source rocks. According to the ingredients, kerogen may be broken down into four distinct forms (Tissot and Welte, 1984).

Table 4.2 The potential of a source rock to contain organic matter, as determined by its TOC (wt. %) values, according to Alexander et al., 2011.

<b>Kerogen Type</b>	<b>Nature of Kerogen</b>	<b>Constituents</b>	<b>H-C ratio</b>	<b>O-C ratio</b>	<b>Petroleum Type</b>
<b>I</b>	Sapropelic	Lake, Algae	1.65	0.06	Oil Prone
<b>II</b>	Liptinic	Marine Algae, Pollen & Spores	1.28	0.1	Both Oil & Gas
<b>III</b>	Humic	Terrestrial Organic Materials like Plants & Woods	0.84	0.13-0.2	Gas Prone
<b>IV</b>	Inert	Organic debris & highly oxidized materials	....	...	No Hydrocarbons

#### 4.5 Vitrinite Reflectance

Vitrinite reflectance ( $R_o$ ) is an important factor to consider when determining the degree of organic metamorphism (McCartney and Teichmuller, 1972; Shibaoka et al., 1973). The ratio of  $R_o$  to a rock's age is proportionate.

Table 4.3 Classifying different values of  $R_o$  based on the type of hydrocarbon.

<b>(<math>R_o</math>%)</b>	<b>Hydrocarbon type</b>
<b>&lt;0.5</b>	Immature
<b>0.5-1.5</b>	Oil Window
<b>1.26-2.6</b>	Gas Window
<b>2-3</b>	Dry Gas
<b>3</b>	Over Cooked

The equation 4.1 was used in order to calculate the formation temp for the sembar in the Tarai deep-02 well.

$$FT = \frac{BHT-ST}{TD} * FD \quad (4.1)$$

Where,

FT is formation Temperature.

BHT is Bottom Hole Temperature.

ST is Surface Temperature.

TD is Total Depth.

FD is Formation Depth.

The graphical technique was used to figure out the Vitrinite Reflectance for the Sembar using this Formation Temperature as a reference.

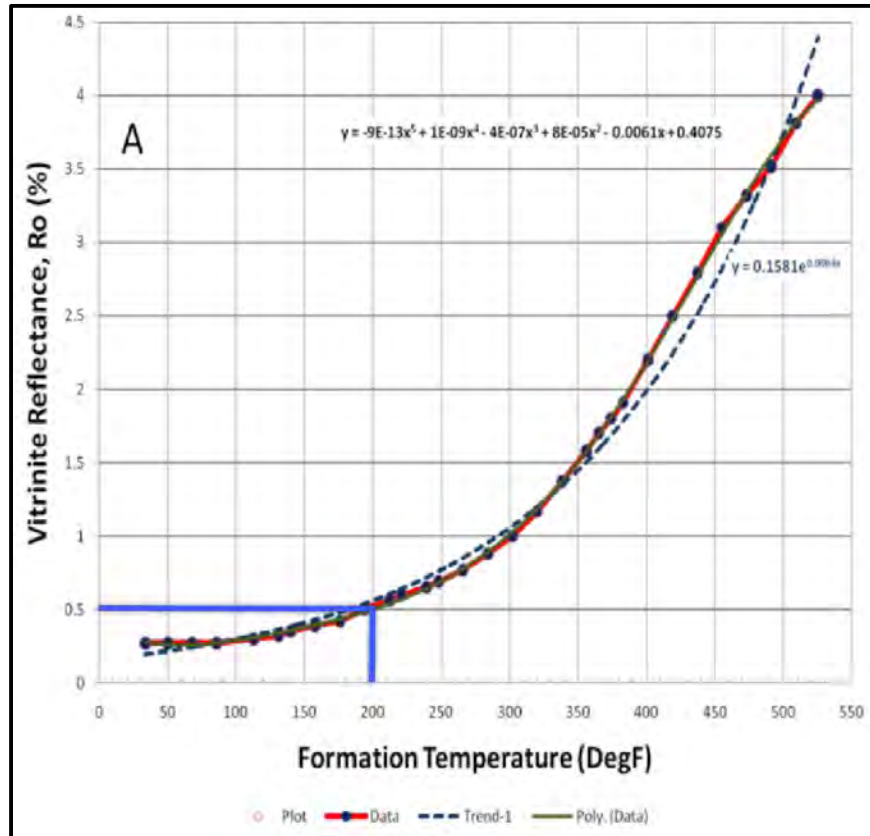


Figure 4.3 Modifying the formation temperature and Ro model following the work of Hill et al., 2007.

It was determined that the vitrinite reflectance for the Sembar in the Tarai Deep -02 well was 0.56.

#### 4.6 Level of Maturity (LOM):

The Level of Metamorphism (LOM) is a key aspect of geology that describes the degree of alteration that a rock has undergone due to high temperature and pressure. The process of metamorphism can change the texture, mineralogy, and chemical composition of a rock, and the LOM is used to quantify these changes. It is commonly determined by analyzing the rank of coal

found in the rock. Coal rank is a measure of the maturity of the original organic matter and is determined by the amount of carbon, volatile matter, and ash content.

There are several methods for determining the LOM, one of which is the graphical method. The graphical method plots the Vitrinite Reflectance values of a specific rock against the corresponding LOM values. Vitrinite Reflectance is a measure of the degree of coalification of the organic matter in the rock and is often used as a proxy for the LOM. The plot of these values forms a curve that can be used to estimate the LOM of a specific rock.

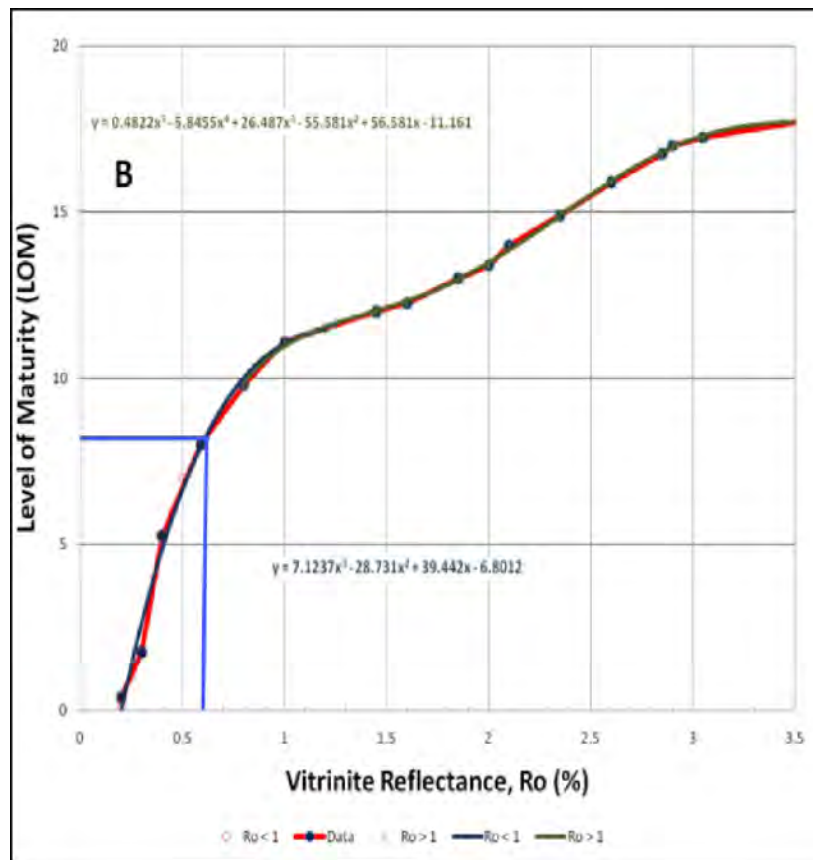


Figure 4.4 Modifications made to the temperature, LOM and RO Model after (Alyousuf et al., 2011).

In the Sembar formation of the Tarai deep 2 well, the LOM value was found to be between 8 and 9 using the graphical method. This means that the rock in this formation has undergone a moderate degree of metamorphism.

As the source rock matures, its carbon-based content is converted into gaseous or liquid hydrocarbon and replaces the formation of water. This process is known as maturation and is a key aspect of petroleum geology. The conversion of organic matter into hydrocarbons is accompanied by changes in the physical and chemical properties of the rock. These changes can be observed in

well logs, which are used to measure various physical properties of the rock such as resistivity, density, and porosity.

The log response of a source rock is different from that of a non-source rock, due to the presence of hydrocarbons. For example, source rocks typically have higher resistivity and lower porosity than non-source rocks, which can be used to identify them in subsurface studies. The LOM is an important factor that helps to identify and evaluate the potential of source rocks for hydrocarbon generation.

#### **4.7 Well Log Response in Tarai Deep-02**

As source rocks mature, a significant portion of the carbon-based content (organic matter) is transformed into gaseous or liquid hydrocarbon through the process of thermal maturity. This hydrocarbon fills the pore spaces within the rock, replacing the formation water, as shown in figure 3.1 (Passey et al., 1990). This process leads to a change in the conductivity of logs in source rocks in comparison to non-source rocks. The change in conductivity is due to the substitution of the formation of water with hydrocarbon in the pore spaces. As a result, the log response in a source rock is different from that in a non-source rock. These variations in log responses can be used to identify source rocks, and to determine their level of thermal maturity. A brief overview of each log in a source rock, and how it is affected by the process of maturation, is provided below.

##### **4.7.1 Gamma Ray Log**

The natural gamma radiation emitted by organic-rich formations can be measured using a tool called the Gamma Ray Log (GR log). High gamma-ray intensity intervals are often associated with facies that are rich in organic matter. This is because there is a correlation between uranium and organic matter, and this relationship has led to an increase in the use of gamma-ray spectral tools (Swanson, 1960).

GR logs measure the gamma radiation emitted by the rock formation and show high values when there is a high concentration of uranium in the formation. This is typically found in marine sediments, which contain high amounts of organic matter that can absorb the uranium. The presence of uranium in these sediments can be an indicator of the potential for hydrocarbon generation. A gamma ray log is a standard tool in the petroleum industry for identifying and evaluating the potential of source rocks.

It is important to note that the GR logs can be affected by other natural radioactive elements present in the rock formation, such as potassium and thorium, so it is important to use it in conjunction with other logs, such as resistivity logs, to accurately identify potential hydrocarbon-bearing formations.

#### **4.7.2 Sonic Log:**

The Sonic log is a tool used to measure the acoustic transit time of a formation. The method operates by transmitting an auditory pulse across the formation and measuring the amount of time required for the pulse to finish its path through the structure. The transit time and the primary ( $V_p$ ) and secondary ( $V_s$ ) velocities of the rock are inversely related, which means that as the transit time increases, the velocities decrease. The velocities can be calculated from the Sonic log data, which is useful for characterizing the rock formation.

The Sonic log is particularly useful for identifying organic-rich formations such as shale because the presence of organic material like hydrocarbons in the formation can cause the primary velocity to be low and the transit time to be high. This is because the organic material slows down the acoustic pulse as it travels through the rock. The total organic carbon (TOC) content also influences the response of Shear wave velocity, which can also be measured using the Sonic log.

The Sonic log is often used in combination with other logs, such as the resistivity log, to improve the accuracy of the measurements and to provide a better estimate of the TOC content of the formation. This is because the Sonic log measures the velocity of the rock, while the resistivity log measures the electrical properties of the rock. By combining the information from both logs, geologists can get a more complete picture of the rock formation and identify potential hydrocarbon-bearing formations more accurately.

#### **4.7.3 Neutron Log**

The neutron log is a tool used to measure the density of a rock formation. It works by sending neutrons into the rock and measuring the number of neutrons that are scattered or absorbed by the rock. The neutron log readings are high in shale formations because the low density of the organic matter in shale, compared to other rocks, causes the hydrogen content in shale to be relatively higher. This results in a higher neutron scattering signal, which is interpreted as high porosity.

However, it is important to note that the neutron log is not a reliable estimator of rock properties when used on its own. In the case of organic-rich intervals, the neutron log can indicate high porosity, but it is not a definitive indicator of hydrocarbon presence or volume.

To accurately estimate the volume of gas in shale gas reserves, geologists use a grouping of density and NPHI logs. The density log calculates the bulk density of the rock, while the neutron log calculates the hydrogen index, which is associated with porosity of the formation. Together, these two logs provide a more accurate estimate of the gas volume in the shale formation. However, this approach is only applicable in the absence of clay-rich formations, as clay minerals can affect the readings of the density and neutron logs.

#### **4.7.4 Density Log**

The density log is a tool used to calculate the bulk density. It works by sending an electromagnetic pulse into the rock and measuring the time to travel through the rock. The density of the rock can then be calculated from the transit time of the pulse.

The density log is particularly useful for identifying organic-rich formations, such as shale because the presence of HC in the rock can cause the density of the rock to be low. Organic-rich intervals in the formation will have a lower trend in the density log reading. Additionally, formations with a high amount of clay minerals have a normal density value of about 2.7 g/cm<sup>3</sup>, which is considered normal. However, a low-density value is typically an indication of organic-rich shale.

The density log can be used in combination with other logs, such as the resistivity log, to improve the accuracy of the measurements and to provide a better estimate of the rock properties. The resistivity log measures the electrical properties of the rock, while the density log measures the bulk density of the rock. By combining the information from both logs, geologists can get a more complete picture of the rock formation and identify potential hydrocarbon-bearing formations more accurately.

#### **4.7.5 Resistivity Log**

Source rocks, such as shale, are often laminated and have anisotropic properties. This means that their electrical and mechanical properties vary depending on the orientation of the rock layers. To measure these properties, geologists use spherically focused logs, which can provide a more accurate picture of the rock formation.



As source rocks mature, the organic matter in the rock increases in resistivity. This is because as the rock matures, the organic matter in the rock is converted into hydrocarbons, which have a higher resistivity than the surrounding rock. Additionally, voids and fractures in the rock can contain free oil, which also contributes to the overall increase in resistivity.

Because of this relationship between resistivity and source rock maturity, resistivity logs are often used as a maturity indicator. They can provide an estimate of how mature a source rock is, and how much hydrocarbon has been generated from the rock.

To get a more complete picture of the source rock, geologists often use a combine porosity logs, with LLD logs. This allows them to estimate the total amount of hydrocarbon present in the rock, as well as the porosity and other rock properties that can affect hydrocarbon production. In Tarai deep well, well log response gives a good insight of the source rock properties.

#### **4.8 TOC calculation from wireline logging**

A source rock, such as shale, typically has a high gamma ray, high neutron porosity, high resistivity, and low-density log values. These properties are commonly used by geologists to identify source rocks and estimate their hydrocarbon potential.

One way to estimate the total organic carbon (TOC) content of source rock is by using the combination of these log values. For example, high gamma ray and high neutron porosity values may indicate a high concentration of organic matter in the rock, which is positively correlated with TOC. Similarly, increase in resistivity values can also indicate a higher concentration of HC in the rock, which is also positively correlated with TOC. Low-density log values may also indicate the presence of organic matter in the rock.

Another method to estimate TOC is by using the ratio of resistivity log values of the source rock to non-source rock. As the source rock matures, the resistivity of the rock increases due to the conversion of organic matter into hydrocarbons. This increase in resistivity can be used to estimate the amount of TOC present in the rock.

Additionally, there are other methods such as Rock-Eval pyrolysis, where an organic-rich sample is heated in controlled conditions and the generated gases are analyzed to estimate the TOC. Or some other methods like a TOC analyzer, where a sample is burned, and the carbon dioxide released is measured to estimate the TOC.

#### 4.8.1 Passey's Log R Method

The  $\Delta\text{LOGR}$  technique is a method that was introduced in 1979 and applied by Exxon/Esso to determine the Total Organic Carbon (TOC) logs in various wells worldwide. Despite the availability of newer methods that can directly determine TOC, the  $\Delta\text{LOGR}$  method remains effective in determining the TOC of clastic and carbonate source rocks (Passey et al., 1990). The method involves superimposing a logarithmic resistivity log on one of the three logs, namely the Neutron, RHOB, and DT log, after adjusting the scale accordingly (Passey et al., 1990). To ensure accurate results, it is recommended to use the Sonic log as the porosity log as borehole environment can affect the NPHI and Density logs (Liu et al., 2012). After that, a baseline is constructed inside a non-source patch that has a fine granularity. The method of setting the baseline is an essential stage that must be carried out by a trained professional, since the accuracy of the findings is very susceptible to variation based on the baseline that is used.

#### 4.8.2 Sonic and Resistivity overlay

The method of overlaying sonic and resistivity curves is widely used to calculate TOC (total organic carbon) values. The first step in the procedure is scaling the logs in such a way that one full logarithmic cycle of the LLD log matches to a certain interval of the acoustic log. In this specific piece of research, the scaling factor that was used was one hundred microseconds per foot, which was similar to two nonlinear resistivity phases.

The first step in the process is to determine the separation between the two curves, which is known as the  $\Delta\text{LOG R}$  curve. This curve is then used as an input within an equation to calculate the TOC curve. The scaling factor used in this study, 0.02, was determined by equating 50 microseconds per foot to 1 29 Ohm.meter, which then makes 1 microsecond per foot equal to 1/50 Ohm.meter, or 0.02 Ohm.meter.

$$\Delta\text{Log}R_{DT} = \text{Log}10\left(\frac{R}{R_{\text{Baseline}}}\right) + 0.02 \times (\Delta t + \Delta t_{\text{Baseline}}) \quad (4.2)$$

$$\text{TOC}_{DT} = \Delta\text{Log}R_{DT} \times 10^{(2.297 - 0.1688 \times \text{LOM})} \quad (4.3)$$

The  $\Delta\text{Log}R_{DT}$ , value represents the segregation between the sonic and resistivity curves, R depicts the resistivity value (LLD log values in Ohmmeter),  $R_{\text{Baseline}}$ , represents the baseline

values for the deep resistivity curve and is coherent to the transit time baseline value,  $\Delta t$ , shows the transit time values from DT4P log  $\mu\text{s}/\text{ft}$ ,  $\Delta t_{Baseline}$ . is the baseline value for time,  $TOC_{DT}$  is the organic carbon values in wt.% calculated by utilizing acoustic log, and LOM is known as level of metamorphism.

Following the establishment of a baseline, the provided values for  $R_{Baseline}$ , and  $t_{Baseline}$ , are utilised to compute the depth of the borehole. TOC values. When applied to both the Tarai-01 and Tarai deep-02 wells, the Passey  $\Delta\text{LOGR}$  method yields an average TOC of 3.58 and 3.04 wt.% and a  $R_o$  of 0.55. These results can be seen in figure 4.5, and 4.6. Overall, the overlay of sonic and resistivity curves is considered to be the best method for TOC calculation, as it allows for accurate determination of TOC values.

DRSML QAU

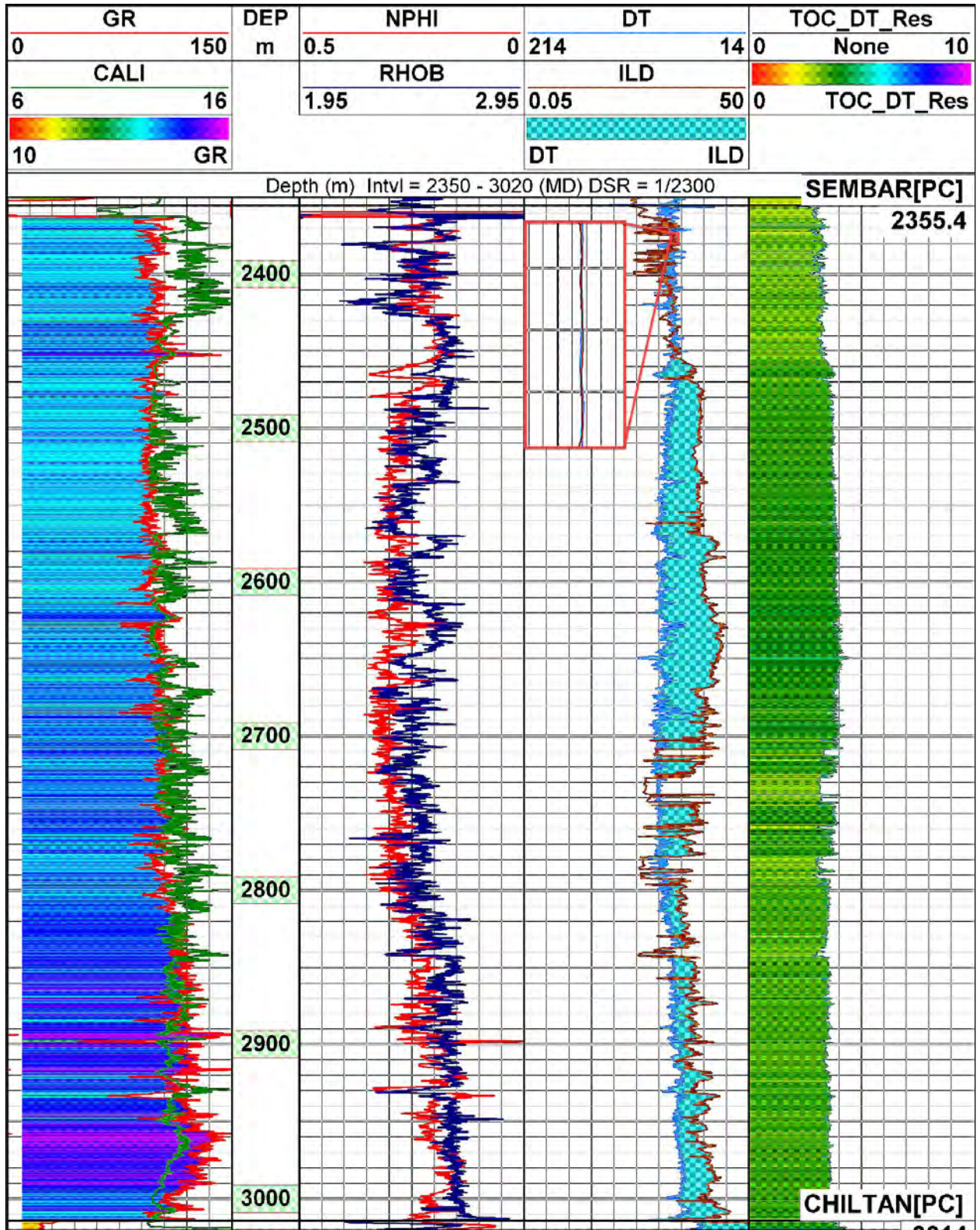


Figure 4.5 To calculate total organic carbon in the Tarai-01 well's Sembar formation, we used a DT/LLD overlay.

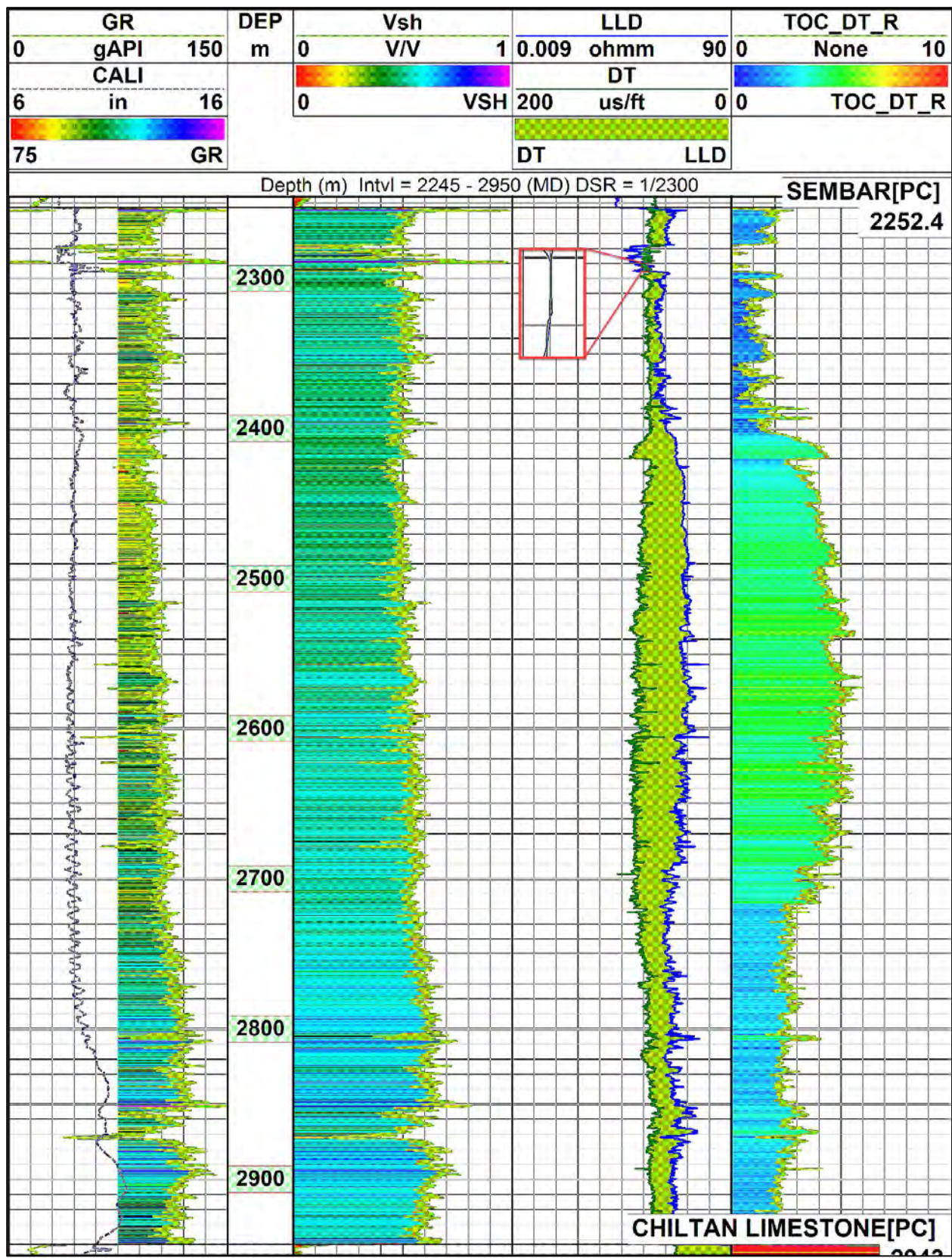


Figure 4.6 DT4P/ resistivity deep intersection for TOC approximation in Sembar formation for Tarai\_Deep\_02 well.

#### 4.8.3 Schmoker's Method:

There is a density difference between the solid organic material and the surrounding matrix because hydro carbon has a lower density than the surrounding rocks. Scientists have discovered a positive linear relationship between total organic carbon (TOC) concentrations and the inverse of RHOB values (Schmoker, 1979). This indicates that total organic carbon values rise with decreasing density of the organic material and decrease with increasing density. This relationship between TOC and density can be used to estimate TOC values in a rock formation by measuring the density of the rock and using the inverse of the density log value to calculate TOC.

$$TOC = A * \left(\frac{1}{\rho}\right) - B, \quad (4.4)$$

where A and B are constants, established by the amount of organic matter and the density, respectively. It may also be calculated by comparing the percentage of organic material to the total amount of organic carbon.  $\rho$  is the density log (RHOB). The unit of measurement is weight percentage (wt. %). The equation can be simplified as follows:

$$TOC = \left(\frac{154.497}{\rho}\right) - 57.261, \quad (4.5)$$

where,  $\rho$  is the density log.

TOC computed for Tarai - 01 and Tarai deep-02 well using the Schmoker's method is illustrated in figures 4.7 and 4.9. The average TOC calculated from Schmoker is 2.134wt%, and 4.12 wt%, respectively.

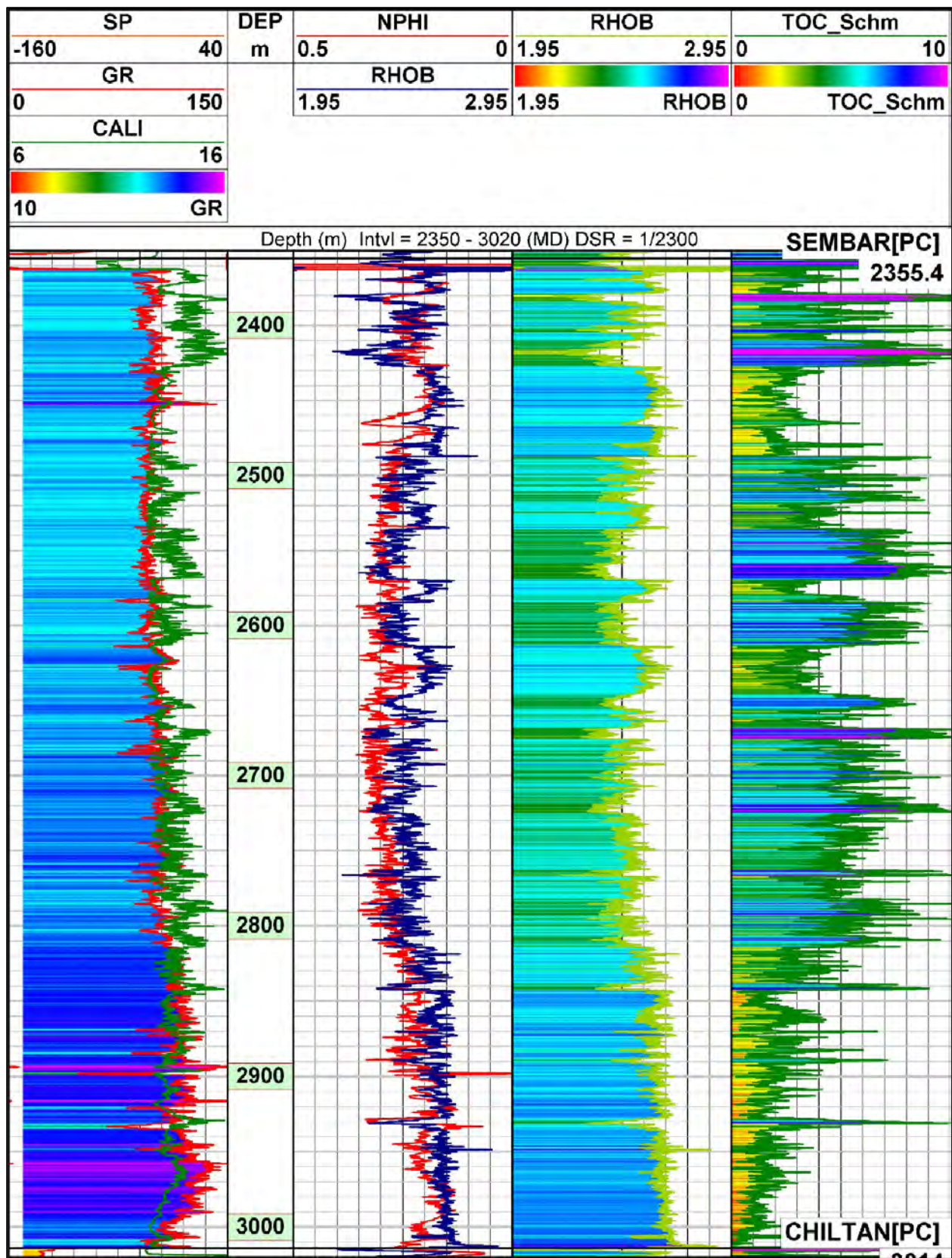


Figure 4.7 Schmoker's Scheme for calculation of TOC for Tarai-01 well.

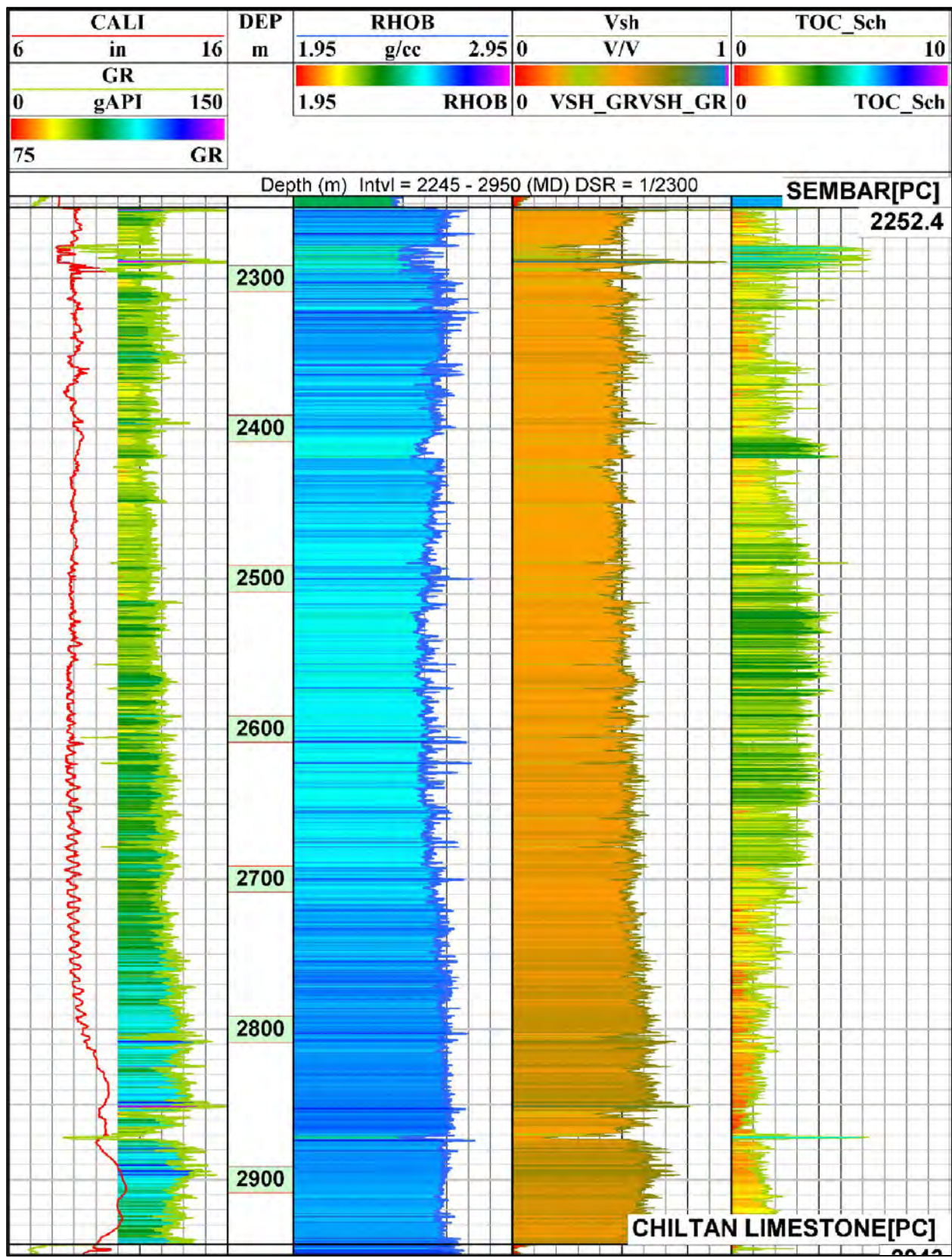


Figure 4.8 Schmoker's Method for calculation of TOC for Tarai Deep-02 well.



#### 4.8.4 Schwarzkopf's Method

Total organic content (TOC) levels estimated from log data need some guesswork and the use of assumptions. Myers and Jenkyns (1992) also calculated TOC using a similar approach. The assumptions made by Schwarzkopf (1992) include the following:

- Non-source rock has a lower organic content trend.
- In terms of porosity and density, the source and non-source intervals are identical.

Instead of using a density log, a sonic log can also be used to estimate TOC in a similar way within a source rock. In contrast to the density log, the selectivity of the acoustic transit time is quite low (Schwarzkopf, 1992). The acoustic log is more sensitive to changes in porosity and lithology type than the RHOB log (Myers and Nederlof, 1984).

Schwarzkopf's approach calculates TOC by comparing the characteristics of source rock and reservoir rock and basing the estimate on the difference. The porosity log is the primary log utilised in this process.

$$porosity = \frac{\rho_{ma} - \rho_{ns}}{\rho_{ma} - \rho_{fl}} \quad (4.6)$$

$$\phi_{ker} = \frac{\rho_s - \rho_{ns}}{\rho_{ker} - \rho_{ma}} \quad (4.7)$$

$$TOC = \frac{0.85 \times \rho_{ker} \times \phi_{ker}}{\rho_{ker} \times \phi_{ker} + \rho_{ma} (1 - porosity - \phi_{ker})} \quad (4.8)$$

where, porosity is water filled porosity value,  $\rho_{ns}$  is density for non-source patch (averaged value of log) in  $g/cc$ ,  $\rho_s$  is source interval density in  $g/cc$ ,  $\rho_{ma} = 2.7 g/cc$ , supposed density of mud-rock,  $\rho_{fl}$  equals Average aquatic density,  $\phi_{ker}$  is pore volume for kerogen packed rock,  $TOC$  is TOC computed in weight percentage.

The organic carbon (TOC) content of a source rock may be estimated using either a density log or a sonic log. The only catch is that the sonic travel time is less sensitive than the density log (Schwarzkopf, 1992). Besides this issue, the acoustic log is more influenced by porosity and lithology type than the density log (Myers and Nederlof, 1984). Figures 4.9 and 4.10 depict the results obtained using the same methods on the Tarai- 01 and Tarai Deep-02 well. The total organic carbon (TOC) in Tarai 1 was determined to be 3.25, and in Tarai deep-02, it was found to be 2.02 correspondingly.

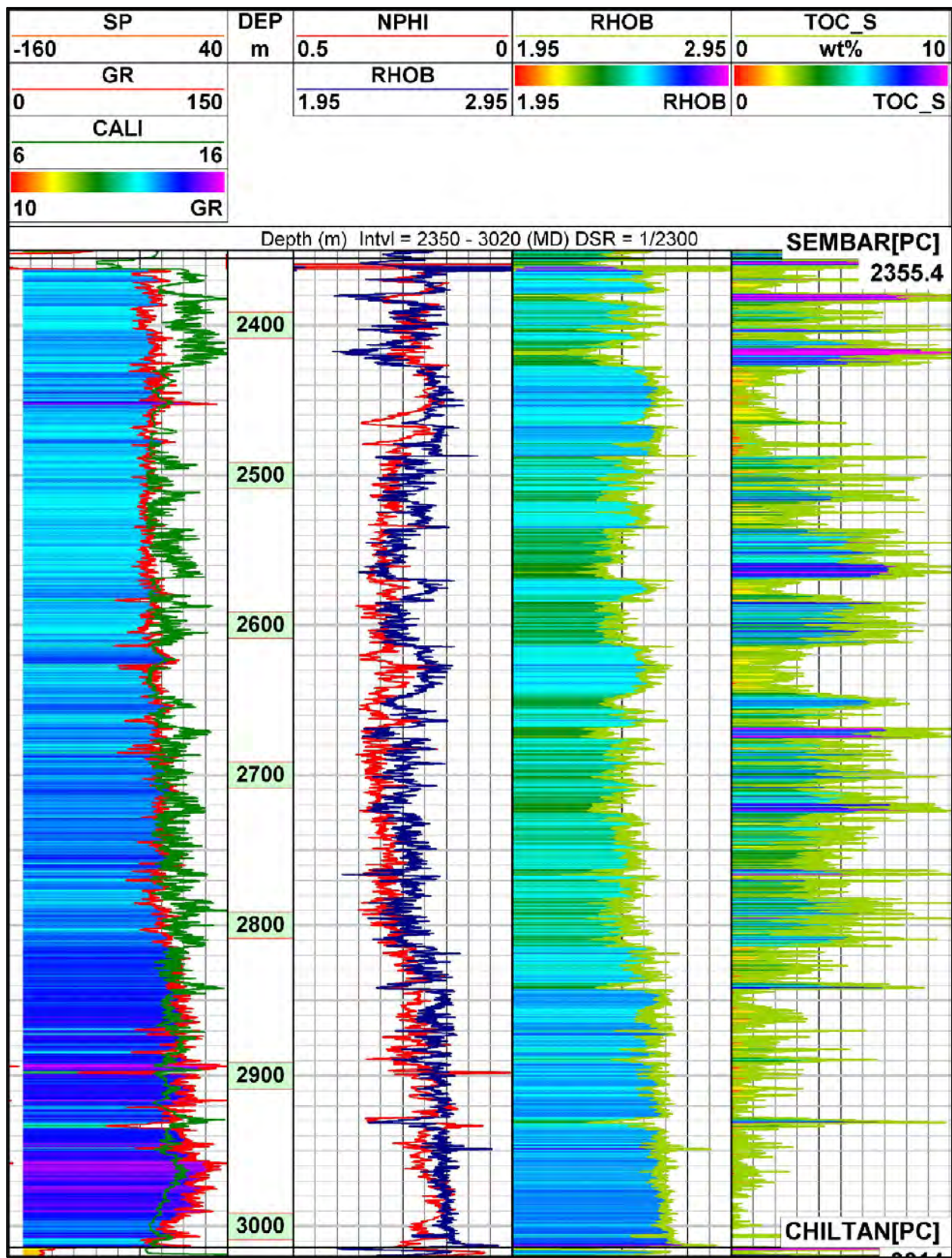


Figure 4.9 The Tarai-01 well's TOC was estimated using the Schwarzkopf process.

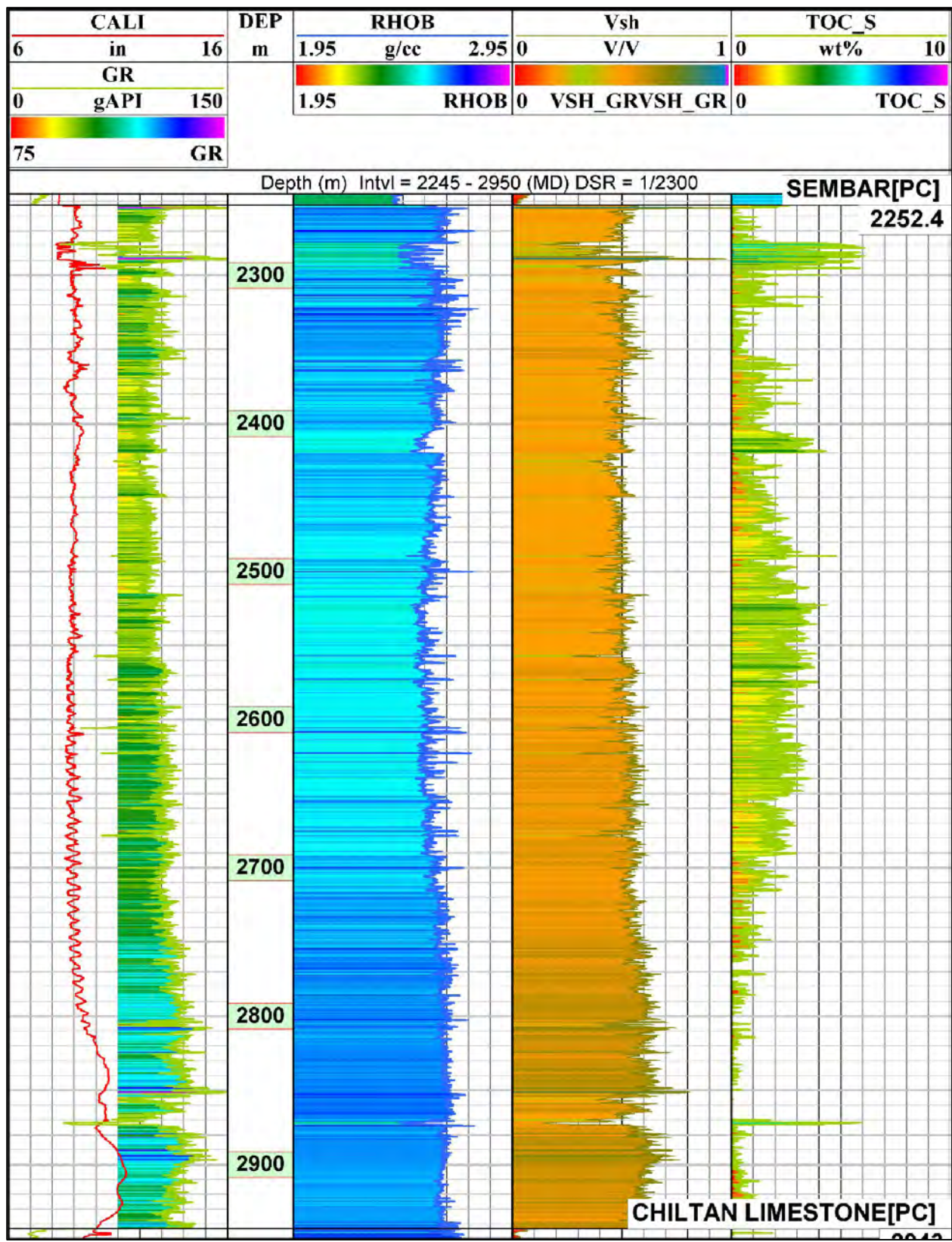


Figure 4.10 Schwarzkopf method for estimation of TOC for Tarai Deep-02 well.

Table 4.4 Results for Tarai-01 and Tarai deep-02's mean TOC as measured by various techniques.

Well Name	PASSEY's METHOD	SCHMOKER METHOD	SCHWARZKOPF METHOD	Ro. (%)
Tarai-01	3.58	4.12	3.25	0.55
Tarai deep-02	3.04	2.13	2.02	0.55

DRSML QAU

## CHAPTER 05

### Shear Velocity Estimation and Rock Physics Modelling for Shales

#### 5.1 Introduction:

Nowadays, Shale gas is a substantial energy source, accounting for almost half of all unconventional gas resources. Shale gas exploration and development are in the exploratory stage because of severe geological conditions, significant heterogeneity, and deep reservoir burials. Thus, geophysical reservoir characterization and fluid detection are crucial for shale gas deposits. Geochemically, Shale is the most prevalent lithology in sedimentary basins (Sondergeld, 2010). As the source and reservoir rock, organic shales exhibit a high degree of anisotropy. Shales have a complex mineralogy, fabric, and organic content, resulting in strong anisotropy. It comprises clay minerals, calcite, feldspar, silts, pyrites and quartz (Guo et al., 2012; Zhu et al., 2012). The kerogen volume proportion within a composite solid, and the form and orientation of pores and fissures all affect the composite solid's effective elastic properties. Clay minerals produce connected phases, while other minerals such as quartz form isolated inclusions, indicating a disconnected phase even at high concentrations, providing a relatively minor contribution to the elastic properties of composite formation. Shale anisotropy is determined by the alignment of clay particles (Homby et al., 1994). The major parameters affected by the organic matter are velocity, density and resistivity of rock in order to characterize shale gas. Due to the low permeability of organic rich shales, hydraulic fracturing is required. Natural stress fractures can also cause anisotropy and affect hydraulic fracturing modelling (Curtis, 2002).

Recent attention has been focused on shales due to kerogen effect concentrations on seismic response and elastic attributes (Zhu et al., 2012). Rock physics modelling establishes a relationship between physical parameters (seismic velocities, elastic moduli etc) and reservoir properties (porosity, saturation, pressure etc), It is used as the foundation for hydrocarbon prediction and the identification of hydrocarbons via the use of seismic data. Various hypotheses about shale deposits have been evolved up to this point. An anisotropic RPM specifically designed for organic-rich shale was developed by Wu et al. (2012). combining kerogen along with some other minerals to derive effective characteristics of the rock. Zhu et al. (2012) calculate the elastic properties of organic content taken as inclusion space, which is compatible with well-log data. Bandyopadhyay et al., (2012) evaluate uncertainties associated with rock properties inversion

of organic shale using Zhu's rock physics model. Zhang et al., (2017) construct an anisotropic rock property model (RPM) for shale rocks by conducting analyses on their development as anisotropic, shale particles and matrix, pores, fractures, and filled pores and cracks. Here, the RPM developed primarily focused on the organic matter effect incorporating multiminerals, porosity, properties of the fluid, and overlooking the comprehensive properties of shale minerals, organic matter, matrix pores, and fluids based on assumptions of (Pan et al., 2020).

After rock physics modelling for predicting well logs, the uncertainty analysis was done using Monte Carlo simulation. The main objective of these simulations is to ensure that the rock physics model reproduces the log data variability. Although rock physics models provide deterministic correlations between input and output parameters such as  $V_p$ , Monte Carlo analysis assigns uncertainties to each variable and predicts the output respectively. As a result, probabilistic models are generated signifying the shale distribution. These simulations can also be used to predict the production effects on the elastic attribute.

The reflection coefficient modelling has been performed after anisotropic rock physics analysis. It is the most efficient approach to characterize a reservoir. AVO analysis helps to obtain subsurface rock characteristics from surface seismic data, which is used to estimate lithology, porosity, and fluid saturation. Anisotropy in shales has a substantial impact on AVO analysis (Tsvankin et al., 2010; Blangy, 1994; Mallick, 2001).

## 5.2 Multilinear regression:

Multilinear regression is a statistical method used to characterise the association between a dependent variable and multiple independent variables. The dependent variable is predicted as a linear combination of independent variables. It is an effective instrument for comprehending the relationship between variables and predicting future outcomes. The general form of a multi-linear regression model can be written as:

$$y = b_0 + b_1x_1 + b_2x_2 + \dots + b_n * x_n + e$$

where  $y$  is the dependent variable,  $x_1$  through  $x_n$  are the independent variables,  $b_0$  through  $b_n$  are the coefficients of the independent variables, and  $e$  is the error term.

The coefficients  $b_0$  through  $b_n$  represent the change in  $y$  for a one-unit change in each independent variable, holding all other variables constant. In other words, they represent the slope of the regression line for each independent variable.

The goal of multi-linear regression is to estimate the values of the coefficient that best fit the observed data. This is typically done using a method called least squares, which minimizes the sum of the squared differences between the observed values of  $y$  and the predicted values of  $y$ .

Once the model is estimated, it can be used to make predictions about the value of the dependent variable for new values of the independent variables.

In our particular instance, we have estimated the link between well data and shear wave by using multiple well log data from the well that is geographically closest to us. The equation that we have developed based on the observed data is as follows:

$$S.S = -0.0502 * GR - 1.945 * \rho - 15.54 * \log_{10}(R_D) + 0.605 * \log(R_{MSH}) + 0.014(CALI) - 0.055 * SP - 0.7 * PE + 10.1 * \log_{10}(R_{LLS}) + 1.92 * CS + 6.322 \quad (5.1)$$

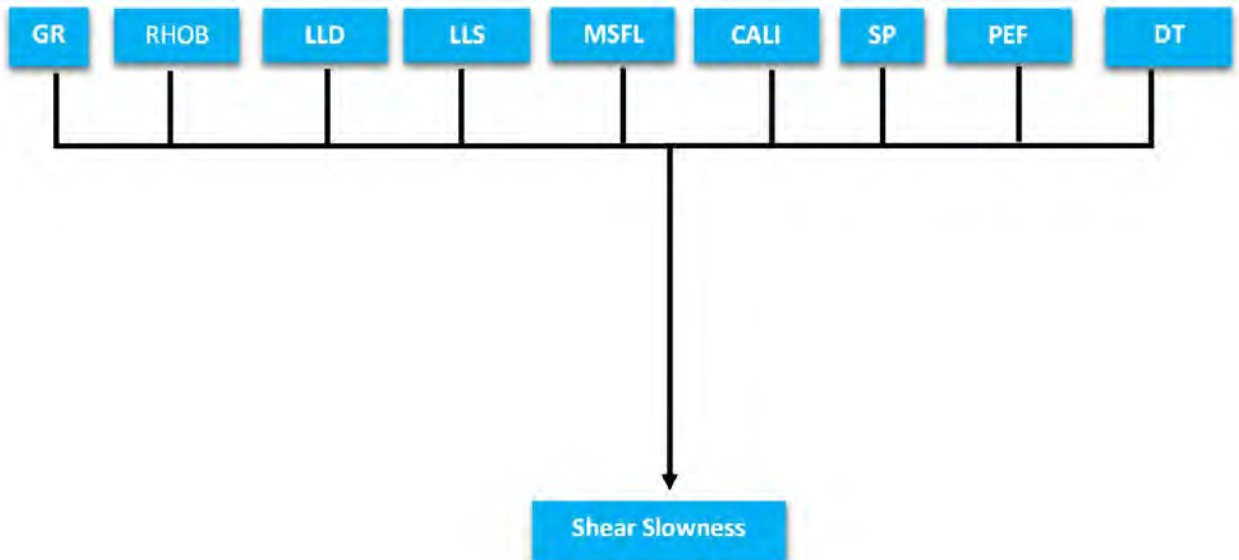


Figure 5.1 Logs used for shear wave calculation

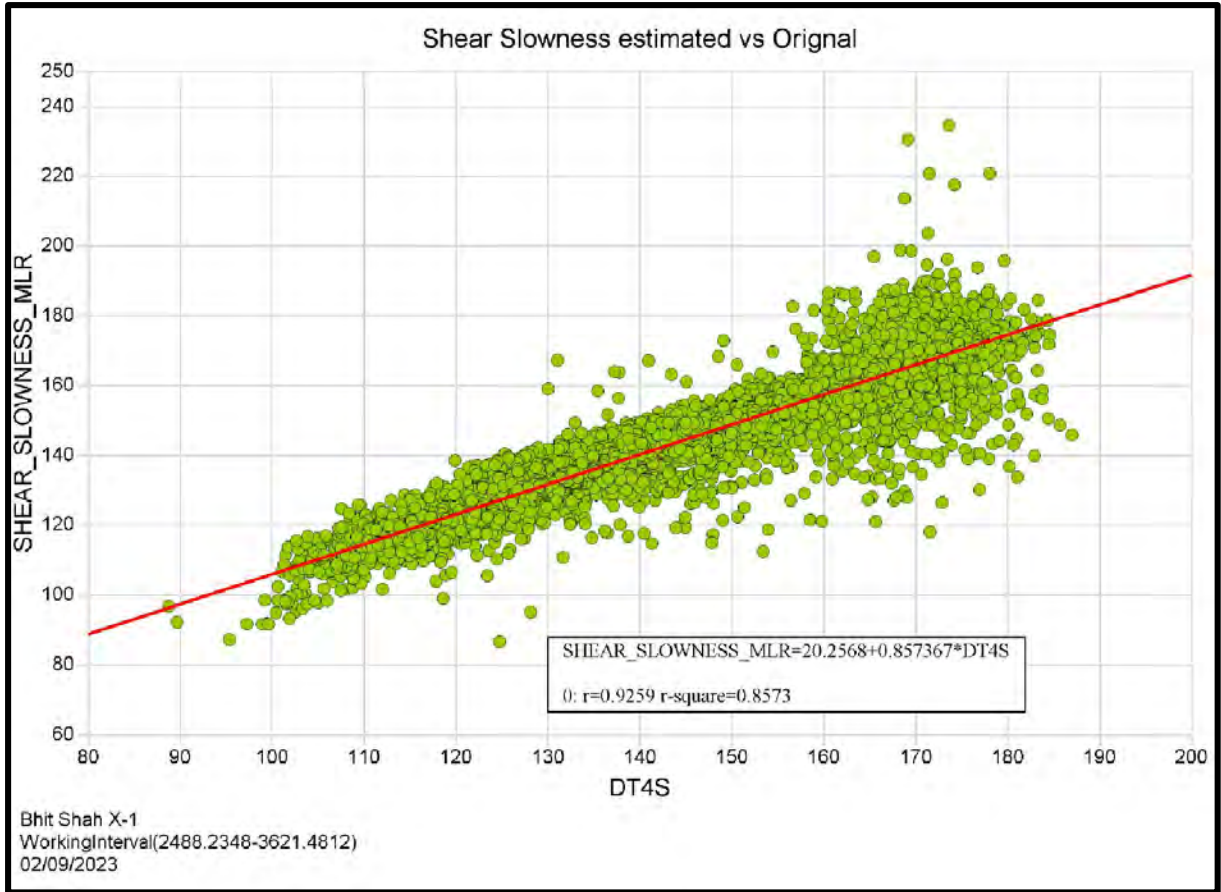


Figure 5.2 Relationship between estimated and original shear slowness

Figure 5.2 depicts the 92% correlation between the original and calculated shear waves calculated using equation (5.1). Logs that were utilized for determining the relation 5.1 are shown in figure 5.1.

### 5.3 The development of the Shale RPM:

It is critical to developing an efficient rock physics model for shale rock characterization. This research emphasizes the elastic rock physics modelling of Patala shale in the Potwar basin along with the uncertainty analysis using Monte Carlo simulation. A workflow is proposed using effective modelling for different shale rock compositions taking into account the matrix, kerogen, fluids, pores etc. The primary objective of this modelling technique is to predict and remodel effective attributes such as density, velocities, and moduli after incorporating significant minerals. This is quite useful in a variety of exploration and production settings to recognize the behaviour of shale rock.



#### 5.4 Voigt-Reuss-Hill (VRH) average:

The first thing that has to be done in order to create a model is to find out the characteristics of the mineral. To build an effective mineralogy, it is better to apply boundaries and averages to account for the fact that the grain arrangement is uncertain. In the quest of estimating the effective moduli of minerals, a simplistic approach to calculate the average of V-R bounds is referred to as the V-RH average.

$$M_{VRH} = \frac{M_V + M_R}{2} \quad (5.2)$$

#### 5.5 SCA model:

Hill, (1965) suggested the SCA model. This model takes into account the pore geometry and interaction of inclusions adjacent to each other so it can be used for rocks with slightly larger inclusion concentrations. Berryman, (1995) defines the SCA for N-phase composites in a general manner given in equations. This technique is used to incorporate complex components and fluid-filled pores with variable geometries into the elastic characteristics of rocks.

$$\sum_{i=1}^n x_i (K_i - K'_{sc}) \beta'^i \quad (5.3)$$

$$\sum_{i=1}^n x_i (\mu_i - \mu'_{sc}) \zeta'^i \quad (5.4)$$

Here,  $i$  denotes the  $i$ th substance,  $x_i$ , is aggregate fraction  $\mu_i$ , and  $K_i$ , are shear, and bulk moduli.  $\beta'_i$  and  $\zeta'_i$  are geometric factors of inclusions.  $\beta'_i$  and  $\zeta'_i$  can be defined in terms of  $K_m$ , and  $\mu_m$  i.e bulk and shear modulus of matrix.

$$\beta'^i = \frac{K_m + \frac{4}{3}\mu_i}{K_i + \frac{4}{3}\mu_i + \pi\alpha\mu_m \frac{3K_m + \mu_m}{3K_m + 4\mu_m}} \quad (5.5)$$

$$\zeta'^i = \frac{1}{5} \left[ \frac{8\mu_m}{4\mu_i + \pi\alpha\mu_m \left(1 + 2\frac{3K_m + \mu_m}{3K_m + 4\mu_m}\right)} + \frac{K_i + \frac{2}{3}(\mu_i + \mu_m)}{K_i + \frac{4}{3}\mu_i + \pi\alpha\mu_m \frac{3K_m + \mu_m}{3K_m + 4\mu_m}} \right] \quad (5.6)$$

#### 5.6 Kuster-Toksöz (K-T) model:

K-T model calculates the dry rock properties of rock. It assumes the pore shape to be ellipsoidal, which is defined by aspect ratio. There is a decrease in velocity with an increase in the porosity of an object (Toksöz et al, 1976). Keys and Xu (2002) used a simplistic approach to estimate effective modulus of dry rock by making an assumption of dry-rock Poisson's ratio is constant with respect to porosity.

$$K_{dry} = K_m(1 - \phi)^P \quad (5.7)$$

$$G = G_m(1 - \phi)^q \quad (5.8)$$

Here,  $K_d$  and  $\mu_d$  represents bulk & shear moduli of dry rock, having porosity  $\omega$ .  $\mu_m$ , and  $K_m$  are the effective shear and bulk moduls of mineral constructing a rock correspondingly.

$$K_{sat} = K_{dry} + \frac{(1 - \frac{K_{dry}}{K_m})^2}{\frac{\phi}{K_f} + \frac{(1-\phi)}{K_m} - \frac{K_{dry}}{K_m^2}} \quad (5.9)$$

In addition, the K-T method is used in order to assess the elastic properties of kerogen and fluid combination (oil, gas, water), assuming that the fluid is already enclosed in Kerogen. Stiffness can be found using relation:

$$\frac{K_{ke}}{K_k} = \frac{1 + \left[ \frac{4\mu_k(K_f - K_k)}{(3K_f + 4\mu_k)K_k} \right] S}{1 - \left[ \frac{3(K_f - K_k)}{(3K_f + 4\mu_k)K_k} \right] S} \quad (5.10)$$

$$\frac{\mu_{ke}}{\mu_k} = \frac{(1-S)(pK_f + 8\mu_k)}{9K_k + 8\mu_k + S(6K_k + 12\mu_k)} \quad (5.11)$$

Where,  $\omega_f$ ,  $\omega_k$ , are fluid and kerogen volume,  $\mu_k$ , and  $K_k$ , are shear and bulk moduli of kerogen  $\mu_{ke}$ , and  $K_{ke}$ , are effective shear & bulk moduli of fluid.

### 5.7 Gassmann's equation:

Gassmann (1951) calculates the modulus of rock that has been saturated by comparing it to the moduli of dry rock, minerals, and pore fluids that are already known. Gassmann's equations are applicable only in the absence of stiffness in the pore filling fluid. The saturated moduli of rock are expressed as:

$$K_{sat} = K_{dry} + \frac{(1 - \frac{K_{dry}}{K_m})^2}{\frac{\phi}{K_f} + \frac{(1-\phi)}{K_m} - \frac{K_{dry}}{K_m^2}} \quad (5.12)$$

$$\mu_{sat} = \mu_{dry} \quad (5.13)$$

$$K_{dry} = \frac{K_{sat} \left( \frac{\phi K_{matrix}}{K_{fluid}} + 1 - \phi \right) - K_{matrix}}{\frac{\phi K_{matrix}}{K_{fluid}} + \frac{K_{sat}}{K_{matrix}} - 1 - \phi} \quad (5.14)$$

Here  $K_d$ ,  $K$ ,  $K_f$ , and  $K_m$  represents the bulk modulus of dry rock, rock saturated, pore fluid, mineral, respectively  $\mu_d$ , and  $\mu$ , refers to shear modulus of dry and saturated rock porosity is denoted by  $\omega$ .

### 5.8 Backus averaging method:

In the research that Vernik and Nur (1992) conducted, the authors formed the assumption that the shale rock is a multilayer composite that is made up of laminated clay minerals and kerogen of lamination in texture, as well as a combination of all the other minerals. The result of applying the anisotropic Backus averaging is a transversely isotropic equivalent medium, which may be characterised by the following five effective stiffnesses:

$$\begin{aligned}
 c_{11}^* &= \langle c_{11} - c_{13}^2 c_{33}^{-1} \rangle + \langle c_{33}^{-1} \rangle^{-1} \langle c_{33}^{-1} c_{13} \rangle^2, \\
 c_{33}^* &= \langle c_{33}^{-1} \rangle^{-1}, \\
 c_{13}^* &= \langle c_{33}^{-1} \rangle^{-1} \langle c_{33}^{-1} c_{13} \rangle, \\
 c_{55}^* &= \langle c_{55}^{-1} \rangle^{-1}, \\
 c_{66}^* &= \langle c_{66} \rangle.
 \end{aligned}
 \tag{5.15}$$

In equation (5.15), the weighted average of a physical quantity  $\alpha$  according to our rock physics model is defined as

$$\langle \alpha \rangle = f_c \alpha_c + f_k \alpha_k + f_m \alpha_m,
 \tag{5.16}$$

where  $c$ ,  $k$ , and  $m$  stand for laminated clay mineral, kerogen, and a mixture of all other compositions, respectively.  $m$  stands for a mixture of all other compositions. The weight for the average is denoted by the parameter  $f$ .

### 5.9 The shale properties analysis and rock physics model process

Initially, we investigate the shale minerals properties. Shale contains clay, sand, carbonate, and other minerals (Wang et al. 2010). Elemental log analysis shows that significant minerals in shale are clay, calcite, quartz and organic content i.e. kerogen as well. We propose an approach of calculating the equivalent elastic modulus of rock matrix using the SCA model.

Secondly, we analyse the pore and fluid properties. Shale is a dense, low-permeable reservoir mostly containing water and gas. Because of its large micropore volume and surface area, clay minerals may absorb more fluids. (Ding et al. 2012). So, it has a lot of bound water and adsorbed gas. This research divides pores into two types: linked micro-pores with immovable fluid

and detached micro-pores with mobile liquids (Zhang et al. 2015a, b). The K-T model posits that stationary fluid micropores are sparsely dispersed with minimal connectivity in shale. And the movable fluid micro-pores are connected. So, the dry pores are added using K-T and DEM models, then saturated with Gassmann low- frequency relations. In this approach, kerogen is taken as isotropic.

- The shale rock physics effective model workflow can be summarized as follows:
- The shale rock consists of matrix i.e. clay, calcite and kerogen
- The elastic modulus characteristics of minerals (clay, calcite, and quartz) are determined using the V-R-H average.
- Using SCA model, organic matters and a mineral mixture is incorporated in order to compute the elastic moduli of "rock matrix."
- To estimate dry rock elastic properties, pores and cracks are added using K-T and DEM model, taking kerogen as a background substance. The fluid properties i.e., bulk modulus of brine is estimated using Batzle and Wang relation.
- To obtain the elastic properties of saturated rock, Backus averaging relation is used by adding the pore fluids to the dry rock. Then we determine the velocities of the P and S-waves.

The flow chart of the built shale rock physics model is shown below:

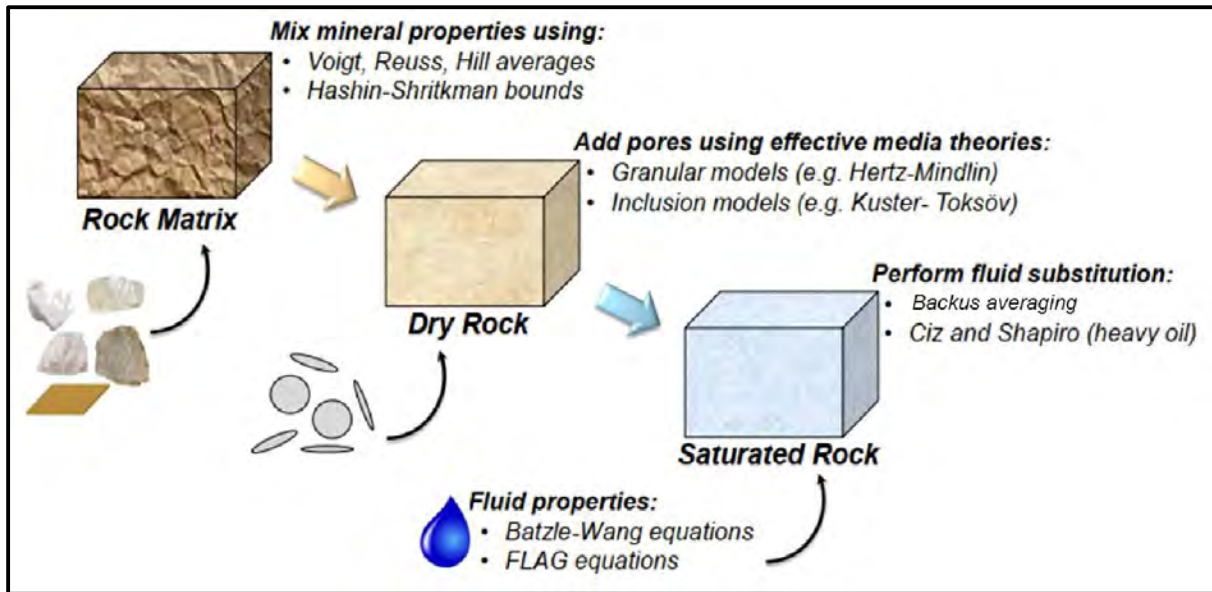


Figure 5.3 Work flow for construction of petro elastic model (Courtesy, CGG).

### 5.10 Rock Physics Modelling for Sembar formation:

Before constructing RPM, lithology log is generated. The lithofacies are based on  $V_{sh}$ , TOC and density log. Different cut-offs are applied on the given parameters, as a result three lithofacies i.e. light shale, dense shale and calcite are generated. Light shale is the targeted shale having maximum  $V_{sh}$  and TOC value. Input parameters required for constructing rock physics model for the Sembar formation primarily include: volume fractions, densities, elastic moduli of matrix (light shale, dense shale, and calcite), organic content, porosity of shale, fluid saturation etc. Here, Tarai deep-02 has been taken as a reference well for which rock physics model is constructed. The model is used to predict P- & S-wave velocity of both wells, compared with recorded wireline log data.

Figure shows the modelled elastic parameters such as  $V_p$ ,  $V_s$ ,  $Rho$  compared by the well data of Tarai deep-02. Track 4 shows the lithofacies classified for Sembar formation. The red curve shows the modelled values of  $V_p$ ,  $V_s$ , and  $Rho$  using constructed rock physics model, which are well correlated with the recorded values of well log data shown with black curve. The targeted formation i.e. Sembar Formation is highlighted at depth of 2254.3-2943m for Tarai deep-02 depicting a good correlation of predicted and measured values of petroelastic attributes. The cross plots of modelled and recorded data of Meyal-05 showing the correlation between elastic parameters is given in figure 4.5(a,b,c). The correlation normally depends upon the two factors i.e. correlation coefficient (CC) and normalized root mean square (NMRS) value, which lies between-

1 to 1. Predicted Rho curve shows 95% correlation with real well log values of Rho, predicted Vp shows 81% while Vs is 91% correlated with measured Vp and Vs calculated using backus average relation for shear wave calculation and NMRS value lies between 0.4-0.5.

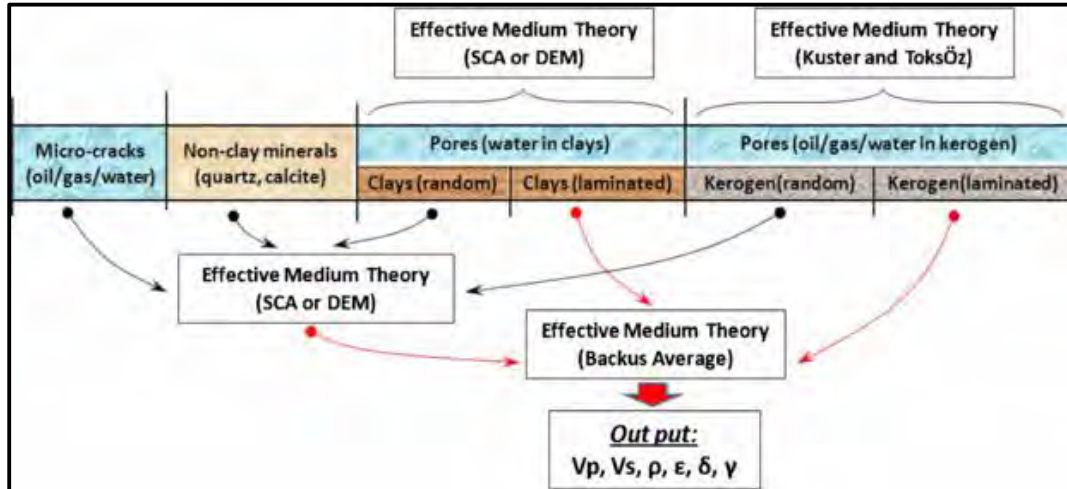


Figure 5.4 Methodology utilized in the development of the Rock physics model.

By implying constructed rock physics model for Sembar formation, our lithofacies are well classified on the measured data i.e. shale, sand and limestone. The different cross plots of Petro-elastic parameters for Tarai deep-02 demarcating each facie is shown in figure 5.5.

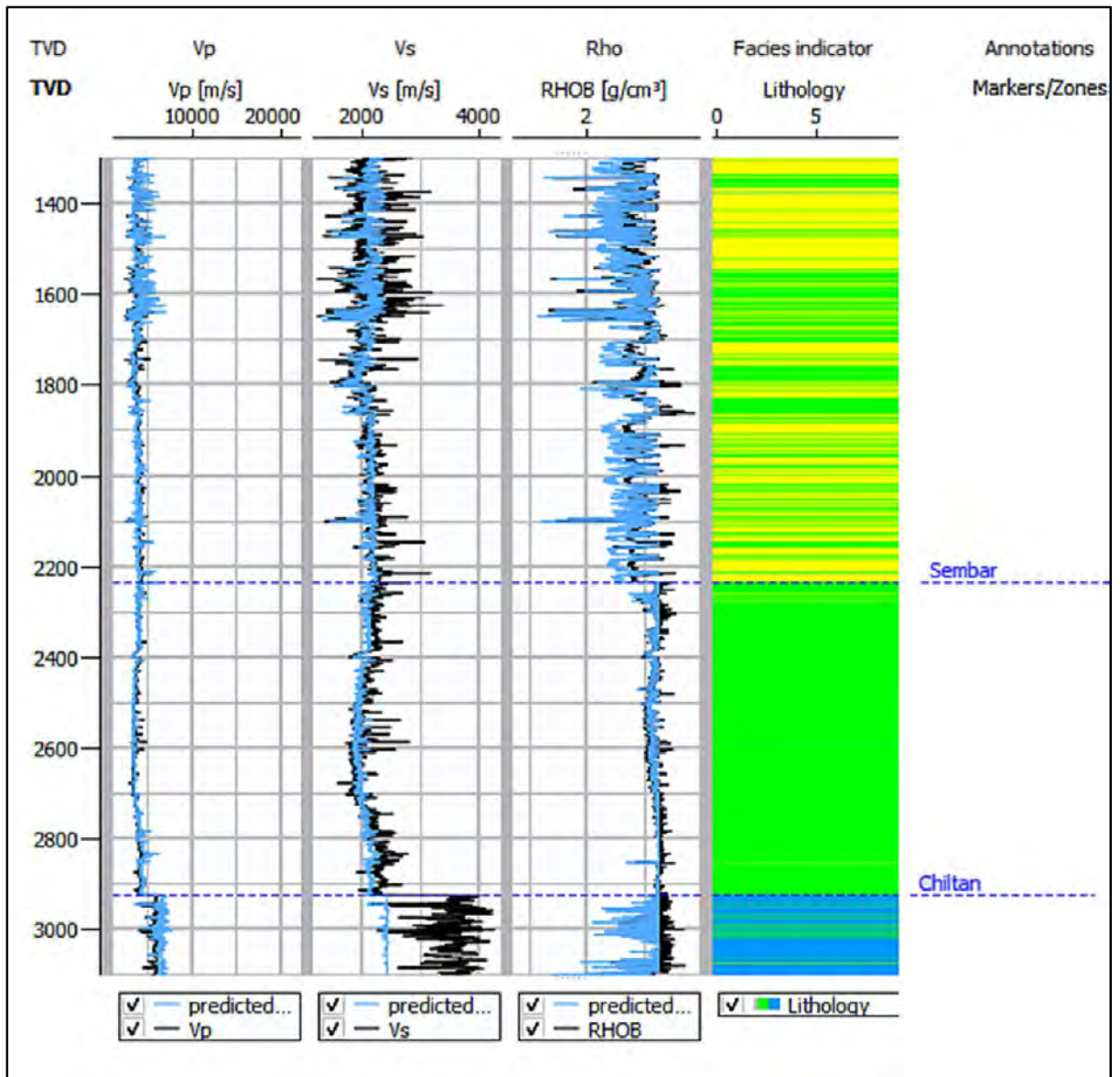


Figure 5.5 Results of real well logging data and modelled well log data i.e. Vp, Vs, and Rho of Tarai deep-02

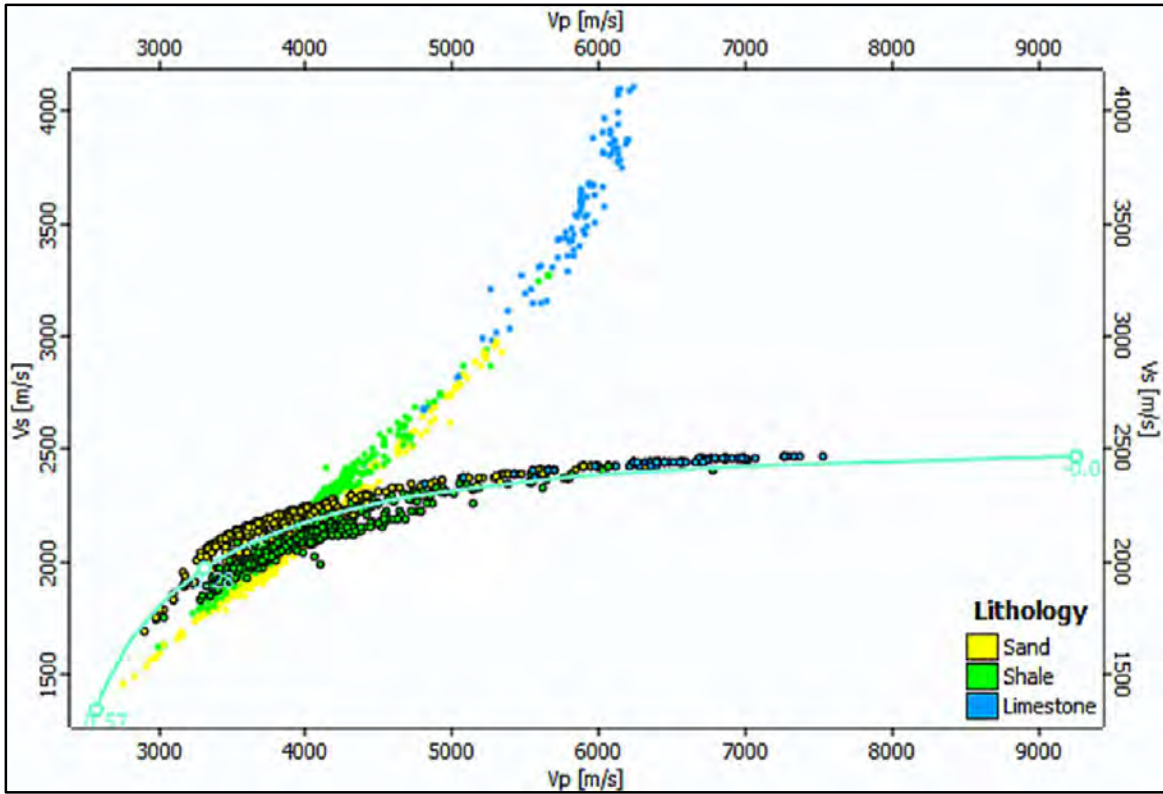


Figure 5.6 Petro-elastic parameters of Sembar formation estimated by rock physics model differentiating each facie ( $V_p$  vs  $V_s$ ).

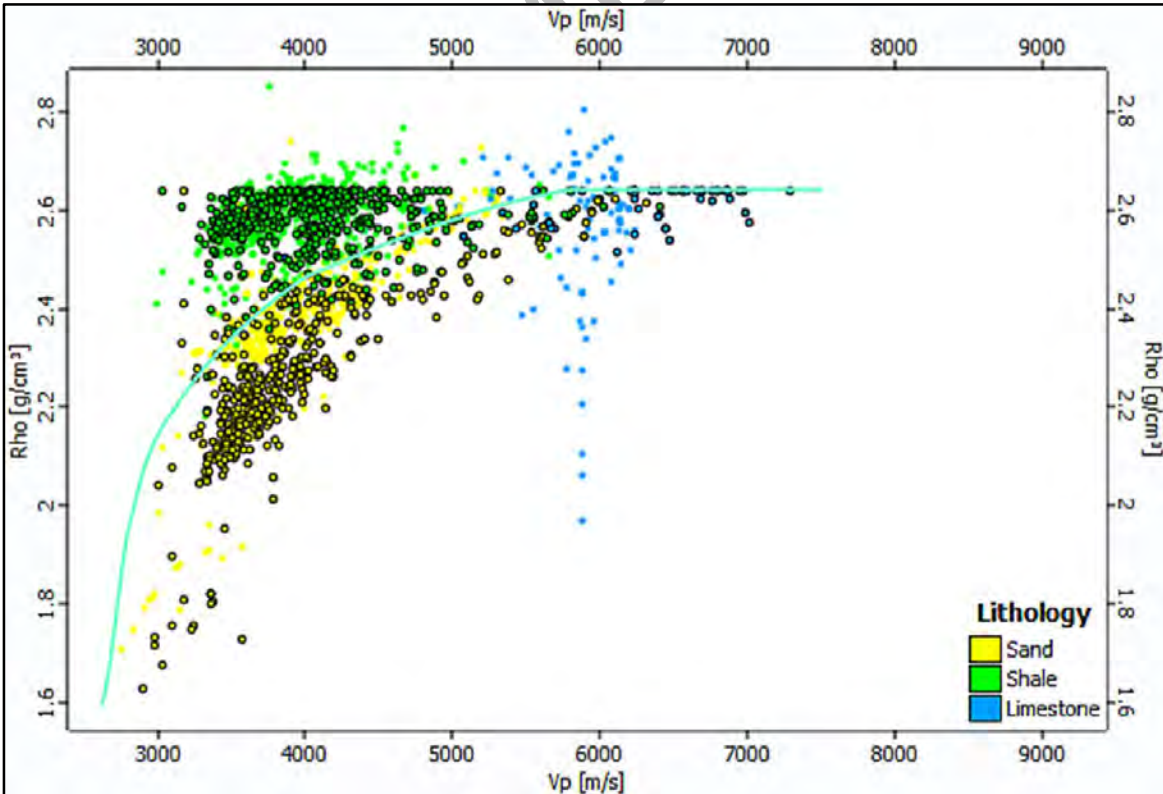


Figure 5.7 Petro-elastic parameters of Sembar formation estimated by rock physics model differentiating each facie ( $V_p$  vs  $Rho$ ).



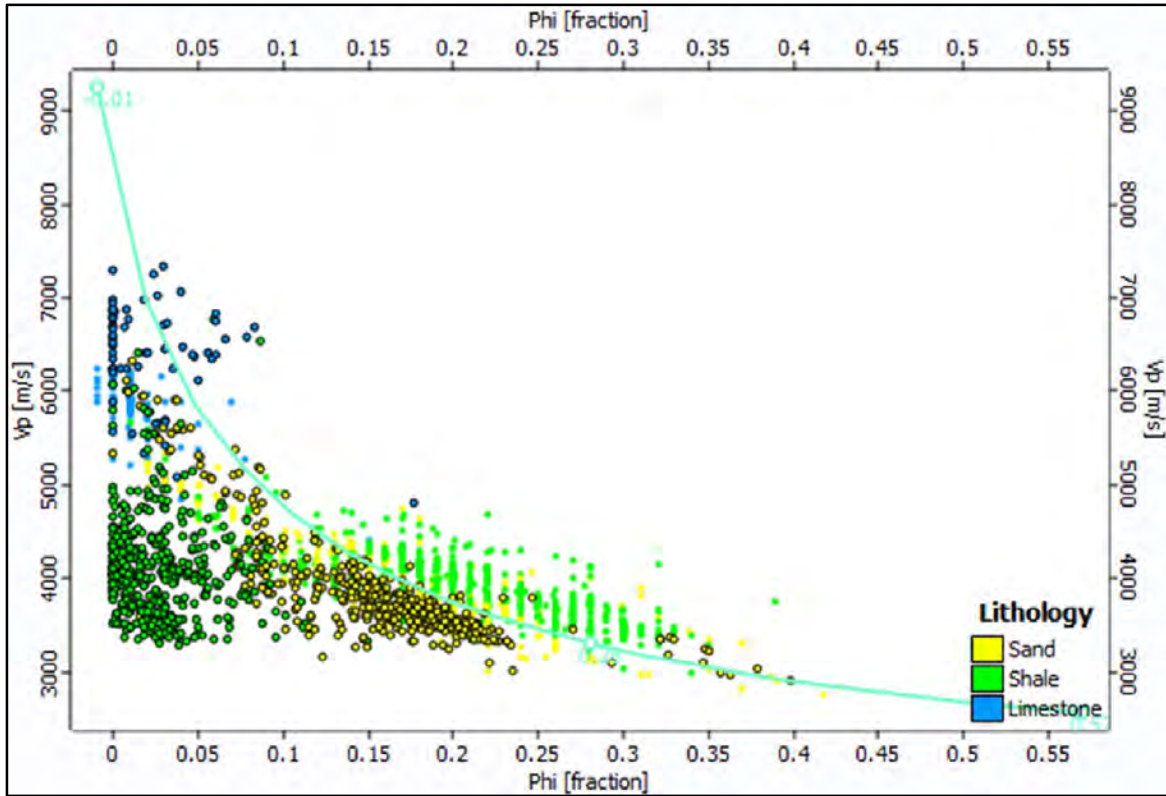


Figure 5.8 Petro-elastic parameters of Sembar formation estimated by rock physics model differentiating each facie (Phi vs  $V_p$ ).

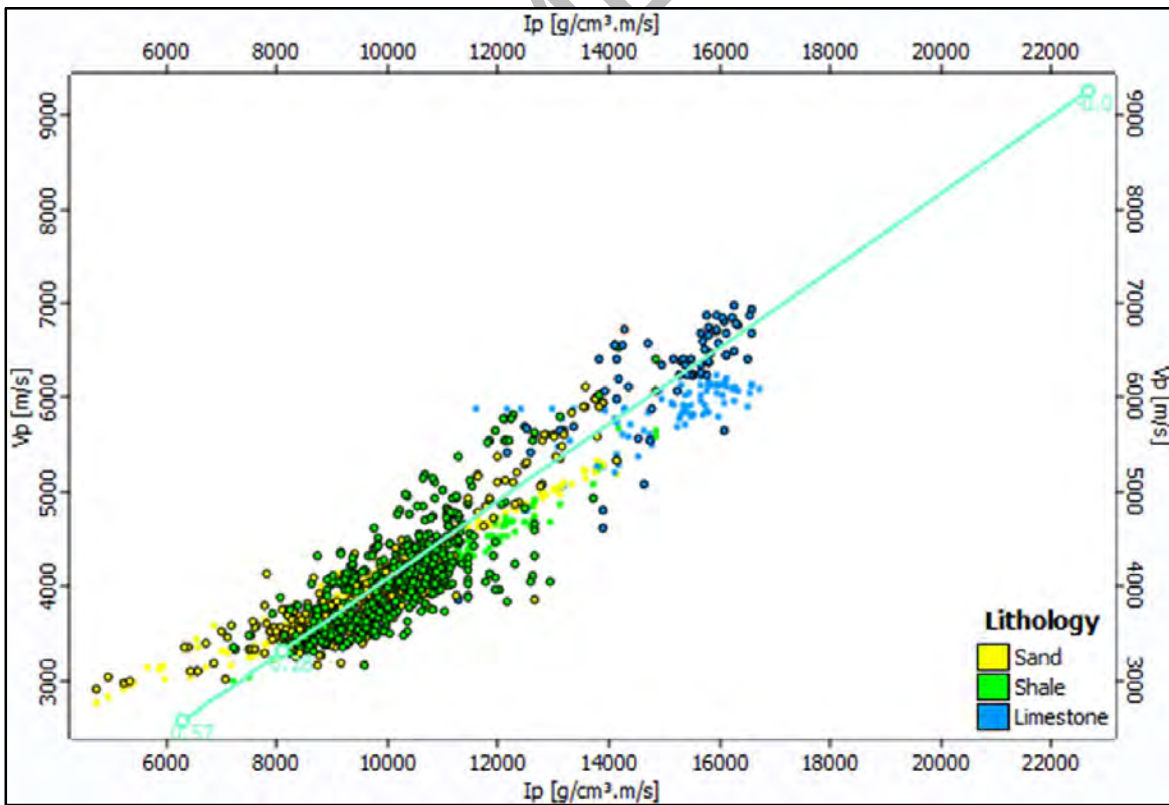


Figure 5.9 Petro-elastic parameters of Sembar formation estimated by rock physics model differentiating each facie (Phi vs  $V_p$ ).

### 5.11 Uncertainty Analysis using Monte Carlo Simulation:

The Standard Monte Carlo (MC) Simulation is a stochastic strategy for evaluating uncertainty. This technique models the unknown parameter with random numbers. Thus, the derived input values are used in a series of simulations to provide a range of estimations and their associated probability (Adjei et al., 2019). One significant advantage of the MC approach is that it is independent of the quantity of random samples used in the input (Alkhatib & King, 2013). Although rock physics models give deterministic correlations between input components and output parameters such as  $V_p$ .  $V_s$ . Monte Carlo simulation quantifies the uncertainty associated with each variable and thereby predicts the output as probabilistic distribution function (Pdf) as shown in figure

Probabilistic distribution function (PDF) defines the distribution, used to specify the probability of the random variables, depending upon the type. There are certain types of distributions which can be used as an input:

- **Normal probability distribution** can be defined by mean and standard deviation
- **Discrete probability distribution** specifies the set of possible outcomes in discrete manner.
- **Uniform probability distribution** refers to the events that have same possibility of occurring. It is specified by two parameters,  $x$  and  $y$ , which refers to minimum and maximum value.
- **Beta probability distribution** is also a form of continuous distribution with two shape parameters i.e.  $a$  &  $B$ , defined on the interval  $[0, 1]$ . These two factors are responsible for the shape of distribution. It encompasses all potential probabilities.

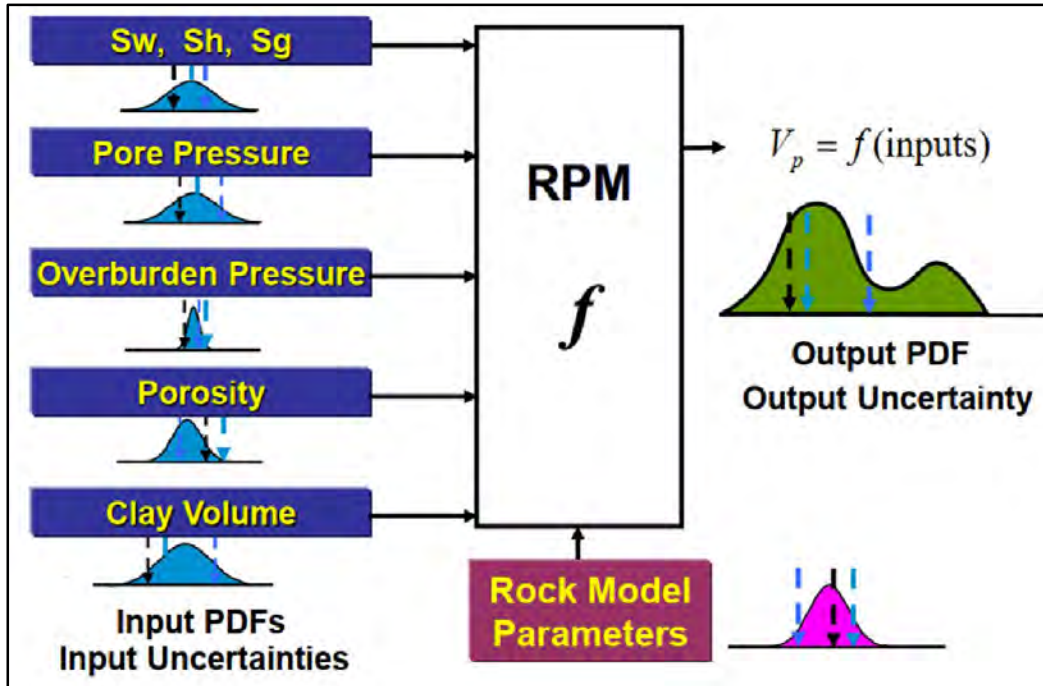


Figure 5.10 Uncertainty analysis of deterministic rock physics model.

### 5.12 Uncertainty Analysis of Sembar shales:

The PERT parameterization of beta distribution is ideally suited for defining rock physics properties. The elastic parameters such as  $V_{sh}$ ,  $\text{Phit}$ ,  $\rho$ ,  $V_p$ ,  $V_s$ ,  $I_p$  are cross plotted against each other defined by the density of points. Using petro-elastic model developed for shale, the two parameters i.e. Volume of Shale ( $V_{sh}$ ) and porosity ( $\text{Phit}$ ) are taken as an input. Applying the beta distribution, maximum, minimum values and mode are estimated based on shale model. Deviation is adjusted to 0.65 by comparing the log distribution and beta distribution. Shape factor is generally reciprocal of standard deviation at mode. Input distribution is given in table as:

Table 5.1 Values used for uncertainty analysis

Parameters	Distribution	Min	Mode	Max	Deviation
$V_{sh}$	Beta	0.45	0.75	0.78	1
$\text{Phit}$	Beta	-0.04	0.01	1.2	0.07

The Iman-Conover technique is used to simulate the correlations between the input variables (figure). The threshold applied to  $V_{sh}$  is 1, due to which porosity is negatively associated with shale volume i.e. - 0.4. As a result, Pdf contours i.e. P-10, P-50, P-90 are generated based on density points as shown in figure. This can also be used to simulate the production effects on elastic

attributes. The red points show the high-density region i.e. 90% probability of shale that lie within center, purple points show the low-density region i.e. 10% probability of shale while yellow points show the moderate probability of shale i.e. 50% distribution of shale.

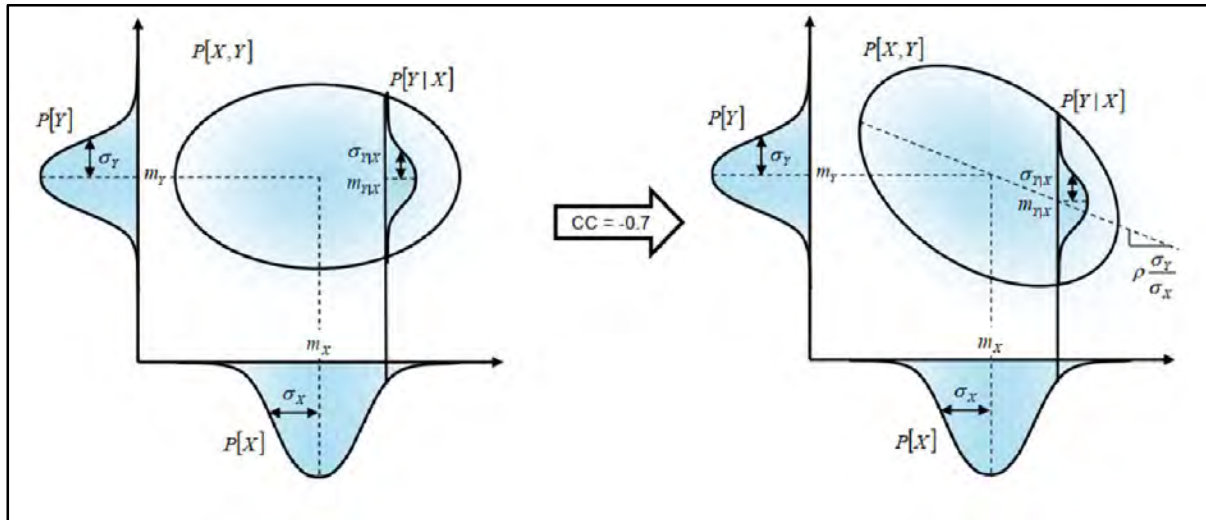


Figure 5.11 Iman-Conover technique to simulate the correlation between input variables.

It clearly shows that measured data was scattered, while after applying analysis using Monte Carlo simulation, data was standardized with minimum deviation. Such values can be valuable for lithofacies classification over seismic section as well.

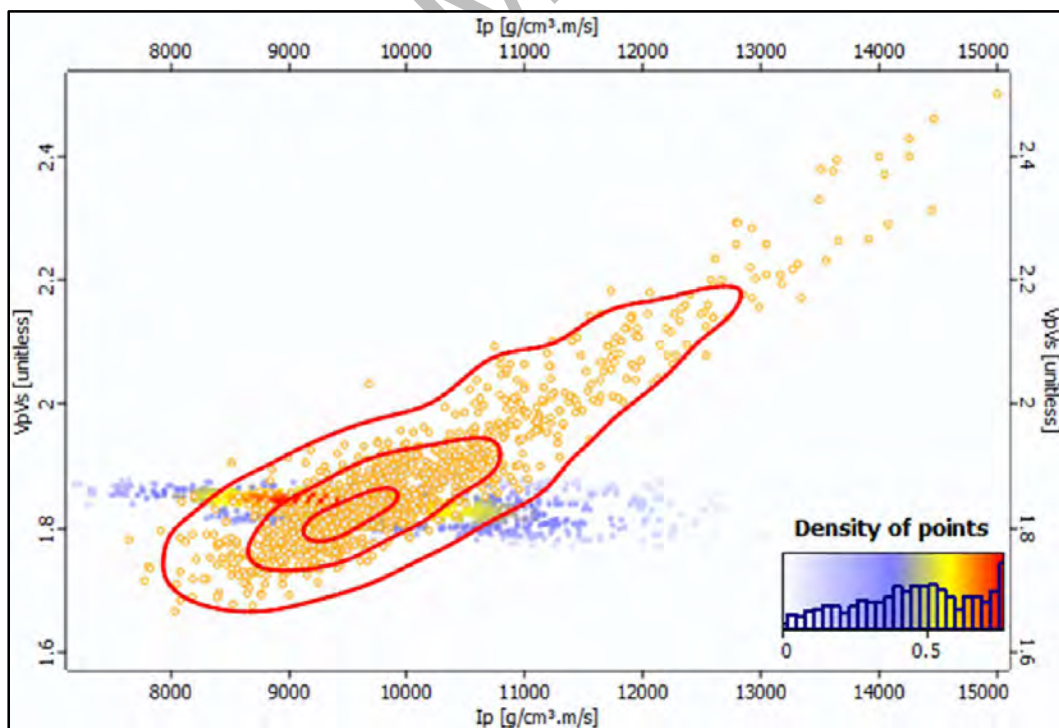


Figure 5.12 Probability density function plots of elastic parameters depicting shale distribution. (Ip vs VpVs ratio).

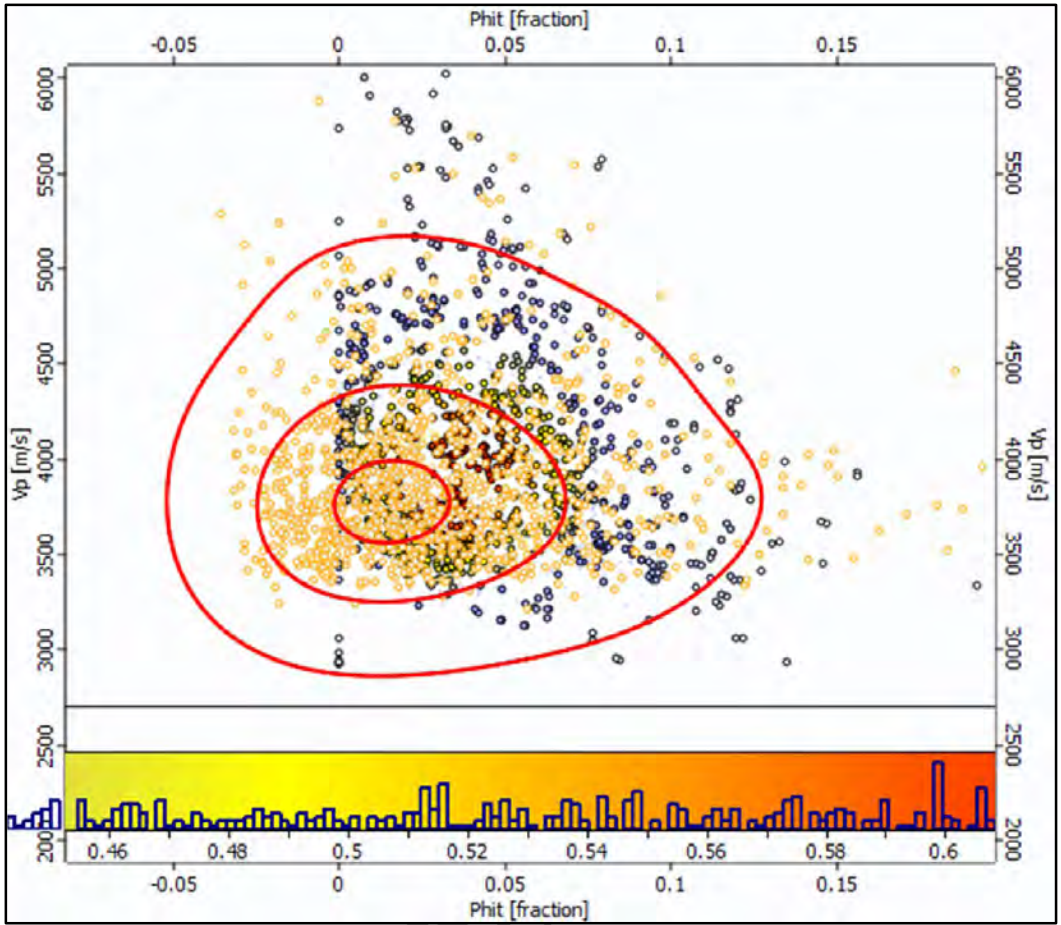


Figure 5.13 Probability density function plots of elastic parameters depicting shale distribution. (Phit vs Vp).

DRS

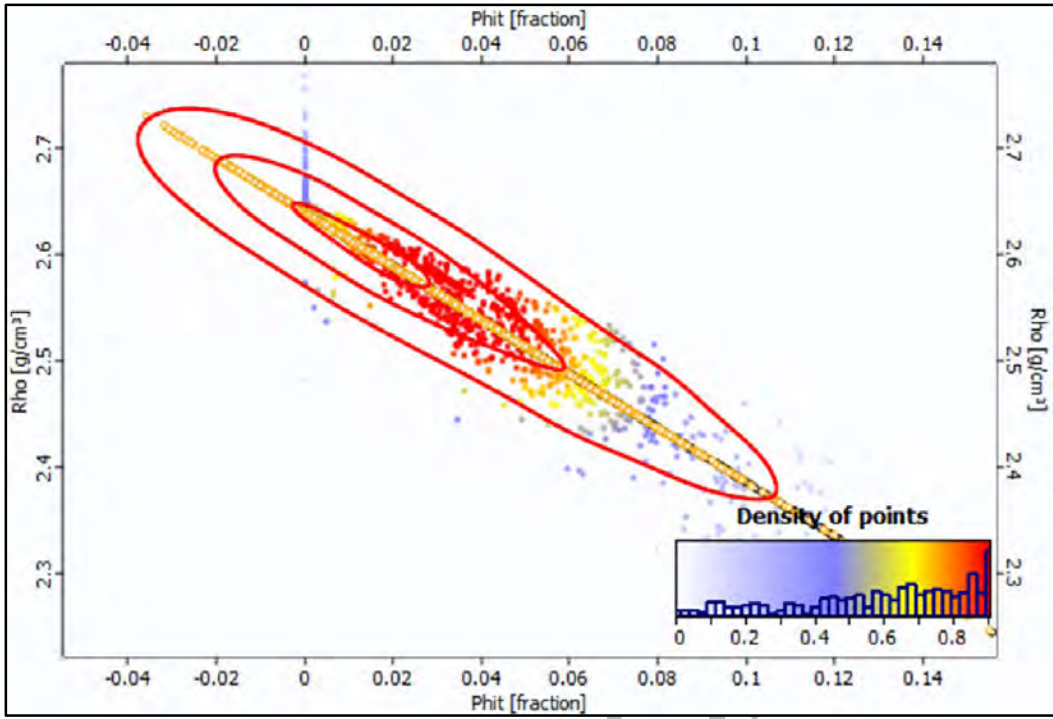


Figure 5.14 Probability density function plots of elastic parameters depicting shale distribution. (Phit vs Rho).

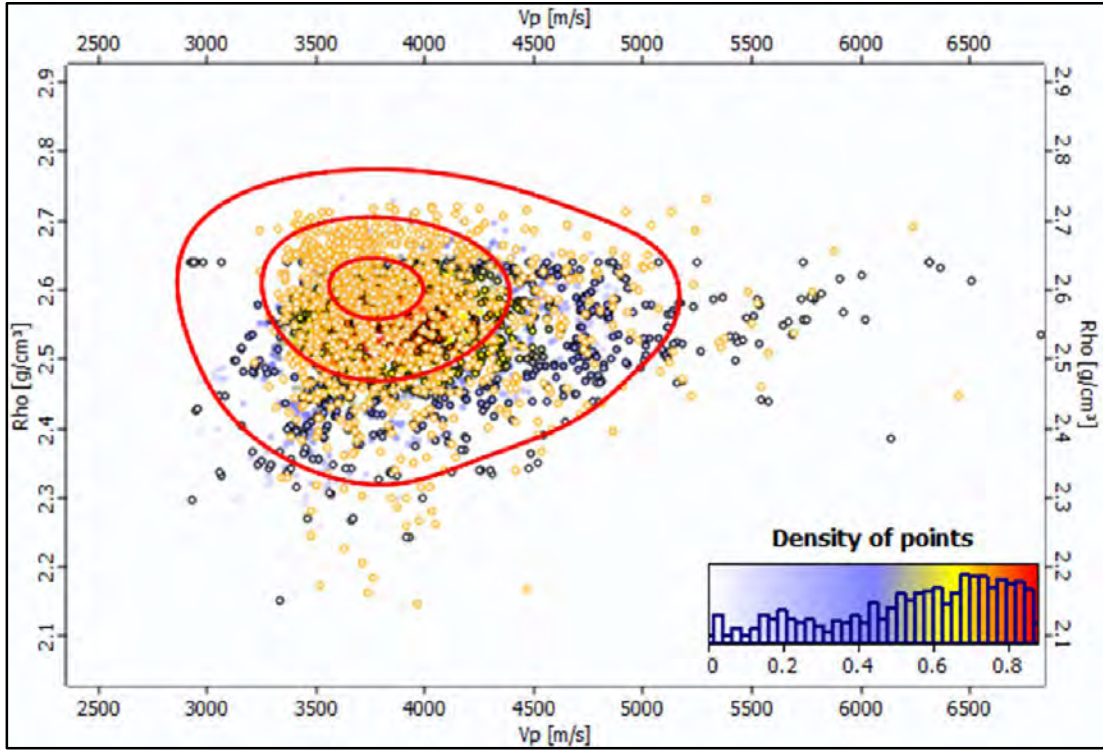


Figure 5.15 Probability density function plots of elastic parameters depicting shale distribution. (Vp vs Rho).

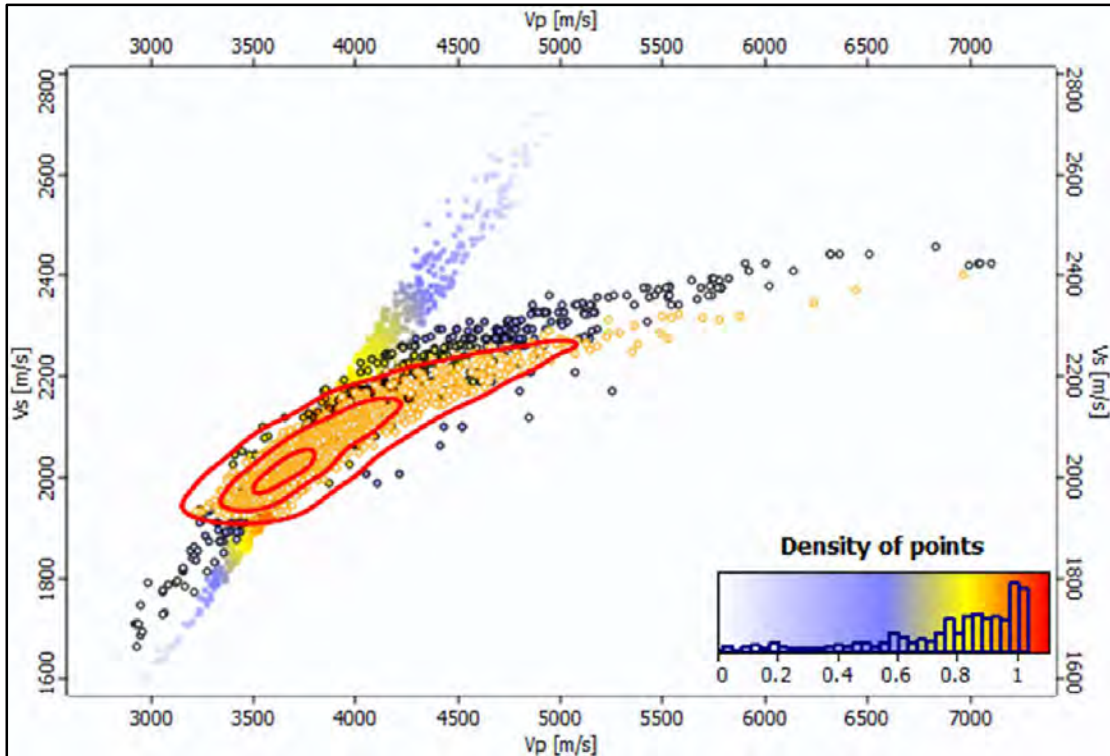


Figure 5.16 Probability density function plots of elastic parameters depicting shale distribution. (Vp vs Vs).

DRSML

## Chapter 6

### Geostochastic Inversion

For reservoir characterization, the construction of precise three-dimensional models of petrophysical properties is necessary, and these models must be placed within a geological setting. The structural seismic analysis is the foundation upon which the reservoir model is constructed, yet its use in the generation of the 3-dimensionally populated petrophysical properties is not very frequent. This is due to a number of factors, some of which include a deficiency in the availability of a 3D dataset, the inability to quantitatively connect seismic data to reservoir characteristics, an insufficiency in the amount of vertical resolution required to develop accurate property models, as well as other factors (Rowbotham et al., 2003). The availability of 3D seismic may solve the second problem by offering seismically determined impedance volumes as a seismic parameter that can be specifically linked to a reservoir feature (for example, 9). The lack of vertical resolution in classification applications has proved more difficult to rectify. Stochastic seismic inversion with higher vertical resolution is one method for developing exact 3D reservoir property models (Gunning & Glinsky, 2003).

Geostatistical techniques are widely used to estimate different geophysical features from seismic and well-log data. Geostatistical methods make use of the sample points, also known as the petrophysical characteristics of the well, and interpolate the data by constructing a surface for each site based on the observed locations (Haas and Dubrule, 1994). Deterministic and geostatistical interpolation are the two main types of approaches used in the field of geostatistics (Russell et al., 1999). Deterministic interpolation methods rely on mathematical functions, while geostatistics uses both mathematical and statistical methods (Hampson et al., 2001). There are many methodologies available for determining reservoir parameters using interpolation techniques. Among these techniques, the most often utilised is Geostochastic inversion (GeoSI), which transforms bandlimited seismic data to high frequency seismic data. GeoSI employs the notion of decreasing the sample interval to 1 ms, enabling inversion results to enhance reservoir models with minimal mistakes (Rowbotham et al., 2003).

Since the middle of the 1990s, there have been significant breakthroughs in the approach that is taken to geostatistical inversion. These developments may be seen most prominently in the integration of data and the conditioning of reservoir models with seismic data and earlier rock



physics information. In a sequential process, the stochastic impedance realizations are converted using various statistical techniques, including collocated co-kriging (Doyen et al. 1989), Bayesian classification, and linear regression functions, to fill reservoir modeling with seismic conditioned reservoir properties (Coulon et al., 2005). Co-simulation of lithofacies and impedance, for example (Torres-Verdin and Sen, 2004), was a fairly early development. The rationale of using seismic directly to condition reservoir properties in a 3D model that use the facies concept is credible (Saussus and Sams, 2012). For example, unless saturation is incorporated in the inversion model, it is difficult to verify that elastic features are consistent with a saturation height function (Sams et al., 2011). Theoretically, applying all restrictions simultaneously results in deeper integration and a more robust and consistent reservoir models.

Recent research has concentrated on developing stochastic algorithms that expand beyond acoustic inversion and into simultaneous elastic inversion. This requires the joint inversion of many partial angle stacks in order to estimate  $Z$ , and  $Z$ , or, in better circumstances,  $V_p$ ,  $V_s$ , and  $p$ . The use of position stochastic inversion in a stricter Bayesian framework has also received some attention. In this situation, the answer to a seismic inverse issue and the degree of uncertainty associated with it are described using a posterior distribution function.

Reservoir models created only from log data have excellent vertical resolution, but poor areal (horizontal) resolution. This is because the resolution qualities of the log data provide a high vertically resolution but a low spatial resolution. The reason for this is due to the fact that the log data has both of these features. The areal resolution of seismic data (the bin size of 3D surveys) is rather good, while the vertical resolution is quite poor (function of the seismic frequency content and velocity of the reservoir). Stochastic seismic inversion offers a unique framework for integrating the benefits of seismic and well log data (Marion et al., 2000). The seismic data are responsible for providing the stochastic impedance volumes with the areal resolution, whereas the log data that are used in the inversion approach provide the technique with the vertical resolution. The created high-quality 3D volumes are ideal for detailed property development. The usual stochastic inversion has a vertical resolution of about 1-2 metres on average. It is often on this scale that models of petrophysical reservoir properties are constructed. Impedance data, together with well log data, may be utilised to build reservoir property models like as porosity (Rowbotham et al., 2003b). On the basis of sequential Gaussian simulation, (Haas and Dubrule 1994) established the first practical use of geo-statistics in seismic inversion. During each and every trace of the

seismic survey, and the well log data (both density and sonic) are employed to create pseudo-logs. A synthetic seismogram is created with the help of the pseudo-impedance log, and then it is compared to the real seismic trace recorded at that point. At any given time, the inversion solution is the simulation that yields a synthetic seismogram that most closely resembles the observed seismic trace. The vertically cell size, not seismic data frequency, determines the simulated log data's vertical resolution. The GeoSI software generates a three-dimensional volume that takes into consideration both the log data and the seismic data and has an aerial resolution comparable to that of seismic data and a vertical resolution comparable to that of log data.

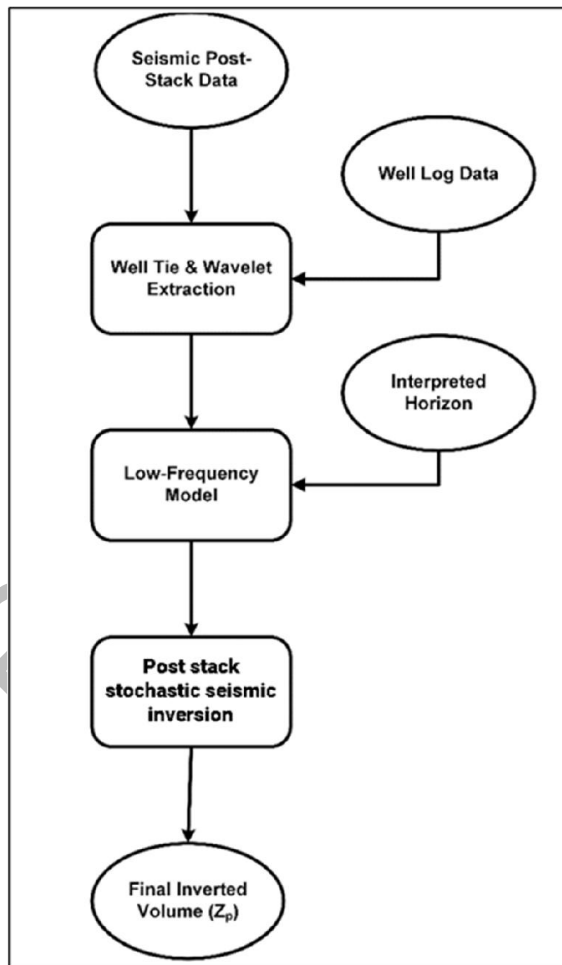


Figure 6.1: Adopted workflow to perform stochastic inversion (courtesy CGG).

### 6.1 Seismic to well tie and Wavelet Extraction

The obtained wavelets must be scaled to fit the stratum model. There were numerous angle stacks for pre stack data, and separate wavelets were recovered from seismic data for each one.

Following that, the wavelets were scaled in order to be employed in the stratum (GeoSI previous) model

The inversion was performed only on the selected time window 960-1100ms in which the horizons of interest lie. The inversion results show colored layers displaying different values of acoustic impedance for each layer. The stochastic inversion results show a good lateral variation in acoustic impedance which can be used for depicting shelling out sequence.

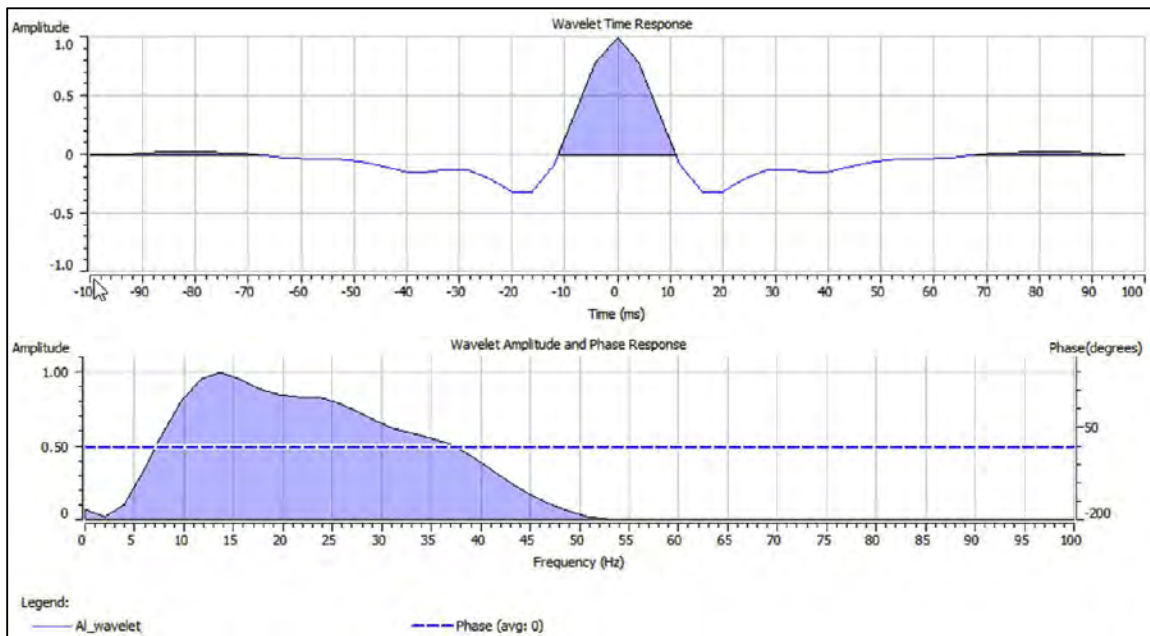


Figure 6.2: Extracted statistical angle dependent wavelet for seismic

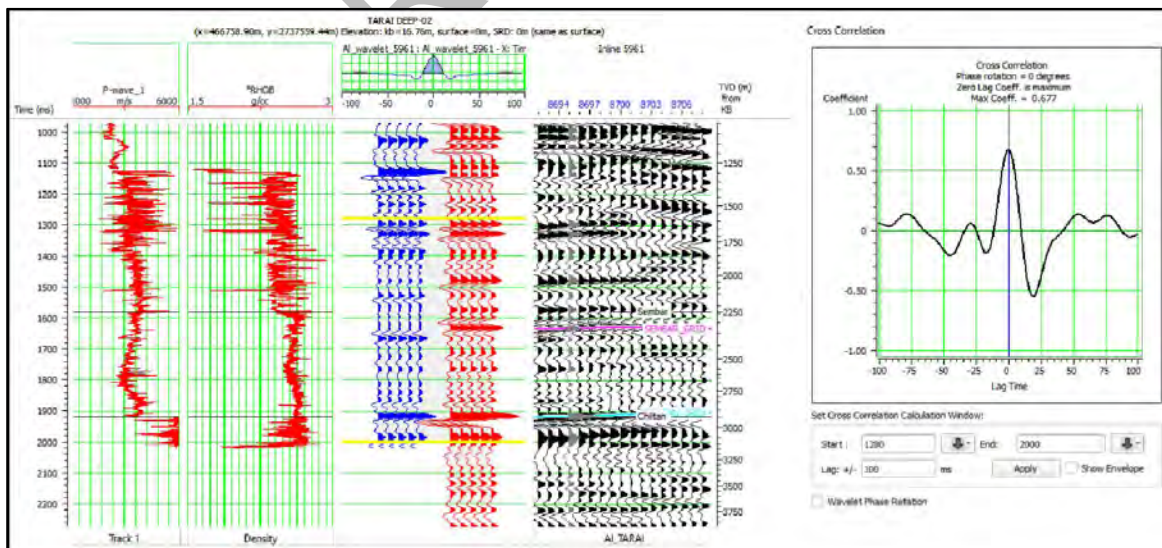


Figure 6.3 Well to seismic tie at well location.

## 6.2 Low Frequency Model

Similarly, each inversion approach, including GeoSI, begins with a connection between well and seismic. Maximum correlation was obtained using the well-to-seismic tie done in PSSI. Similarly, the LFM, also known as the Strata Model in GeoSI, is derived from a previously completed inversion approach, and a subsequent model is constructed. After identifying the seismic horizon using the interpolation method, the low frequency  $Z_p$ ,  $Z$ , and  $p$  models were built. This was done while ensuring that the structural tendencies were maintained. As a result, in order to effectively conduct the stochastic inversion, these LFM are employed as previous models.

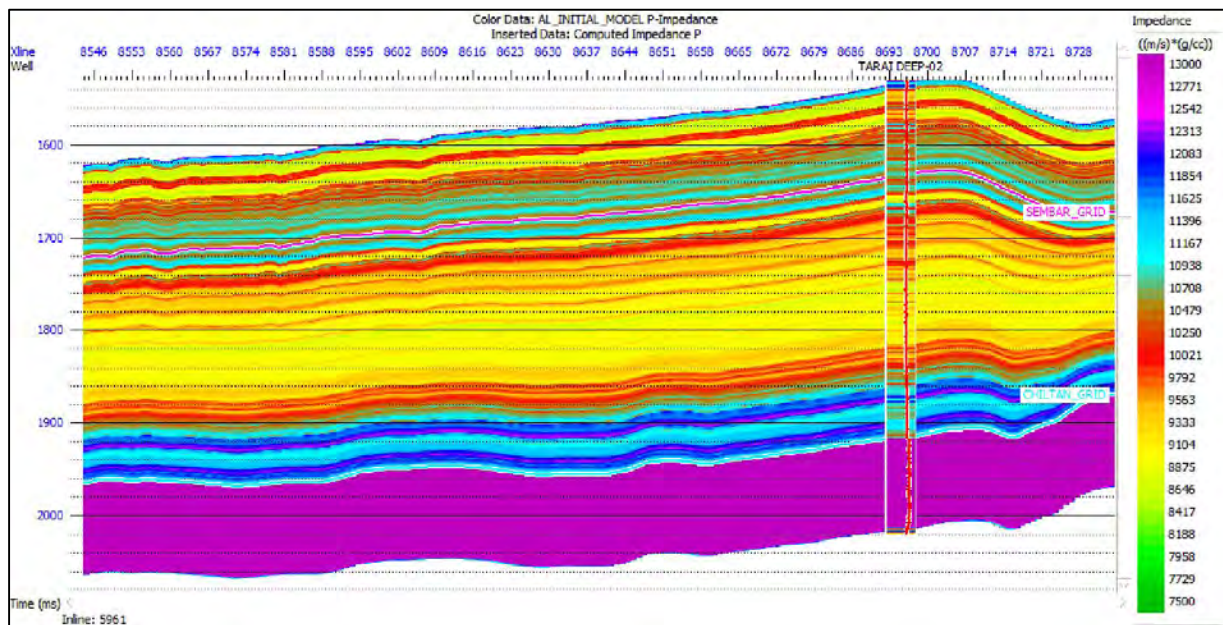


Figure 6.4 A low impedance geo strata model for In-line 5961 built by applying lower and upper impedance limit.

## 6.3 Prior Model (SI Model)

In traditional inversion, the initial model (LFM) is often generated by combining well logs throughout the full seismic volume, while GeoSI needs a prior model using specified characteristics and additional seismic data limitations. Using regular domain samples that were initially set at 1 millisecond, a high-resolution stratigraphic grid that corresponds to petrophysical parameters was produced. The stratigraphic geo-cellular grid comprised of three strata of confirmable fine scale, ranging from Chiltan to Sembar formation. To accommodate the variable thickness and depositional tendency, the layer thickness was fixed at 0.1ms to achieve excellent resolution. Figure 6.5 depicts the parameters utilised to obtain the previous model.  $Z$ , and 2 were

chosen as the appropriate types of inversion for this research, whilst the background trend was given to the previously created stratum model,

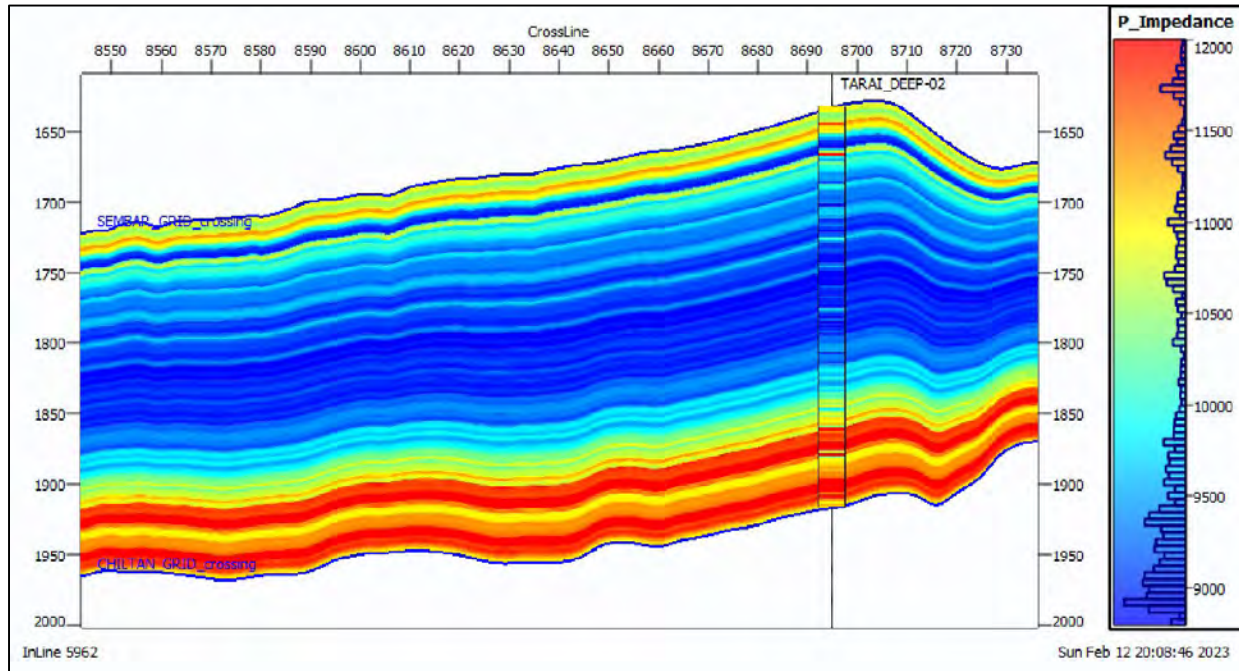


Figure 6.5 SI Model interpreted from the strata model on inline 5962.

## 6.4 Variograms

For both sparse (well) and rich (seismic) data, a variogram may be used as a measurement of geographical variances (spatial consistency or changes in space). Variograms are used to calculate stratigraphic grid spatial variations using a statistical technique and Kriging/Co-kriging processes. Due to the fact that the values of these "regionalized variables" have a geographical (posterior) distribution, these variograms deal with a kind of variable that is neither completely random nor deterministic. The presence or absence of a specific component or structure in a sample therefore depends heavily on its position on the depositional surface as represented by the grid (Saussus and Sams, 2012). Three points are used to evaluate a theoretical variogram: range, nugget, and sill. The range is the potential outcomes between the minimum value and the largest value. The variogram readings will eventually cease changing and hit a "plateau" at some point. This is referred to as the range. All of the data points that fall within the "range" will be given weight and included in the computations, but any data points that fall outside of the range will not be considered (Liu et al., 2018). The number that corresponds to "Sill" in the variogram is the point at which the change in that graph ceases. Because the sill has no geographical link to the reference

point, offset is irrelevant. The data points in this case are not utilised to compute the unknown value. "Nugget" depicts the origin's discontinuity. Although it should be zero, sampling error and data point small scale variability lead it to be non-zero (Bosch et al., 2012).

#### **6.4.1 Vertical and horizontal variograms**

Variogram models in stochastic inversion (GeoSI) encompass vertical and horizontal modelling. Vertical variograms were created using high-quality log data, and horizontal ranges were approximated using seismic data while taking structural and stratigraphic changes into account. Vertical study was carried out over three layers: "layer 1" (from Upper Goru to Lower Goru 1), "layer 2" (from Lower Goru 1 to lower Goru 1 basement).

#### **6.5 Facies Classification**

At that point, a simple equation was used in the (Litho-SI) procedure on the modelled wells to apply a basic definition for the reservoir facies. The simplest technique for identifying facies is a gamma-ray log. As a result, a (40 API) threshold was used to distinguish between reservoir (40 API) and non-reservoir (>40 API) facies (Supplementary F). The reservoir portion from layer 1 to layer 150 was subjected to the facies categorization. Using the well data to estimate the Gas sand, shaly sand, sandy, shale and shale ratio, suggesting a high Net to Gross value in the reservoir portion. In order to produce the geo-bodies volume realizations, the connection analysis was done after the classification was performed to the inverted model.

#### **6.6 Probability Density Functions (PDF's)**

Noise in the data, as well as mistakes in the modelling procedures, induce variances in the inversion findings. As a consequence, GeoSI gives a superior solution by providing various outcomes iteratively in realizing subsurface features. This not only produces better resolution data than the input, but also allows for the quantification of uncertainty within the reservoir model's probable scenarios. As a result, Monte Carlo simulation (MCS) based on Bayesian categorization offers a reliable method for predicting probability distributions for hydrocarbon facies.

#### **6.7 Inverted impedance section**

The layered strata model, scaled wavelet, and facies classification were used to run 50 realizations. to generate 50 different distribution scenarios for the sand, shale, and calcite, together with volume realizations for the geobodies and connectivity analyses. Due to the fact that

stochastic inversion is founded on geostatistical techniques, a variogram analysis is essential in order to replicate the spatial variation in each of the directions. The inversion variogram matched the well-matched data cloud with a consistent trend, as shown in Shown in fig 6.6. As shown in Fig. 6 only 14 no realizations of the facies volumes and geo-bodies were retrieved, and give us better co-relation with impedance

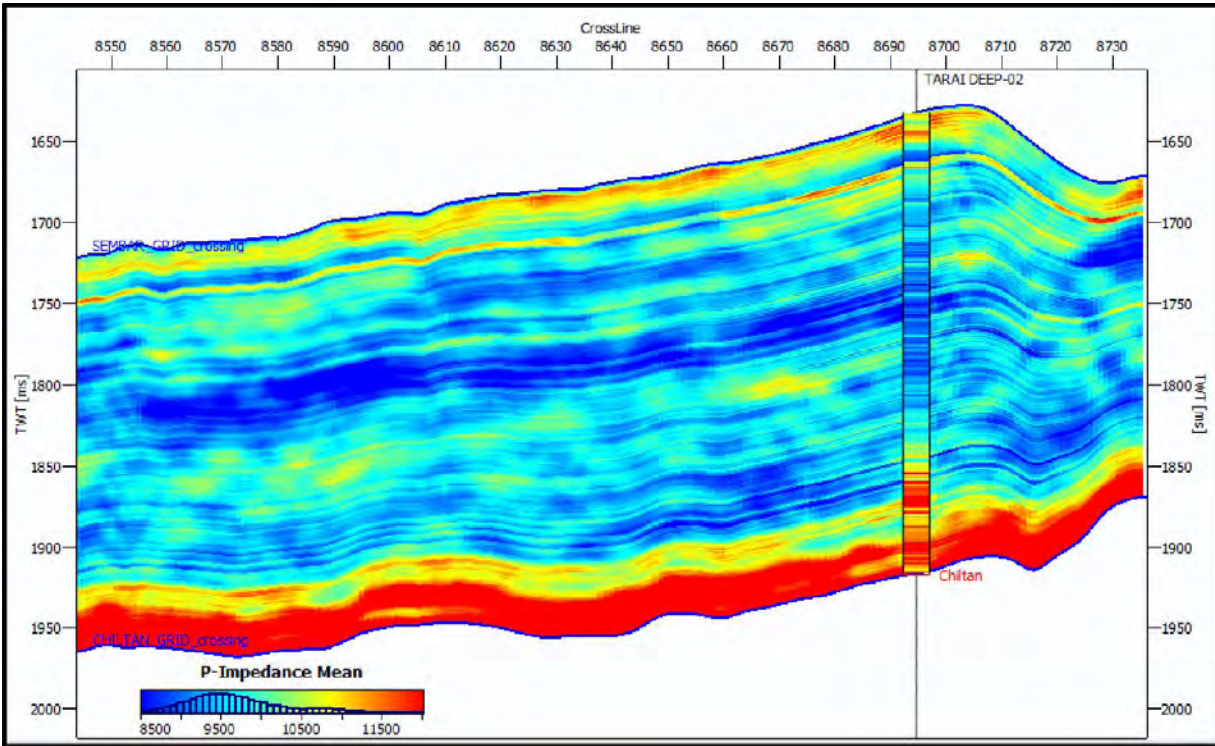


Figure 6.6 Inverted Imprudence sections on In-line 5961.

## 6.8 Spatial Distribution of TOC

TOC logs determined from different techniques in chapter 4 are calibrated with the inverted impedance sections. Keeping in mind the contrast in resolutions of both data sets, the regression technique is valid only after upscaling of the well data in accordance with the seismic resolution (Ali et al., 2019). Vertical resolution of seismic data can be determined after extracting the dominant frequency ( $f$ ) and velocity ( $v$ ) at the respective zone of interest. Wavelength for the seismic data at that zone can be determined using the equation 6.1.

$$\lambda = \frac{v}{f} \quad (6.1)$$

where,  $\lambda$  is wavelength. The value obtained from  $\lambda/4$  will give the vertical resolution of seismic data. The dominant frequency for a seismic data is determined though amplitude spectrum (Ali et al., 2019).

Values taken from inverted sections are obtained according to the depths for up-scaled well log data. TOC obtained from each technique is plotted against acoustic impedance from inverted section. A linear regression line is obtained which should have a correlation coefficient value ( $R^2$ ) exceeding 0.7. The equation for that line is then used to develop the seismic TOC sections. The plot obtained is for both high and low TOC values against the Acoustic impedance values and then utilized to estimate the high and low TOC values on the seismic section.

### 6.9 Seismic Passey TOC sections from impedance model:

Seismic inverted sections for TOC calculated from Passey's method was developed from the cross plot between acoustic impedance and TOC obtained fig 6.7. Regression line was applied as:

$$y = -0.000980666 * x + 13.0857 \quad (6.2)$$

The correlation for the data set was more than 0.7. Seismic section for Passey is illustrated in fig 6.8.

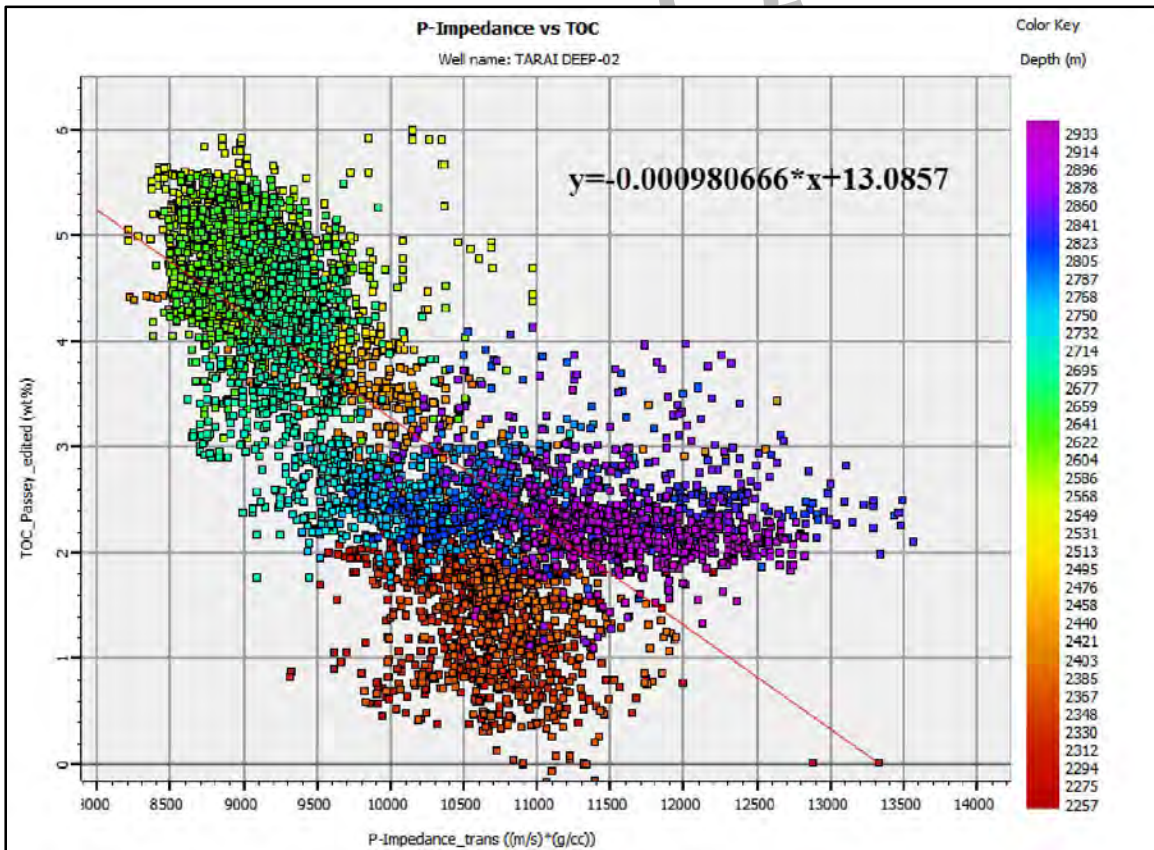


Figure 6.7 Cross-plot of P-impedance and TOC calculated from Passey.



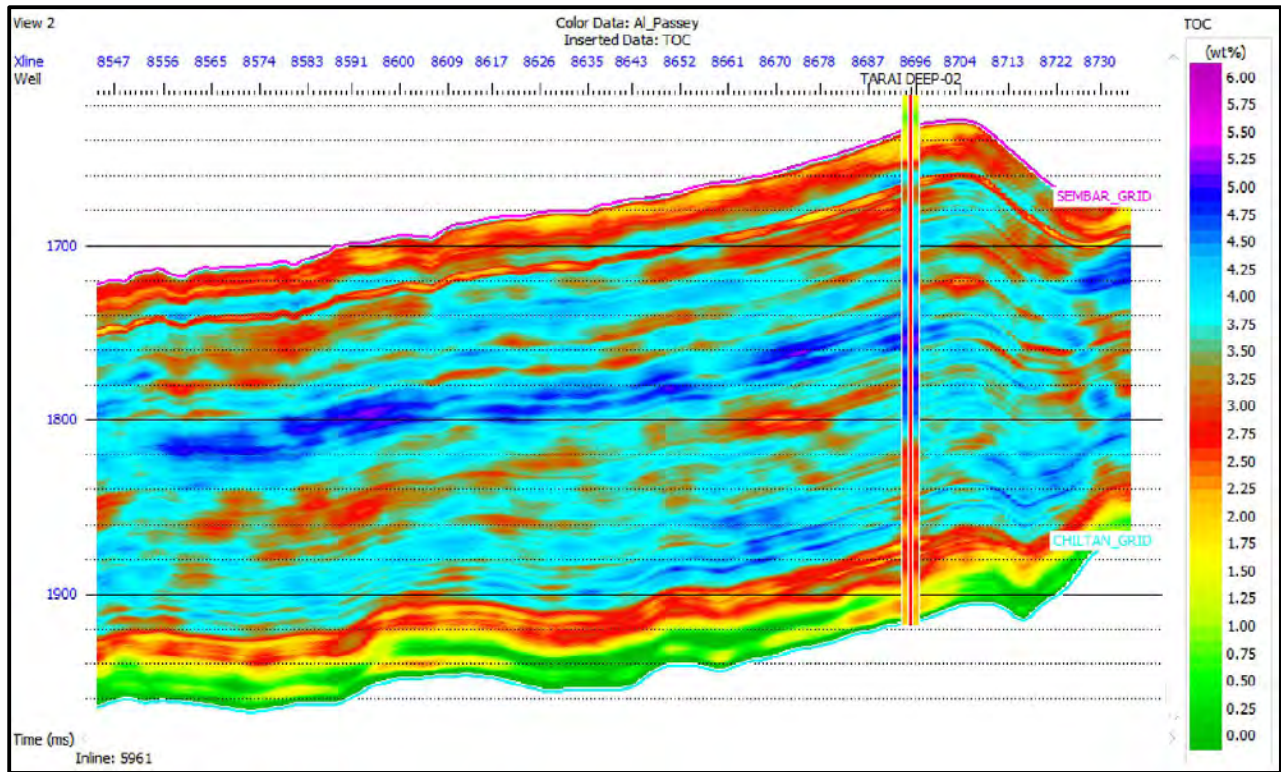


Figure 6.8 Inverted seismic section for TOC obtained from Passey.

### 6.10 Seismic Schmoker TOC sections from impedance model:

Seismic inverted sections for TOC calculated from Passey's method was developed from the cross plot between acoustic impedance and TOC obtained fig 6.9. Regression line was applied as:

$$y = -0.000912151 * x + 11.2801 \quad (6.3)$$

The correlation for the data set was more than 0.73. Seismic section for Passey is illustrated in fig 6.10.

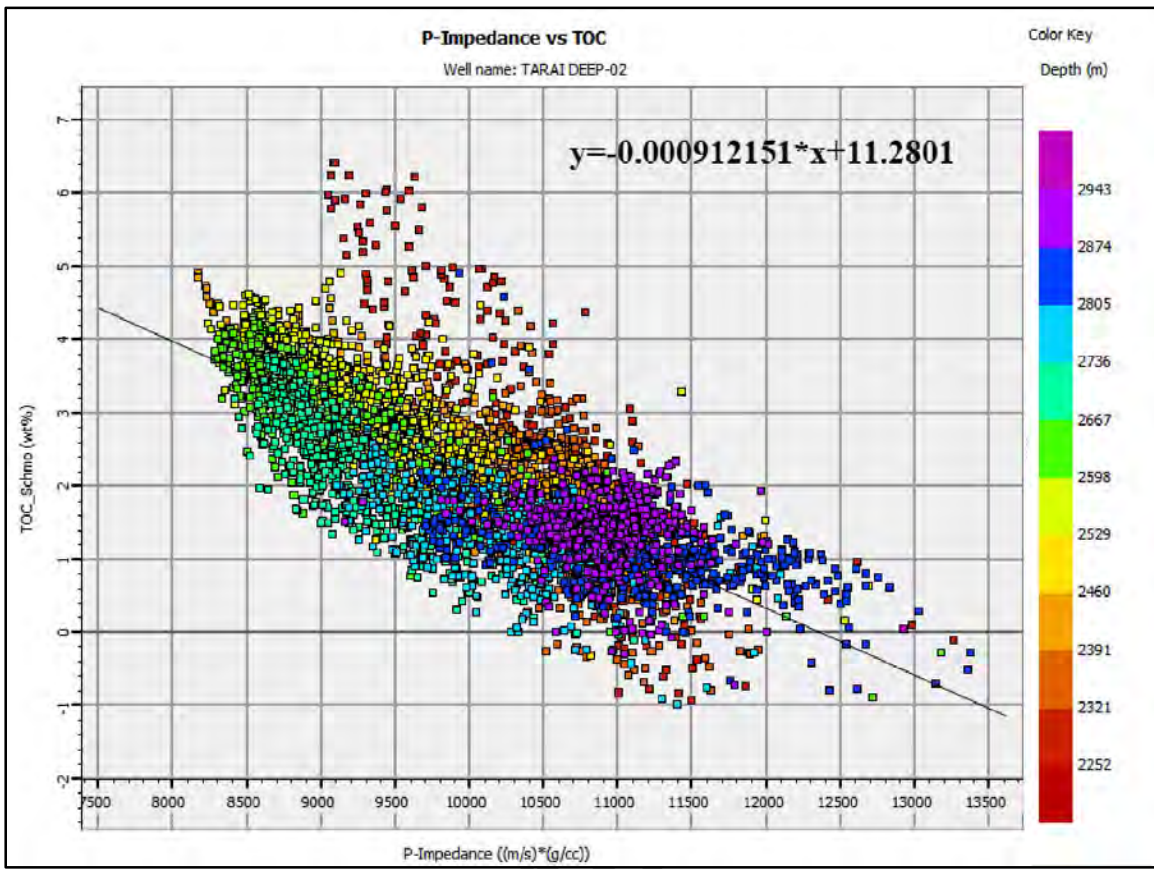


Figure 6.9 Cross-plot of P-impedance and TOC calculated from Schmoker.

DRS

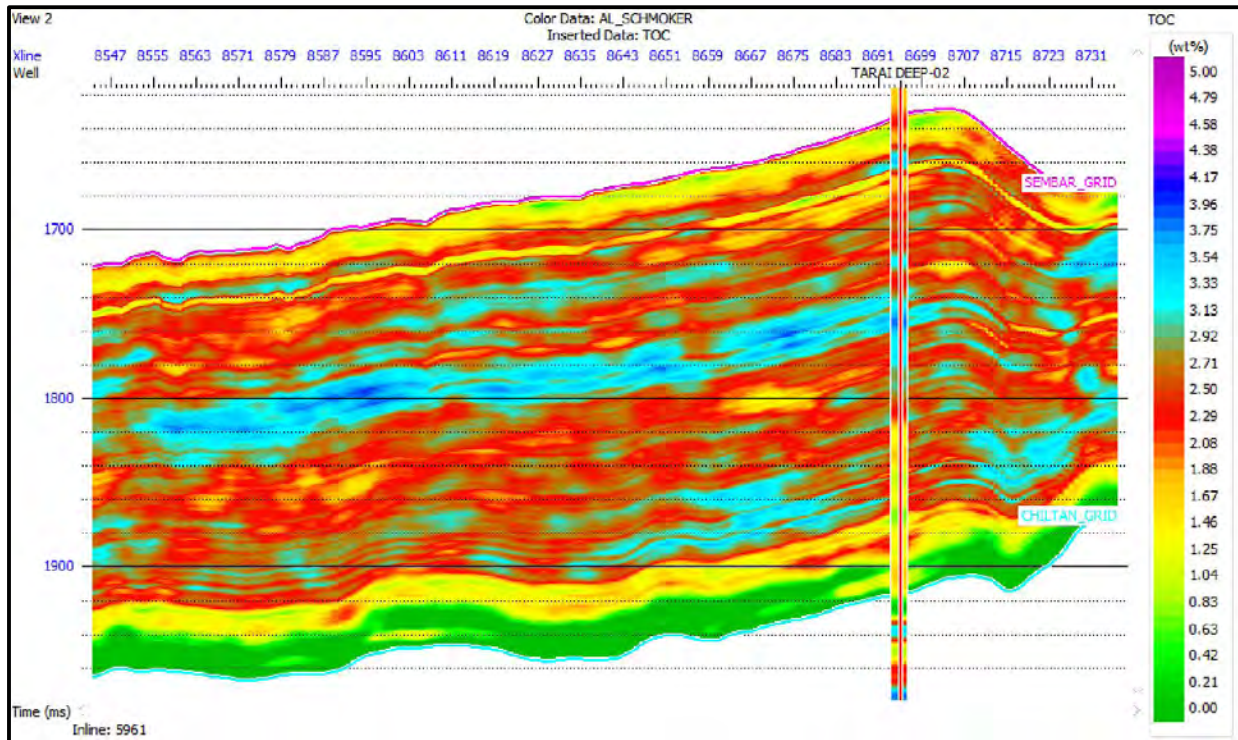


Figure 6.10 Inverted seismic section for TOC obtained from Schmoker.

### 6.11 Seismic Schwarzkopf TOC sections from impedance model:

Seismic inverted sections for TOC calculated from Schwarzkopf method was developed from the cross plot between acoustic impedance and TOC obtained fig 6.11. Regression line was applied as:

$$y = -0.000109245 * x + 12.0638 \quad (6.4)$$

The correlation for the data set was more than 0.76. Seismic section for Passey is illustrated in fig 6.12.

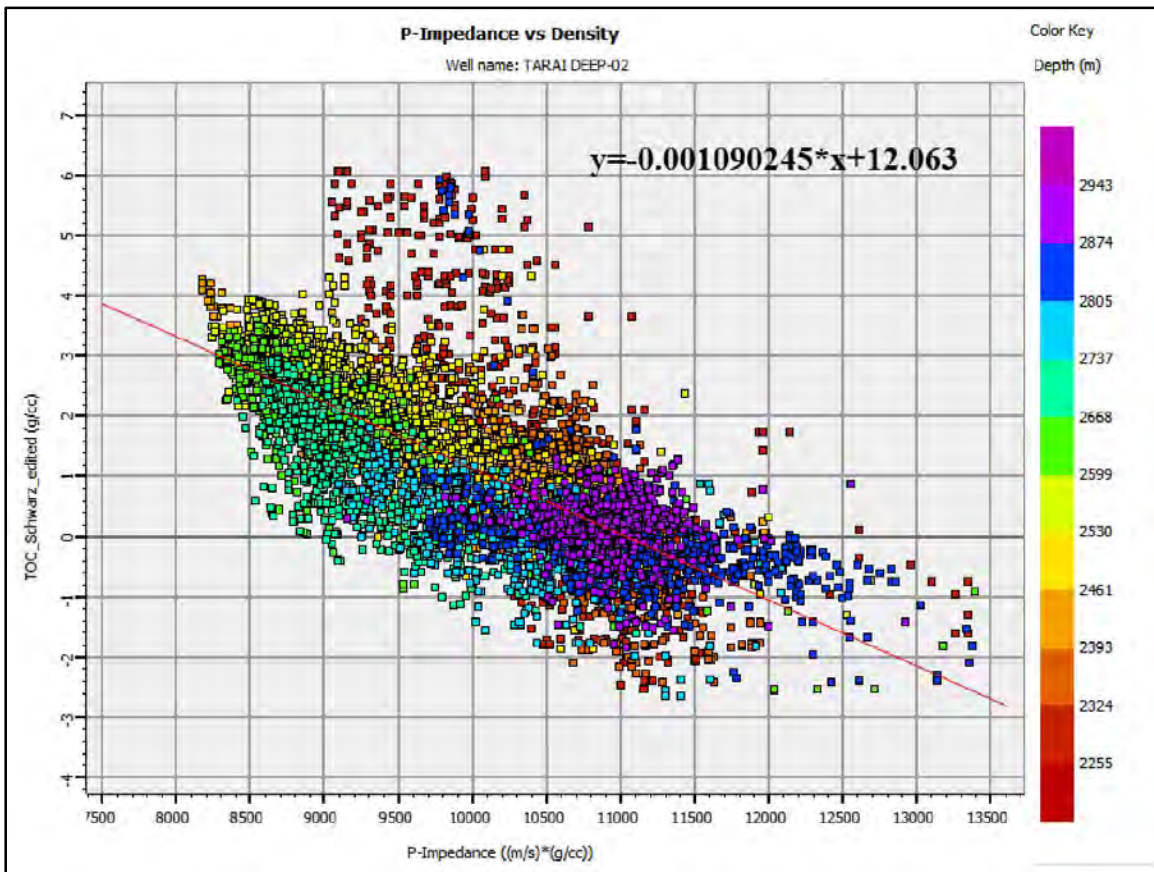


Figure 6.11 Cross-plot of P-impedance and TOC calculated from Schwarzkopf.

DRS

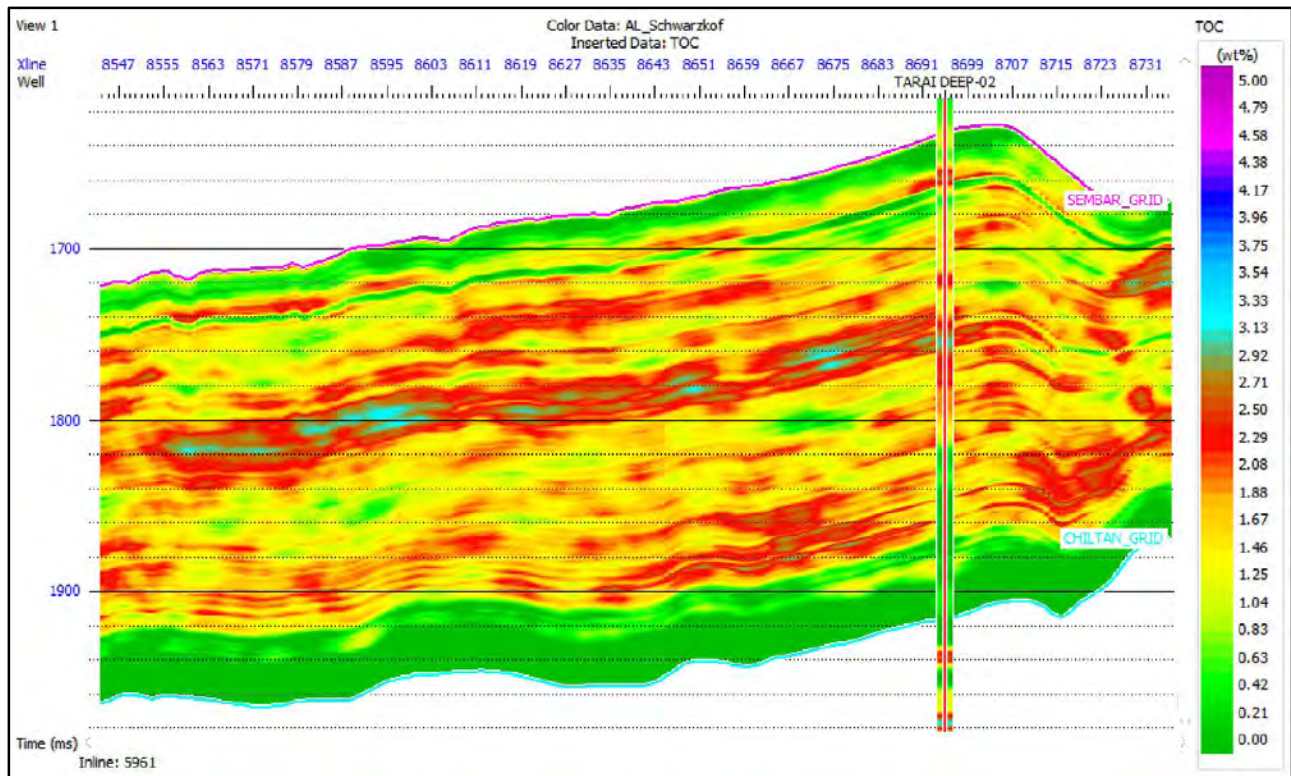


Figure 12 Inverted seismic section for TOC obtained from Schwarzkopf.

DRSML

## DISCUSSION AND CONCLUSIONS

This research presents an integrated examination of the Sembar Formation in the Tarai Area of the Lower Indus Basin in Pakistan in terms of the potential of unconventional reservoirs. The Tarai Deep – 02 well log information was employed for this purpose. A high oil/gas production rate and the existence of the Sembar Formation, the principal source rock in the Lower Indus Basin, made the region favourable for unconventional source study. In terms of the region's prospective shale oil/gas resource, the Sembar Formation has not been thoroughly studied and utilised as an unconventional resource.

Since the Tarai Deep – 02 well was drilled to the Chiltan Formation, its data was used. This makes it an exceptional well for producing effective results using well logs. Creating a connection between well and seismic data is the first stage of interpretation. Utilizing the DT and RHOB logs, a synthetic seismogram was generated for seismic to well tie development. Due to the considerably lower resolution of seismic data, the synthetic seismogram correlation is sometimes low. Making an accurate tie is crucial for precise horizon marking. After establishing a precise tie, the horizons of interest were marked on the seismic section, beginning with the seismic line closest to the well and then extending the interpretation to other lines. Each section's faults were identified and linked using the fault polygon approach. The generation of time and depth grids that depict the regional distribution of the Sembar Formation, which is gently sloping westward.

To qualify as a potential unconventional resource, a source rock must have a high TOC concentration. The Sembar was analysed and subsequently identified as a probable source rock using a variety of techniques for calculating TOC values. Methodologies based on distinct log data inputs might possibly respond differently to a degree. If the log data is erroneous, this difference can be significant. Before using the approach, it is therefore essential to consider the availability and quality control of well logs. The approach of Passey introduces a variable that integrates the influence of amount of organic maturity into the calculation. This value is referred to as the Ro. The visual assessment of the average Ro value was 0.56. In Tarai – 01, the Passey's Log R method, Schmoker's method, and Schwarzkopf methodology gave average values (in weight percent) of 3.58 (DT/LLD), 4.12 (Schmoker), and 3.58 (Schwarzkopf), respectively. In Tarai Deep – 02, the Passey's Log R techniques, Schmoker's method, and Schwarzkopf methodology generated average values (in weight percent) of 3.04 (DT/LLD), 2.13 (Schmoker), and 2.04 (Schwarzkopf).

According to the computed TOC logs, values in the range of 2 to 4 wt.% indicated that the Sembar formation has the potential to serve as an unconventional reservoir.

Rock physics modeling is applied to the well data to calculate the elastic parameters of the lithologies. The calculated properties are true or near to true representation of subsurface. These elastic properties are then used in stochastic inversion. Initial strata model was calculated and then used as an input to develop the SI model. The inverted volume indicates low to medium impedance values in the Sembar Formation.

TOC logs from each technique are cross-plot with the impedance log to develop a relationship between them. Based upon the regression equation, the volumes of TOC have been generated which indicates good spatial TOC distribution throughout the Sembar Formation, particularly in the middle portion. Passey TOC section shows high TOC values of about 4%. Schmoker TOC section show an average of about 2 to 3% spatially distributed throughout the Formation. Schwarzkopf based TOC section depicts 1.5 to 2.5% TOC values. Overall, TOC in the area is about 2 to 3% distributed in the Sembar Formation making it a potential prospect as an unconventional resource. The conclusions of the dissertation are as follows:

- The Sembar Formation in the study area is dipping toward west and its thickness is increasing towards north-east.
- The average TOC values within the Sembar Formation, calculated from the Passey, Schmoker and Schwazkopf, methods, are 3.31, 3.1, and 3.07 wt% respectively.
- The  $V_p$ ,  $V_s$ , and  $\rho$  estimated from the rock physics model segregate the facies and improved the inversion results.
- The uncertainty analysis based on P10, P50, and P90 models confirmed the presence of shale in the Sembar Formation.
- The spatial distribution of the TOC log estimated from each method shows that the TOC distribution in area is about 2-3 wt% and is particularly high in the middle portion of the formation.

## REFERENCES

- Abbasi AH, Mehmood F, Kamal M (2014) Shale oil and gas: lifeline for Pakistan. Sustainable Development Policy Institute, Islamabad, pp 85–87
- Adjei, S., Wilberforce, A. N., Opoku, D., & Mohammed, I. (2019). Probabilistic approach for shale volume estimation in Bornu Basin of Nigeria. *Petroleum and Gas Engineering*, 49.
- Ahmad N, Mateen J, Shehzad K, Mehmood N, Arif F (2011) Shale gas potential of Lower Cretaceous Sembar Formation in Middle and Lower Indus Basin, Pakistan. In: Assoc Pet Geol/Soc Pet Explor-Ann Tech Confer, pp 235–252
- Ahmad N, Mateen J, Shehzad K, Mehmood N, Arif F (2011) Shale gas potential of Lower Cretaceous Sembar Formation in Middle and Lower Indus Basin, Pakistan. In: Assoc Pet Geol/Soc Pet Explor-Ann Tech Confer, pp 235–252
- Ahmad, N., Mateen, J., Chaudry, K. S., Mehmood, N., & Arif, F. (2013). Shale gas potential of lower Cretaceous Sembar Formation in middle and lower Indus basin, Pakistan. *Pakistan Journal of Hydrocarbon Research*, 23, 51-62.
- Alam, M. S. M., Wasimuddin, M., & Ahmad, S. S. M. (2002, November). Zaur Structure, A Complex Trap in a Poor Seismic Data Area. In BP Pakistan Exploration & Production Inc. Annu. Tech. Conf.(ATC), Islamabad, Pakistan, November (pp. 2-4).
- Alexander, T., Baihly, J., Boyer, C., Clark, B., Waters, G., Jochen, V., ... & Toelle, B. E. (2011). Shale gas revolution. *Oilfield review*, 23(3), 40-57.
- Ali, A., Alves, T. M., Saad, F. A., Mateeullah, T., & Hussain, M. M. (2018). Resource potential of gas reservoirs in south pakistan and adjacent indian subcontinent revealed by post-stack inversion techniques. *Journal of Natural Gas Science and Engineering*, 49, 41–55.



- Al-Rahim, A. M., & Hashem, H. A. (2016). Subsurface 3D prediction porosity model from converted seismic and well data using Model-based inversion technique. *Iraqi Journal of Science*, 57(1A), 163-174.
- Alyousuf, T., Algharbi, W., Algeer, R., et al., 2011. Source rock characterization of the Hanifa and Tuwaiq mountain formations in the Arabian basin based on rock-eval pyrolysis and the modified delta log R method. SPE/DGS Saudi Arabia Section Technical Symposium and Exhibition.
- Aziz, O., Hussain, T., Ullah, M., Bhatti, A. S., & Ali, A. (2018). Seismic based characterization of total organic content from the marine Sembar shale, Lower Indus Basin, Pakistan. *Marine Geophysical Research*, 39, 491-508.
- Bandyopadhyay, K., Sain, R., Liu, E., Harris, C., Martinez, A., Payne, M., & Zhu, Y. (2012). Rock property inversion in organic-rich shale: Uncertainties, ambiguities, and pitfalls. In *SEG Technical Program Expanded Abstracts 2012* (pp. 1-5). Society of Exploration Geophysicists.
- Barclay, F., Bruun, A., Rasmussen, K. B., Alfaro, J. C., Cooke, A., Cooke, D., & Roberts, R. (2008). Seismic inversion: Reading between the lines. *Oilfield Review*, 20(1), 42-63.
- Berryman, J. G. (1995). Mixture theories for rock properties. *Rock physics and phase relations: A handbook of physical constants*, 3, 205-228.
- Blangy, J. P. (1994). AVO in transversely isotropic media—An overview. *Geophysics*, 59(5), 775-781.
- Blyth, F. G. H., & De Freitas, M., 2017. *A geology for engineers*. CRC Press.
- Bocora, J. (2012). Global prospects for the development of unconventional gas. *Procedia-Social and Behavioral Sciences*, 65, 436-442.
- Bowman T (2010) Direct method for determining organic shale potential from porosity and resistivity logs and identify possible resource play. In: AAPG annual convention, New Orleans, pp 11–14

- Carcione, J. M. (2000). A model for seismic velocity and attenuation in petroleum source rocks. *Geophysics*, 65(4), 1080-1092.
- Carcione, J. M., Helle, H. B., & Avseth, P. (2011). Source-rock seismic-velocity models: Gassmann versus Backus. *Geophysics*, 76(5), N37-N45.
- Chesnokov, E. M., Tiwary, D. K., Bayuk, I. O., Sparkman, M. A., & Brown, R. L. (2009). Mathematical modelling of anisotropy of illite-rich shale. *Geophysical Journal International*, 178(3), 1625-1648.
- Cooke, D., & Can't, J. (2010). Model-based Seismic Inversion: Comparing deterministic and probabilistic approaches. *CSEG Recorder*, 28-39
- Curtis, A., & Snieder, R. (2002). Probing the Earth's interior with seismic tomography. *International Geophysics Series*, 81(A), 861-874.
- Dewhurst, D. N., Siggins, A. F., Sarout, J., Raven, M. D., & Nordgård-Bolås, H. M. (2011). Geomechanical and ultrasonic characterization of a Norwegian Sea shale. *Geophysics*, 76(3), WA101-WA111.
- Dobrin and Savit., 1988, *Geophysical Exploration*, Hafner Publishing Co.
- EIA, U., 2013. *Annual Energy Outlook*. US Energy Information Administration, Washington, DC, pp. 60e62.
- Eickhoff G, Alam S (1991) On the petroleum geology and prospectivity of Kirther Range and Sibi Trough, Southern Indus Basin, Pakistan. BGR/HDIP, Hannover
- Farah AG, Lawrence RD, De J (1984) An overview of the tectonics of Pakistan. In: Haq BU, Mil Liman JD (eds), *Marine geology and oceanography of the Arabian Sea and coastal Pakistan*. Van Nostrand and Reinhold Co., New York, pp 161–176
- Gavotti, P. E. (2014). Model-based inversion of broadband seismic data (Master's thesis, Graduate Studies).
- Gavotti, P., Lawton, D., Margrave, G., & Isaac, H. (2013). Poststack

- Glasson, J., & Therivel, R. (2013). Introduction to environmental impact assessment. Routledge.
- Glorioso, J. C., & Rattia, A. (2012, March). Unconventional reservoirs: basic petrophysical concepts for shale gas. In SPE/EAGE European unconventional resources conference & exhibition-from potential to production (pp. cp-285). European Association of Geoscientists & Engineers.
- Gnos, E., Immenhauser, A., & Peters, T. J. (1997). Late Cretaceous/early Tertiary convergence between the Indian and Arabian plates recorded in ophiolites and related sediments. *Tectonophysics*, 271(1-2), 1-19.
- Guo, Z., Chapman, M., & Li, X. (2012). A shale rock physics model and its application in the prediction of brittleness index, mineralogy, and porosity of the Barnett Shale. In SEG technical program expanded abstracts 2012 (pp. 1-5). Society of Exploration Geophysicists.
- Hasany, S. T., & Saleem, U. (2012). An integrated subsurface geological and engineering study of Meyal Field, Potwar Plateau, Pakistan. *Search and Discovery Article*, 20151, 1-41.
- Hill, R. (1965). Theory of mechanical properties of fibre-strengthened materials—III. Self-consistent model. *Journal of the Mechanics and Physics of Solids*, 13(4), 189-198.
- Hill, R. J., Zhang, E, Katz, B. J., et al., 2007. Modeling of gas generation from the Barnett shale, Fort Worth Basin, Texas.
- Holmes, M., Holmes, D., & Holmes, A., 2011. A petrophysical model to estimate free gas in organic shales. In Annual Conference and Exhibition, Huston, Texas, AAPG Search and Discovery Article Vol. 40781.
- Hornby, B. E., Schwartz, L. M., & Hudson, J. A. (1994). Anisotropic effective-medium modeling of the elastic properties of shales. *Geophysics*, 59(10), 1570-1583.

- Iqbal MWA, Shah SMI (1980) A guide to stratigraphy of Pakistan, vol 53. GSP, Quetta
- Kadri IB (1995) Petroleum geology of Pakistan. Pakistan Petroleum Limited, Karachi, pp 35–37
- Kazmi AH, Snee LW (1989) Geology of world emerald deposits: a brief review. Van Nostrand Reinhold, The Netherland, pp 165–228
- Kazmi, A. H., & Jan, M. Q. (1997). Geology and tectonics of Pakistan. Graphic publishers.
- Kemal, A., Zaman, A. S. H., & Humayon, M. (1991, November). New directions and strategies for accelerating petroleum exploration and production in Pakistan. In Proceedings, International Petroleum Seminar (pp. 16-57).
- Khalid, P., Qureshi, J., Din, Z. U., Ullah, S., & Sami, J. (2019). Effect of kerogen and TOC on seismic characterization of lower cretaceous shale gas plays in lower Indus Basin, Pakistan. *Journal of the Geological Society of India*, 94, 319-327.
- Kneller, E. A., Albertz, M., Karner, G. D., & Johnson, C. A. (2013). Testing inverse kinematic models of paleo crustal thickness in extensional systems with high-resolution forward thermo-mechanical models. *Geochemistry, Geophysics, Geosystems*, 14(7), 2383-2398.
- Liu, L., Shang, X., Wang, P., Guo, Y., Wang, W., & Wu, L. (2012). Estimation on organic carbon content of source rocks by logging evaluation method as exemplified by those of the 4 th and 3 rd members of the Shahejie Formation in western sag of the Liaohe Oilfield. *Chinese Journal of Geochemistry*, 31, 398-407.
- Mallick, S. (2001). AVO and elastic impedance. *The leading edge*, 20(10), 1094-1104.

- Mavko, G., Mukerji, T., & Dvorkin, J. (1998). *The rock physics handbook: Tools for seismic analysis in porous media*: University of Cambridge.
- McCartney, J. T., & Teichmuller, M., 1972. Classification of coals according to degree of coalification by reflectance of the vitrinite component. *Fuel*, 51(1), 64-68.
- Meyer, B. L., & Nederlof, M. H. (1984). Identification of source rocks on wireline logs by density/resistivity and sonic transit time/resistivity crossplots. *AAPG bulletin*, 68(2), 121-129.
- Meyer, B.L. and Nederlof, M.H., 1984. Identification of source on wireline logs by density/resistivity and sonic transit time/resistivity crossplot. *AAPG Bulletin* 68, 121-129.
- Miller, R. G., & Sorrell, S. R. (2014). Introduction: the future of oil supply. *Philosophical Transactions: Mathematical, Physical and Engineering Sciences*, 1-27.
- Myers, K. J., & Jenkyns, K. F. (1992). Determining total organic carbon contents from well logs: an intercomparison of GST data and a new density log method. *Geological Society, London, Special Publications*, 65(1), 369-376.
- Onajite, E. (2013). *Seismic data analysis techniques in hydrocarbon exploration*. Elsevier.
- Pan, X. P., Zhang, G. Z., & Chen, J. J. (2020). The construction of shale rock physics model and brittleness prediction for high-porosity shale gas-bearing reservoir. *Petroleum Science*, 17, 658-670.
- Passey, Q. R., Bohacs, K. M., Esch, W. H., Klimentidis, R., and Sinha, S., 2010. From oil-prone source rock to gas-producing shale reservoir-geologic and petrophysical characterization of unconventional shale gas reservoirs. *Society of Petroleum Engineers (SPE 13150): International oil and gas conference and exhibition 8-10 June, Beijing, China*, 1–29.

- Passey, Q. R., Creaney, S., Kulla, J. B., Moretti, F. J., & Stroud, J. D. (1990). A practical model for organic richness from porosity and resistivity logs. AAPG bulletin, 74(12), 1777-1794.
- Peters, K. E., & Cassa, M. R. (1994). Applied source rock geochemistry: Chapter 5: Part II. Essential elements.
- Porth, H., & Raza, H. A. (1990). On the geology and hydrocarbon prospects of Sulaiman Province, Indus Basin, Pakistan. Unpublished technical report, Bundesanstalt für Geowissenschaften und Rohstoffe, Hannover/Hydrocarbon Development Institute, Pakistan, 127.
- Raza HA, Ali SM, Ahmed R, Ahmed J (1990) Petroleum geology of Kirther Sub-Basin and part of Kutch Basin. Pak J Hydrocarbon Res 2(1):29–73
- Sayers, C. M. (2013). The effect of kerogen on the AVO response of organic-rich shales. The Leading Edge, 32(12), 1514-1519.
- Schmoker, J.W., 1979. Determination of organic content of Appalachian Devonian shales from foreformation-density logs. AAPG Bulletin, 63: 1504–1537.
- Schwarzkopf, T.A. 1992. Source rock potential (TOC + hydrogen index) evaluation by integrating well log and geochemical data. Org Geochem 19(4):545–555
- Selley, R. C. (1985). Elements of Petroleum Geology, W. H.
- Sen, M. K. (2006). Seismic inversion. Richardson, TX.: Society of Petroleum Engineers.
- Shah, S. M. I. (2009). Stratigraphy of Pakistan (memoirs of the geological survey of Pakistan). The Geological Survey of Pakistan, 22.
- Sharma, R. K., & Chopra, C. (2013, September). Unconventional reservoir characterization using conventional tools. In 2013 SEG Annual Meeting. OnePetro.

- Sheriff R. E., Telford W. M., and Geldart L. P., 1990, Applied geophysics, Cambridge University Press.
- Shibaoka, M., Bannett, A. J. R., & Gould, K. W., 1973. Diagenesis of organic matter and occurrence of hydrocarbon in some Australian sedimentary basins. The APPEA Journal, 13(1), 73-80.
- Slatt, R. M., & Abousleiman, Y. (2011). Merging sequence stratigraphy and geomechanics for unconventional gas shales. The Leading Edge, 30(3), 274-282.
- Songergeld, C. H., Newsham, K. E., Comisky, J.T., Rice, M.C., & Rai, C. S., 2010. Petrophysical considerations in evaluating and producing shale gas resources. Society of Petroleum Engineers. SPE 131768.
- Songergeld, C. H., Newsham, K. E., Comisky, J.T., Rice, M.C., & Rai, C. S., 2010. Petrophysical considerations in evaluating and producing shale gas resources. Society of Petroleum Engineers. SPE 131768.
- Swanson, V. E. (1960). Oil yield and uranium content of black shales (No. TID-27491). Geological Survey, Washington, DC (USA).
- Telford, W.M., Geldart, L.P., Sheriff, R.E., and Keys, D.A., 1999, Applied Geophysics, Cambridge University Press, London
- Tsvankin, I., Gaiser, J., Grechka, V., Van Der Baan, M., & Thomsen, L. (2010). Seismic anisotropy in exploration and reservoir characterization: An overview. Geophysics, 75(5), 75A15-75A29.
- Tsvankin, I., Gaiser, J., Grechka, V., Van Der Baan, M., & Thomsen, L. (2010). Seismic anisotropy in exploration and reservoir characterization: An overview. Geophysics, 75(5), 75A15-75A29.
- Vishal, V., Rizwan, M., Mahanta, B., Pradhan, S. P., & Singh, T. N. (2022). Temperature effect on the mechanical behavior of shale: Implication for shale gas production. Geosystems and Geoenvironment, 1(4), 100078.

- Vernik, L., & Nur, A. (1992). Ultrasonic velocity and anisotropy of hydrocarbon source rocks. *Geophysics*, 57(5), 727-735.
- Wandrey CJ, Law BE, Shah AH (2004) Sembar Goru/Ghazij composit total petroleum system, Indus and Sulaiman-kirther Geological Province, Pakistan and India. *USGS Bulletin*, pp 1–23
- Welte, D. H., & Tissot, P. (1984). *Petroleum formation and occurrence*. Springer-verlag.
- Wenk, H. R., Lonardelli, I., Franz, H., Nihei, K., & Nakagawa, S. (2007). Preferred orientation and elastic anisotropy of illite-rich shale. *Geophysics*, 72(2), E69-E75.
- Wu, X., Chapman, M., Y. Li, X., & Dai, H. (2012, June). Anisotropic elastic modelling for organic shales. In 74th EAGE Conference and Exhibition incorporating EUROPEC 2012 (pp. cp-293). EAGE Publications BV.
- Zaigham, N. A., & Mallick, K. A. (2000). Prospect of hydrocarbon associated with fossil-rift structures of the southern Indus basin, Pakistan. *AAPG bulletin*, 84(11), 1833-1848.
- Zhang, F., Li, X. Y., & Qian, K. (2017). Estimation of anisotropy parameters for shale based on an improved rock physics model, part 1: theory. *Journal of Geophysics and Engineering*, 14(1), 143-158.
- Zhang, F., Wang, L., & Li, X. Y. (2020). Characterization of a shale-gas reservoir based on a seismic amplitude variation with offset inversion for transverse isotropy with vertical axis of symmetry media and quantitative seismic interpretation. *Interpretation*, 8(1), SA11-SA23.
- Zhu, Y., Xu, S., Payne, M., Martinez, A., Liu, E., Harris, C., & Bandyopadhyay, K. (2012, November). Improved rock-physics model for shale gas reservoirs. In 2012 SEG Annual Meeting. OnePetro.



- Zou, C., Zhao, Q., Zhang, G., & Xiong, B. (2016). Energy revolution: From a fossil energy era to a new energy era. *Natural Gas Industry B*, 3(1), 1-11.